UNIVERSIDADE D
COIMBRA

Saulo Jorge Beltrão de Queiroz

SPECTRO-COMPUTATIONAL COMPLEXITY ANALYSIS FOR WIRELESS COMMUNICATIONS

Doctoral thesis submitted to the Doctoral Program in Information Science and Technology, supervised by Professors Edmundo Monteiro and João P. Vilela, and presented to the Department of Informatics Engineering of the Faculty of Sciences and Technology of the University of Coimbra.

September 2021

Faculdade de Ciências e Tecnologia
da Universidade de Coimbra

Análise Da Complexidade Espectro-Computacional Para Comunicações sem Fios

Saulo Jorge Beltrão de Queiroz

Tese no âmbito do Programa de Doutoramento em Ciências e Tecnologias da Informação, orientada pelo Professor Doutor Edmundo Monteiro e pelo Professor Doutor João P. Vilela, e apresentada ao Departamento de Engenharia Informática da Faculdade de Ciências e Tecnologia da Universidade de Coimbra.

Setembro de 2021

1 2 9 0

UNIVERSIDADE D
COIMBRA

This work is partially supported by the European Regional Development Fund (ERDF), through the Regional Operational Programme of Lisbon (POR LISBOA 2020), the Competitiveness and Internationalization Operational Programme (COMPETE 2020) of the Portugal 2020 framework from the Portuguese Foundation for Science and Technology (FCT) [projects 5G with Nr. 024539 (POCI-01-0247-FEDER-024539), CONQUEST (CMU/ECE/0030/2017), SWING2 (PTDC/EEI-TEL/3684/2014, POCI-01-0145-FEDER-016753), MobiWise (P2020 SAICTPAC/001/2015)], the MIT Portugal Program [Project SNOB-5G with Nr. 045929 (CENTRO-01-0247-FEDER-045929)], and the reasearch funding agency of the brazilian state of Paraná fundação araucária.

To the one that raised from dead.
Dedicado Àquele que ressurgiu dos mortos.

"I am the resurrection and the life. Whoever believes in Me will live, even though he dies."

John 11:25

Acknowledgements

This work was possible thanks to the help of several people. First, I would like to thank the One everything came from: "Jesus Christ ... for of him, and through him, and to him, are all things: to whom be glory forever. Amen!".

During the years of this work, I received support from some very special people. Of them, my beloved wife Dulcina Queiroz deserves my deepest gratitude. About eleven years ago, I mentioned her in the acknowledgment of my master thesis. Now, after all these years, my gratitude has grown. Thank you for all your love, support, companionship, and sincere words of enthusiasm. I love you!

This work required me to travel between Brazil and Portugal several times. In Portugal, I had the valuable support of my wife's family, especially my father-in-law João Oliveira and mother-in-law Dulcina Aquino. In Brazil, I'd like to thank my parents José and Silvana for the priceless principles of life given to me. Also, I'd like to thank my sisters Sheyla and Sheylane for their sincere votes of success to me.

I would like to thank my advisors, professors Edmundo Monteiro and João Vilela, for sharing their experience, valuable technical contributions, and this great opportunity given to me. Thank you for accepting the challenge of advising a Ph.D. student full of other academic assignments and investing your time in my academic formation. I'm very happy to have you as part of my professional history.

I also would like to thank the incentives from my colleagues of the Academic Department of Informatics of the Federal University of Technology in Brazil and the support from the colleagues of the LCT group and CISUC.

Finally, I would like to thank all people that somehow contributed to the accomplishment of this work.

Abstract

This thesis introduces the spectro-computational complexity (SC) analysis of communication signal algorithms. The SC analysis stems from a novel mathematical model that unifies indicators of performance of the information theory, such as capacity, throughput, and spectral efficiency (SE), along with indicators of the theory of computational complexity (CC), such as processing runtime, the number of computational instructions and asymptotic lower bound. The proposed analysis exploits the fact that both classes of performance indicators can be written as a function of the signal's spectral bandwidth W.

This thesis defines the SC throughput $SC(W)$ of a communication signal algorithm as the ratio between the number of modulated bits $B(W)$ and the CC $T(W)$ required to turn the bits into the signal. Thus, an asymptotic analysis on W reveals the necessary CC (or SE improvement) to prevent the nullification of $SC(W)$ as W grows. Based on $SC(W)$, novel definitions derived from and homologous to concepts of the CC and information theory fields are defined, such as SC capacity, SC efficiency, optimal SC algorithm, and comp-limited signals (from computation-limited, as a reference to the homologous power- and band-limited signal regimes). With the assistance of the SC analysis, novel capacity-complexity scaling laws are presented for Orthogonal Frequency Division Multiplexing (OFDM) and some variants.

In a case study, an optimal mapper for OFDM with Index Modulation (IM) was designed, implemented, and evaluated. Such ideal mapper reaches the maximal SE gain over OFDM but its complexity had been considered computationally intractable by the OFDM-IM literature. Based on the SC analysis, the exact asymptotic complexity required to sustain the maximal SE gain was demonstrated as linear (rather than exponential) on the number of subcarriers.

In other case study, it was shown that the complexity of the FFT algorithm causes the throughput of OFDM to nullify on the number of subcarriers N. The FFT constraint that N must grow as a power of two 2^i ($i > 0$) translates into an exponential complexity on i as spectrum widens. In general, it is shown that the throughput of FFT-based waveforms (e.g. OFDM) nullifies on N unless the lower bound complexity of the Fourier transform problem verifies as linear on N, which implies in faster-than-FFT algorithms and remains an open question in computer science. Based on the SC analysis, an algorithm is proposed to an alternative formulation in which an N-point transform is replaced by several smaller transforms. This formulation is employed by OFDM in its vectorized form (V-OFDM) in order to mitigate the cyclic prefix overhead of OFDM. Thus, the proposed algorithm can replace FFT in V-OFDM. By relaxing the power of two constraint of N and, with the parameterization of the number of smaller transforms, it was verified that the complexity of the proposed algorithm can

grow linearly on N rather than exponentially on i.

The presented case studies illustrate how the SC analysis can guide waveform designers towards the optimal balance between capacity and complexity in the extremely large signals expected for future wireless networks.

Keywords: Wireless Signal Performance, Computational Complexity, Channel Capacity, Index Modulation, Vector OFDM.

Resumo

A presente tese introduz a análise da complexidade eSpectro-Computacional (SC) para algoritmos de sinais de comunicação. A análise SC baseia-se em um novo modelo matemático que unifica indicadores de desempenho da teoria da informação como capacidade, débito de sinal e eficiência espectral (SE), com indicadores da teoria da complexidade computacional (CC) como tempo de execução, número de instruções computacionais e cota assimptótica inferior de um problema computacional. A análise proposta explora o facto de que ambas classes de indicadores de desempenho podem ser escritas como função da largura espectral do sinal W.

Nesta tese, o débito SC $SC(W)$ de um algoritmo de sinal de comunicação como a razão entre o número de bits modulados $B(W)$ e a CC $T(W)$ necessária para transformar os bits em sinal. Assim, uma análise assimptótica em W revela a CC mínima (ou a melhoria de SE) necessária para impedir que $SC(W)$ tenda a zero a medida que W cresce. Baseado no débito $SC(W)$, novas definições derivadas e homólogas a conceitos dos campos da CC e da teoria da informação são apresentadas como capacidade SC, a eficiência SC, algoritmo SC óptimo e sinais comp-limited (do inglês "computation-limited", em referência aos regimes homólogos *power-* e *band-limited*). Com a assistência da análise SC, novas leis de escalabilidade conjungando capacidade e complexidade são apresentadas para a forma de onda OFDM e algumas de suas variantes.

Em um estudo de caso, um mapeador óptimo para OFDM com modulação por índice (IM) é projetado, implementado e avaliado. O referido mapeador óptimo maximiza o ganho SE do OFDM-IM sobre o OFDM mas a complexidade resultante tem sido conjecturada como intratável pela literatura. Baseado na análise SC, a complexidade assimptótica exacta necessária para assegurar o ganho SE máximo foi demonstrada como linear (em vez de exponencial) no número de subportadoras.

Em outro estudo de caso, verificou-se que a complexidade do algoritmo FFT faz com que o débito do OFDM tenda a zero a medida que o número de subportadoras N cresce. A limitação da FFT em que N deve crescer como uma potência de dois 2^i $(i > 0)$ leva a uma complexidade exponencial em i a medida que a largura do espectro aumenta. De forma geral, é mostrado que o débito de formas de onda baseadas na FFT (e.g. OFDM) tende a zero a menos que a cota inferior do problema da transformada de Fourier de N pontos verifique-se como linear, exigindo-se, assim, algoritmos mais rápidos que a FFT, o que permanece uma questão em aberto da ciência da computação. Com o suporte da análise SC, um algoritmo é proposto a uma formulação alternativa em que uma transformada de N pontos é substituida por várias transformadas menores. Tal abordagem é empregada pela forma de onda OFDM vectorial (V-OFDM) a fim de mitigar a sobrecarga do prefixo cíclico do OFDM. Assim, o algoritmo proposto é uma alternativa à FFT no V-OFDM. Pelo relaxamento de N como

potência de dois e com a parametrização do número de transformadas menores, verificou-se que a complexidade do algoritmo proposto cresce linearmente em N em vez de exponencialmente em i.

Os estudos de casos apresentados ilustram como a análise SC pode conduzir projetistas de formas de onda rumo ao balanceamento óptimo entre a capacidade e a complexidade de sinais extremamente largos esperados nas redes sem fio do futuro.

Palavras-chave: Desempenho de Sinais Sem Fios, Complexidade Computacional, Capacidade de Canal, Modulação por Índice, OFDM Vectorial.

Foreword

The results reported in this thesis were accomplished with resources of Laboratory of Communication and Telematics (LCT) of the Centre for Informatics and Systems of the University of Coimbra (CISUC). The publications of this thesis were partially supported by the following projects:

- **Project MobiWise** (P2020 SAICTPAC/001/2015)
- **Project CONQUEST** (CMU/ECE/0030/2017)
- **Project 5G - Components and Services for 5G Networks** (POCI-01-0247-FEDER-024539)
- **Project SWING2** (POCI-01-0145-FEDER-016753 and PTDC/EEI-TEL/3684/2014)
- **Project SNOB-5G** (CENTRO-01-0247-FEDER-045929)

The outcome of this work led to technical presentations, open source softwares and publications, as listed below.

Open source library: Queiroz, S. (2020). lib-ofdmim: The OFDM with index modulation library mapper. `https://github.com/sauloqueiroz/lib-ofdmim`.

Technical presentations:

- Queiroz, S. and Vilela, João P. and Monteiro, E., "**Index Selector Task for OFDM with Index Modulation: A Cost Analysis**". 26°Seminário da Rede Temática de Comunicações Móveis (RTCM), 2019.
- Queiroz, S. and Vilela, João P. and Monteiro, E., "**What is the Cost of the Index Selector Task for OFDM with Index Modulation**". °IEEE Wireless Days, Manchester, UK, 2019.

Publications:

- Queiroz, S., Vilela, J., and Monteiro, E. (2019). What is the cost of the index selector task for OFDM with index modulation? In IFIP/IEEE Wireless Days (WD) 2019, Manchester, UK.
- Queiroz, S., Silva, W., Vilela, J. P., and Monteiro, E. (2020). Maximal spectral efficiency of OFDM with index modulation under polynomial space complexity. IEEE Wireless Communications Letters, 9(5):1–4.
- Queiroz, S., Vilela, J. P., and Monteiro, E. (2020). Optimal mapper for OFDM with index modulation: A spectro-computational analysis. IEEE Access, 8:68365–68378.

- Queiroz, S., Vilela, J. P., and Monteiro, E. (2020). Is FFT Fast Enough for Beyond-5G Communications? Technical Report ArXiv n. 2012.07497 (under review on IEEE Transactions on Signal Processing).

Contents

List of Figures

List of Algorithms

List of Tables

Acronyms

ASIC	Application-Specific Integrated Circuit
ADFT	Approximate Discrete Fourier Transform
BER	Bit-Error Rate
CP	Cyclic Prefix
IQ	In-phase Quadrature
ITU	International Telecommunication Union
SNR	Signal-to-Noise Ratio
FPGA	Field Programmable Gate Array
GPP	General Purpose Processor
ASE	Area Spectral Efficiency
SE	Spectral Efficiency
DAC	Digital-to-Analog Converter
RF	Radio Frequency
ADC	Analog-to-Digital Converter
DSP	Digital Signal Processing
DFT	Discrete Fourier Transform
eMBB	Enhanced Mobile Broadband
IDFT	Inverse Discrete Fourier Transform
FFT	Fast Fourier Transform
FBMC	Filter Bank MultiCarrier
VLSI	Very Large-Scale Integration
UFMC	Universal Filtered MultiCarrier
IM	Index Modulation
PFFT	Parameterized Fast Fourier Transform
PDFT	Parameterized Discrete Fourier Transform
IFFT	Inverse Fast Fourier Transform
OFDM	Orthogonal Frequency Division Multiplexing

V-OFDM Vector OFDM

ISI Inter-symbol Interference

Hz Hertz

SC Spectro-Computational

THz Terahertz

MT Mersenne Twister

VB Vector Block

Symbols

W	Signal bandwidth (Hz)
$C(W)$	Capacity as function of bandwidth (bits/seconds)
$B(W)$	Bits per symbol as function of the bandwidth
$T(B(W))$	Computational complexity as function of $B(W)$
G	Number of algorithms of a waveform proposal
$\mathcal{N}_0$	Noise spectral density (Watts)
$\mathcal{P}$	Received signal power (Watts)
W_{OFDM}	OFDM bandwidth (Hz)
R	Waveform data rate
R_{OFDM}	OFDM data rate
M	Constellation size of the modulation diagram
M	Number of samples per vector block
S	Waveform spectral efficiency
S_{OFDM}	OFDM spectral efficiency
B_{OFDM}	Number of bits in a N-subcarrier OFDM symbol
$B(N)$	Number of bits in a N-subcarrier waveform symbol
$T_{OFDM}(N)$	Period of OFDM symbol with cyclic prefix in seconds
T_{cp}	Length of cyclic prefix in seconds
T_{NYQ}	Nyquist time interval in seconds
N_{cp}	Length of cyclic prefix in samples
$T_{SYM}(N)$	Period of multicarrier symbol in seconds
f_s	Nyquist sampling rate (Samples per second)
Δf	OFDM frequency subcarrier bandwidth
$T(N)$	Computational complexity of a DSP algorithm given an N-size signal
$T_{DFT}(N)$	Computational complexity of the N-point DFT
$SC_{DFT}(N)$	Spectro-Computational throughput of DFT
$SC_i(W)$	Spectro-Computational throughput of i-th waveform algorithm

$SC(W)$	Spectro-computational throughput of a waveform
$SC(N)$	Spectro-Computational throughput of a signal algorithm upon an N-subcarrier input
$T_{MULT}(d)$	Computational complexity to multiply two d-digit numbers
$\mathbf{X}$	Vector of complex frequency domain OFDM symbols
X_i	i-th complex frequency domain sample of a multicarrier symbol
Y_i	i-th complex time domain sample of a multicarrier symbol
$\mathbf{x}_l$	l-th frequency-domain vector block of an multicarrier symbol
$\mathbf{y}_l$	l-th time-domain vector block of an multicarrier symbol
g	Number of subsymbols in an OFDM symbol
N	Number of complex OFDM samples
$\mathbb{Z}$	Set of integers
$\mathbb{C}$	Set of complex number
κ	Wall clock runtime of a computational instruction
$\mathcal{L}_i(B(W))$	Asymptotic complexity lower bound of the i-th waveform algorithm
$\mathcal{L}(B(W))$	Asymptotic complexity lower bound of a waveform

Chapter 1

Introduction

"This is life, life is beautiful and beautiful."

(Gonzaguinha)

Contents

This thesis aims to propose a mathematical model for the joint analysis of indicators of computational complexity – such as processing runtime, number of computational instructions, and asymptotic lower bound – and information theory – such as capacity, throughput, and spectral efficiency – for communication signal algorithms and their associated waveforms. This introductory chapter is organized as follows. Section 1.1 presents motivation and the problem statement. Section 1.2 lists the objectives and summarizes the achieved contributions and Section 1.3 presents the organization of the thesis.

1.1 Motivation and Problem Statement

Throughput is a classic performance indicator of wireless networks. In general terms, it captures how many units of information a given solution is able to transfer within a period of time. In the case of wireless network channels, the number of units of information (i.e., bits) depends on the range of electromagnetic waves assigned to the network (i.e., the spectrum bandwidth) and the ability of the physical layer to put more bits in the spectrum.

The support for faster data rates has been a continuous design target for wireless network standards. The fifth generation of wireless cellular networks

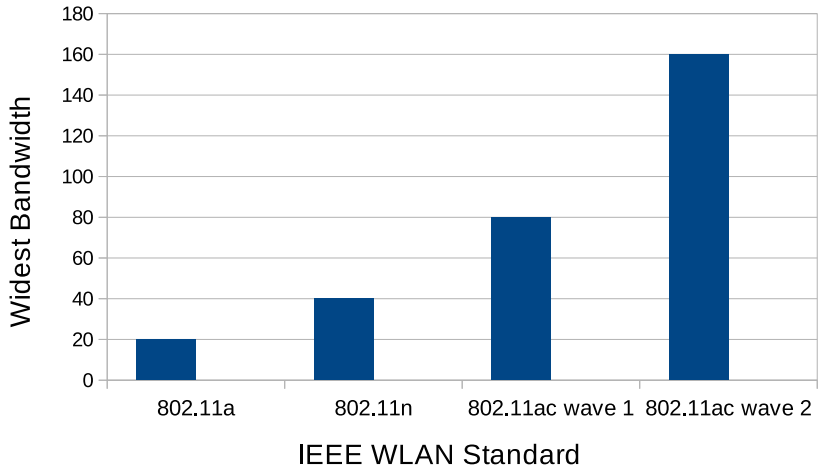

Figure 1.1: Growth of the widest supported bandwidth across the evolution of the IEEE 802.11 WLAN standard [IEEE 802.11, 2016], [802.11, 2013].

(5G) [3GPP, 2018], for example, standardizes the enhanced mobile broadband (eMBB) data traffic service for applications that demands high data rates. Similarly, the evolution of the IEEE 802.11 family of Wireless Local Area Networks (WLANs) standards has been characterized by the support of faster and faster wireless services. As one can observe in Fig. 1.1, the widest supported bandwidth has doubled across different amendments of the WLAN standard in order to assure faster data rates.

Despite the recent evolution of the wireless networks, forecasts based on the past observed data indicate that the mobile traffic will keep growing exponentially over the next decade, requiring wider spectrum bandwidths to support faster data rates [Tariq et al., 2020]. In addition to wider bandwidths, clever physical layer designs are expected to modulate more bits per spectrum in order to increase the efficiency of the spectrum resources. In order words, the improvement of data rate and spectral efficiency improvement will increase the volume of data to be processed. Since the computational complexity of communication signal processing algorithms grow on the number of bits, unprecedented spectrum bandwidth brings not only faster data rates but also unprecedented signal processing complexity. This side effect can prevent the achievement of other performance targets pursued by future communication radio devices such as portability and power consumption, since these indicators are direct related to computational complexity [Blume et al., 2002].

The computational complexity resulting from pursuing faster wireless networks can lead to physical layer designs of unfeasible cost-benefit. In face of that, it is consensual in the literature that less complex algorithms need to be devised [Zhao et al., 2019]. Indeed, a search by the term “low complexity” in the IEEE Xplorer digital library reports more than twenty thousand papers in the broad field of communication signal processing. In spite of that, term “low complexity” seems not to be precisely formalized in the literature. A closer look,

for instance, reveals that the term can be employed even for exponential-time algorithms [Siddiq, 2016], [Zheng et al., 2015], [Zhang et al., 2017].

Moreover, because the classic capacity/throughput analysis taught by communication signal textbooks [Proakis and Salehi, 2008] does not consider complexity as a component of throughput, it is hard – not to say impossible – for current mathematical models to calculate the optimal asymptotic balance between complexity and throughput. In other words, it is not possible to calculate the signal processing lower bound complexity required to sustain the maximum asymptotic throughput. Similarly, the lack of a unified model also prevents one to answer whether complexity creates a bottleneck on throughput as the spectrum bandwidth gets arbitrarily large. These questions become more critical as wireless communication standards need to adopt wider bandwidths and more complex algorithms.

In summary, *the central problem of this thesis is that of investigating the mathematical relationship between the computational complexity of communication signal processing algorithms and the throughput of the processed signal.* By addressing that central problem, other related questions can be also formulated and answered, for example,

- What is the minimal asymptotic complexity required to sustain the maximal *spectral efficiency* of a given waveform?
- How the time complexity of a signal processing algorithm does relate to (or affect the) *capacity* of its corresponding communication channel?
- What lower bound asymptotic complexity is required to prevent the nullification of the *throughput* of the signal as it gets arbitrarily large?

1.2 Objectives and Contributions

In this thesis, we argue that the data rate analysis of wireless communication signals should encompass indicators of the computational complexity overhead in order to support the design of faster wireless communication waveforms under minimal computational complexity. In this sense, we propose a mathematical model that considers indicators of computational complexity (such as processing runtime, number of computational instructions and asymptotic lower bound) and indicators of data rate (such as channel throughput, spectral efficiency and capacity). Such a joint model can fill gaps left by current heterogeneous view of the indicators. For example, at times, novel physical layer proposals reach faster throughput at the expensive of complexity. This hinders the conclusion of comparative performance studies of waveforms because the heterogeneous analysis is unable to reflect the impact of complexity on throughput. Thus, a joint model can answer whether an increase in complexity does pay off throughput.

In other cases, standardization bodies and spectrum management protocols focus on a larger spectrum to provide novel wireless communication standards with faster signal throughput. Conversely, wider signals demand higher processing

runtime. From this, a waveform designer may wonder whether the throughput gain implied by spectrum widening suffices to compensate for the processing time overhead as the spectrum gets arbitrarily larger. In summary, the specific goals of this thesis can be described as follows:

Goal 1 – Proposing a mathematical model that enable the joint analysis of indicators of computational complexity and indicators of data rate for wireless communication signal waveforms;

Goal 2 – Proposing a method to calculate the asymptotic lower bound complexity required by a given physical layer waveform in order to sustain the maximum asymptotic throughput as spectrum gets arbitrarily large;

Goal 3 – Demonstrating the application of the proposed model by

Goal 3.1 calculating the minimal computational complexity required by one or more existing physical layer waveforms;

Goal 3.2 re-designing, if necessary, the analyzed physical layer waveforms in order to achieve the optimal balance between complexity and throughput.

As a consequence of meeting the aforementioned goals, this thesis achieved the following contributions:

- **Contribution 1, The Spectro-Computational (SC) Complexity Analysis**
  The SC analysis results from a novel mathematical model that unifies the throughput of signal waveform to the computational complexity of its associated algorithms. After reviewing the related work, we identified such homogeneous model lacks in the literature. The SC analysis is based on the SC throughput $SC(W) = B(W)/T(W)$ of a signal processing algorithm (subsection 3.2.1) which stands for the computational complexity $T(W)$ spent to modulate $B(W)$ bits into a W-Hertz wireless symbol. Based on that, we identify that a signal algorithm is asymptotically scalable if its throughput does not nullify as the spectrum grows, i.e., $\lim_{W\to\infty} SC(W) > 0$. The conditions of scalability for the throughput of algorithms and waveforms are detailed in subsection 3.2.4. The entire SC complexity model is presented in chapter 3;
- **Contribution 2, Novel Definitions Towards a Unified Theory of Waveform Throughput and Computational Complexity**
  By performing an asymptotic analysis on the SC throughput (having W as variable), Section 3.2.1 presents novel definitions homologous to concepts of the theory of computational complexity and information theory, such as SC capacity, SC efficiency and computation-limited signals. We believe these definitions can serve as foundation for a future unified theory of capacity and complexity.
- **Contribution 3, The Optimal Mapper for OFDM with Index Modulation**

In Chapter 4, the SC analysis is employed to drive the design of an optimal mapper for OFDM with Index Modulation (OFDM-IM). Under its ideal mapping setup, OFDM-IM reaches its maximum spectral efficiency (hence, throughput) gain over OFDM. However, such an optimal setup has been conjectured as computationally intractable by the OFDM-IM literature [Lu et al., 2018], [Basar et al., 2017]. We employ the SC model to capture the trade-off between complexity and spectral efficiency and to calculate the minimum complexity under which the OFDM-IM throughput maximizes. The minimal complexity can be achieved by means of look-up tables but subsection 4.5.1 shows that an N-subcarrier OFDM-IM symbol requires an exponential amount of $\Theta(2^N/\sqrt{N})$ entries. Subsection 4.5.1 presents an optimal OFDM-IM mapper setup under polynomial (rather than exponential) storage complexity. However, that polynomial storage is still asymptotic larger than OFDM's. Then, subsection 4.5.2 demonstrates an optimal OFDM-IM mapper running at the same asymptotic time and storage complexities of an OFDM mapper.

- **Contribution 4, Asymptotic Formalization of the Sampling-Complexity Trade-Off**
  This thesis formalizes what we refer to as the sampling-complexity (or Nyquist-Fourier) trade-off, which accounts for the fact that the complexity of batch-oriented signal algorithms (such as FFT) increases as the Nyquist interval decreases (to improve symbol throughput by gathering more samples per symbol in multicarrier waveforms). By considering the time constraint imposed on the sampling theorem, a novel asymptotic complexity lower bound is presented for the frequency-time transform problem and a practical solution is discussed.

- **Contribution 5, Spectro-Computational Analysis of OFDM and Novel Asymptotic Limits for Fourier Transform Algorithms**
  This contribution consists of the SC analysis of the OFDM waveform. We show that the throughput of the asymptotically dominant algorithm of OFDM (i.e., the Fast Fourier Transform FFT algorithm) nullifies on N. We analyze an alternative formulation of frequency-time transform and identified its conditions of scalability as the number of points grow.

1.3 Thesis Outline

The remainder of this thesis is organized in five chapters, as described below.

- **Chapter 2 – General Background and Literature Review**
  Presents the concepts, definitions and basic assumptions of the thesis. The background comes from computational complexity, analysis of algorithms, communication signals and information theory. The chapter also reviews an analyzes the related literature in performance evaluation of signal waveforms. A summary points to the need of a joint model between compu-

tational complexity and indicators of data rate such throughput, spectral efficiency and capacity;

- **Chapter 3 – The Spectro-Computational Complexity Model**
  Introduces the novel definitions and methodology for the joint model of computational complexity and indicators of data rate of signals waveforms. A step-by-step illustrative analysis is performed on the basic OFDM waveform;
- **Chapter 4 – Optimal Mapper for OFDM with Index Modulation**
  Studies the problem of enabling the ideal mapping setup of the OFDM-IM waveform in order to maximize spectral efficiency gain over OFDM. Reviews the literature showing that OFDM-IM mappers are restricted to compromise approaches that either sacrifices spectral efficiency or computational complexity. Employs the SC model to calculate the minimum complexity under which the spectral efficiency maximizes and presents two designs of optimal mappers;
- **Chapter 5 – Is FFT Fast Enough for Beyond 5G Communications?**
  Reports a detailed joint study of capacity and complexity for the OFDM waveform under arbitrarily large signals. Demonstrates that the throughput scalability of the basic OFDM waveform requires a lower bound complexity of $\Omega(N)$ to the N-point Fourier transform problem, which remains an open question in computer science. This implies that the FFT algorithm prevents the scalability of the OFDM throughput as N grows. Presents an alternative and scalable Fourier transform solution for OFDM in its vectorized form.
- **Chapter 6 – Conclusion and Future Work**
  Presents the conclusions of this thesis, as well as the research directions for future work.

Chapter 2

General Background and Literature Review

"A journey of a thousand miles begins with a single step."

(Lao Tzu)

Contents

THIS chapter introduces the theoretical background and the related literature of the mathematical model proposed in this thesis. The chapter is organized as follows.

Section 2.1 presents the reference radio architecture and the information theory performance indicators referred to along this thesis. Section 2.2 reviews the main concepts and terminologies of computational complexity employed in the mathematical model introduced in this work. Section 2.3 reviews and analyzes the literature in performance evaluation of communication signal algorithms and waveforms. Finally, section 2.4 summarizes the chapter.

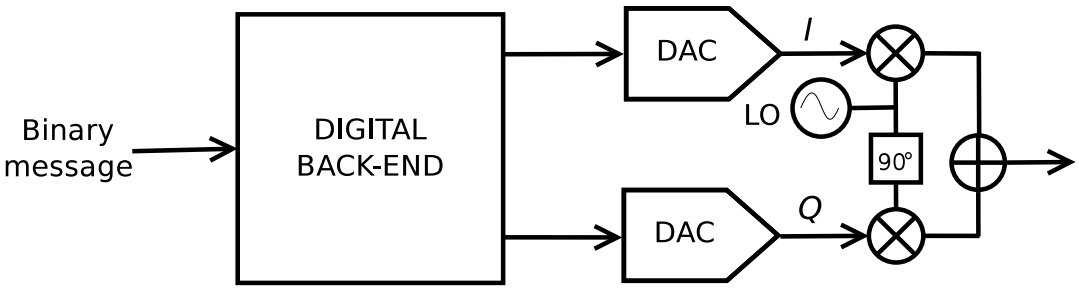

Figure 2.1: Basic In-Phase/Quadrature (I/Q) radio architecture model.

2.1 System and Terminology

In this section, we review the basic terminology, notation and definitions that comes from communication signal and the information theory fields. In subsection 2.1.1, we present the reference radio architecture model for the work. In subsection 2.1.2, we review the OFDM waveform that constitutes the base for the multicarrier waveforms studied in the remainder of this work. In subsection 2.1.3, we review information theory performance indicators for communication signals such as capacity, throughput and spectral efficiency.

2.1.1 Radio Architecture Model

Nowadays wireless telecommunication signal waveforms such as Wi-Fi and cellular networks are based on the basic In-phase/Quadrature (IQ) radio architecture illustrated in Fig. 2.1. This architecture has also been considered for future wireless communication standards [Huang et al., 2019], [Madanayake et al., 2020a]. Next, we overview this architecture for multicarrier signals studied throughout this work.

At the IQ transmitter, the radio reads a sequence of data bits from the upper layers of the network stack. The bits undergo several computations by a sequence of communication signal algorithms that forms the so-called digital back-end of the radio. The radio back-end can be defined either by software – through General Purpose Processors (GPP) or Field Programmable Gate Array (FPGA) – or hardware through, for instance, Application-Specific Integrated Circuits (ASICs).

The outcome of the radio back-end is the digital time domain baseband signal, i.e., a sequence of complex numbers whose real and imaginary parts are labeled as in-phase (I) and quadrature (Q), respectively. Each of these components goes through a particular Digital-to-Analog Converter (DAC) to be translated to the analog domain aiming to modulate the carrier frequency. The modulation consists in multiplying the I and Q components of the baseband signal to the cosine and sine waves generated from the Local Oscillator (LO), respectively.

The LO generates a carrier frequency f_c Hz of a real-valued magnitude $\cos(2\pi f_c t)$ at each time instant t seconds. This carrier is meant to be the real part of the

Figure 2.2: Basic waveform of OFDM transmitter that can implement the digital back-end of the radio architecture shown in Fig. 2.1).

final complex RF signal and is modulated by the in-phase component of the analog baseband signal. Another copy of the carrier produced by the LO is shifted by 90° degrees, yielding a signal of magnitude $\sin(2\pi f_c t)$ that is modulated by the component Q of the baseband signal and is added to the in-phase part of the waveform. The magnitude of the final complex-valued RF signal $s(t)$ is, therefore,

$$s(t) \quad = \quad I\cos(2\pi f_c t) + Qj\sin(2\pi f_c t) \tag{2.1}$$

The resulting shape of the modulated signal waveform and number of bits it carries depend on the logic implemented in the digital back-end. For this reason, the sequence of communication signal algorithms of the radio's back-end are popularly referred to as "waveform" in comparative studies of future standards e.g. [Doré et al., 2017]. We adopt this terminology throughout this work.

At the receiver, homologous reverse steps are performed to recover the digital baseband signal from the analog carrier. Particularly, two Analog-to-Digital Converters (ADCs) sample the complex W-Hz analog signal at a sample rate f_s and an inter-sample time interval T_{NYQ} according to the so-called Shannon-Nyquist sampling theorem [Nyquist, 1928], [Shannon, 1949]. Considering the double DAC/ADC architecture, these quantities are such that

$$f_s \quad \geq \quad W \quad \text{samples/second} \tag{2.2}$$

$$T_{NYQ} \quad = \quad 1/f_s \quad \text{seconds} \tag{2.3}$$

For comprehensive explanation about the IQ radio architecture, please refer to classic textbooks in the field such as [Proakis and Salehi, 2008], [Luzzatto and Shirazi, 2016].

2.1.2 OFDM Waveform

The basic digital back-end of an OFDM radio is illustrated in Fig. 2.2. It is an example of waveform that fills the digital back-end of Fig. 2.1. Because of its cost-benefit between computational/transceiver complexity and throughput performance, OFDM is not only the dominant waveform of nowadays wireless network standards but it has also been considered as reference for future standards [Zaidi et al., 2016].

The sequence of communication signal algorithms of the basic OFDM waveform transmitter are Mapper, Inverse Discrete Fourier Transform (IDFT) and Cyclic

Prefix (CP) insertion. The OFDM mapper maps bits into complex symbols taken from a M-point constellation diagram. The "translation" task of the mapper is usually performed in parallel but some particular implementations can be serialized. This is the case of software-defined radio implementations in which the number of available processors is usually less than the number of subcarriers to map. Each complex point mapped to a subcarrier represents a sequence of $\log_2 M$ bits ($M = 2^p$, $p > 0$) and the number of bits in the N-subcarrier OFDM symbol is

$$B_{OFDM} = N \log_2 M \quad \text{bits} \tag{2.4}$$

The Table 2.1 exemplifies the bit-to-point correspondence of the Quadrature Phase Shift Keying (QPSK) constellation diagram that is adopted by the IEEE 802.11 standard [802.11, 2013].

The IDFT algorithm translates the discrete OFDM symbol from frequency domain to time domain. Denoting $i = \sqrt{-1}$ and $e = \lim_{x\to\infty}(1 + 1/x)^x = 2.718281\ldots$, IDFT computes N time domain samples Y_t ($t = 0, 1, \cdots, N-1$) from N frequency domain samples X_k ($k = 0, 1, \cdots, N-1$) as follows

$$Y_t = \sum_{k=0}^{N-1} X_k e^{j2\pi kt/N} \quad t = 0, 1, \cdots, N-1 \tag{2.5}$$

At the receiver, a DFT algorithm takes the signal back from time to the frequency domain by performing

$$X_k = \sum_{t=0}^{N-1} Y_t e^{-j2\pi kt/N} \quad k = 0, 1, \cdots, N-1. \tag{2.6}$$

To avoid that a symbol overlaps with delayed copies of prior transmitted symbols – which lasts distinct periods by traveling over the different paths of the multipath propagation effect – OFDM introduces a guard time at the beginning of each time domain symbol that consists of its last N_{cp} samples. Considering that T_{SYM} time domain samples are produced by IDFT, the overall duration T_{OFDM} of the OFDM symbol enlarges by T_{cp} seconds as follows [Viswanathan and Mathuranathan, 2018],

$$T_{OFDM} = T_{SYM} + T_{cp} \quad \text{seconds} \tag{2.7}$$

$$T_{cp} = N_{cp} T_{SYM}/N \quad \text{seconds} \tag{2.8}$$

At the OFDM receiver, the signal is processed in the inverse sequence of the transmitter for homologous algorithms, namely, CP remover and DFT and demapper. The demapping task is assisted by a detection algorithm to compute the most likely bit sequence from each received frequency domain noisy symbol.

Table 2.1: Bit-to-point correspondence of IEEE 802.11 QPSK constellation diagram.

Transmission Bits	I	Q
00	-1	-1
01	-1	$+1$
10	$+1$	-1
11	$+1$	$+1$

2.1.3 Information Theory Performance Indicators

The throughput achieved by a given B-bit T_{SYM}-seconds symbol waveform proposal is determined from the symbol data rate R in bits per seconds (bps), which is

$$R = B/T_{SYM} \quad \text{bits/seconds} \tag{2.9}$$

The channel capacity C is the maximum error-free transmission rate achieved by a communication channel [Shannon, 1948] which is also known as the Shannon-limit. That work is among the founding pillars the information theory research field. Under a Signal-to-Noise Ratio (SNR) of SNR (unitless), the capacity of a W Hertz (Hz) channel disturbed by additive white Gaussian noise (AWGN) is given by

$$C = W \log_2(1 + SNR) \quad \text{bits/seconds} \tag{2.10}$$

Assuming an average received power of $\mathcal{P}$ and a noise power density of $\mathcal{N}_0$ in the spectrum bandwidth W, the SNR is given by

$$SNR = \frac{\mathcal{P}}{W\mathcal{N}_0} \tag{2.11}$$

When SNR is much larger than zero ($SNR \ggg 0$ dB) in Eq. 2.10, the channel follows the so-called bandwidth-limited regime (a.k.a. band-limited) in which the capacity grows approximately linearly on the bandwidth. Indeed, spectrum widening has been commonly adopted to enable faster wireless communication standards over the past few years [802.11, 2013], [IEEE 802.11, 2012]. Moreover, spectrum management techniques have been exploited as well e.g. cognitive radios [Akyildiz et al., 2006].

To enable the desired linear performance of band-limited regime in future extremely wide bandwidth waveforms, the SNR must be kept sufficiently large as W grows. This means that the received power $\mathcal{P}$ must improve to compensate the overall resulting noise $W\mathcal{N}_0$ and to assure at least a constant SNR as $W \to \infty$. Towards that, novel techniques such as massive Multiple Input, Multiple Output (MIMO) [Maruta and Falcone, 2020], adaptive power control [Chiang et al., 2008] and multiuser MIMO [Liao et al., 2016] have been envisioned to

provide the SNR implied by the band-limit regime. Hence, for a real constant $k \geq 1$, it is assumed that

$$\lim_{W \to \infty} \log_2 \left(1 + \frac{\mathcal{P}}{W\mathcal{N}_0}\right) \quad = \quad k \geq 1, \tag{2.12}$$

from which,

$$C \quad = \quad Wk \tag{2.13}$$

By contrast, under $SNR \lll 0$ dB, capacity becomes insensitive to bandwidth leading to the so-called the power-limited regime. We assume the band-limited regime in the remainder of this work unless differently mentioned.

The division of R by the amount W Hz of spectrum consumed by the symbol, one gets the spectral efficiency of the waveform – a.k.a. bandwidth efficiency or spectral bit rate – which is

$$S \quad = \quad R/W \quad \text{bits/seconds/Hz} \tag{2.14}$$

In OFDM and its variants, the subcarrier orthogonality imposes

$$\Delta f \quad = \quad 1/T_{SYM} \quad \text{Hz}, \tag{2.15}$$

which yields a bandwidth of

$$W_{OFDM} \quad = \quad N\Delta f \tag{2.16}$$

$$= \quad N/T_{SYM} \quad \text{Hz} \tag{2.17}$$

Under a sampling rate $f_s = W$ samples per second, and considering Eq. 2.17, the Eq. 2.3 for OFDM rewrites as

$$T_{NYQ} \quad = \quad 1/W \quad \text{seconds}, \tag{2.18}$$

which results in an overall OFDM symbol duration of

$$T_{SYM} \quad = \quad NT_{NYQ} \quad \text{seconds} \tag{2.19}$$

Considering the number of bits per symbol (Eq. 2.4), the respective data rate R_{OFDM} and spectral efficiency S_{OFDM} of an N-subcarrier OFDM symbol modulated by an M-ary constellation diagram can be written as [Basar et al., 2013],

$$R_{OFDM} \quad = \quad B_{OFDM}/T_{OFDM} \quad \text{bits/seconds} \tag{2.20}$$

$$S_{OFDM} \quad = \quad B_{OFDM}/(N + N_{cp}) \quad \text{bits/seconds/Hz} \tag{2.21}$$

2.2 Computational Complexity

In this section, we present the main notations and definitions related to the asymptotic analysis of algorithms. These definitions will support the development of the spectro-computational complexity analysis of algorithms we propose throughout this thesis.

2.2.1 Asymptotic Analysis

The asymptotic notation due to [Landau, 1909], [Bachmann, 1894] enables one to compare the order of growth of two given functions $f(N)$ and $g(N)$. In the analysis of algorithms, these functions capture the "complexity" of a given algorithm meaning that they quantify the amount of consumed computational resources upon an input of length N. Common resources are storage or number of computational instructions, usually referred to as "space" and "time" complexities, respectively. These measures are taken based on a given computational model. In this work, we assume the classic Random-Access Machine (RAM) model which is shown to be equivalent to the universal Turing machine [Cook and Reckhow, 1972].

The RAM model focus on counting the amount of basic computational instructions (e.g., data reading, data writing, basic arithmetic, data comparison) regardless of the technology of the underlying computational apparatus. For example, based on the RAM model, one verifies that a classic N-subcarrier BPSK-modulated OFDM mapper needs to map N bits into N real numbers. Thus, the overall time computational resources of any implementation requires N computational instructions, be them implemented sequentially on a software-defined radio or in parallel on a dedicate circuit.

The asymptotic analysis of algorithms concerns about classifying the order of growth of the complexity functions. Thus, the analysis considers $N \to \infty$ rather than specific values of N. Besides, it is assumed non-negative increasing functions whose limits $\lim_{N\to\infty} f(N)/g(N)$ and $\lim_{N\to\infty} g(N)/f(N)$ do exist.

The main asymptotic notations to describe and compare the performance of algorithms are big O ($O(g(N))$), big omega ($\Omega(g(N))$), big theta ($\Theta(g(N))$), little o ($o(g(N))$) and little omega ($\omega(g(N))$). These notations are sets of functions that satisfy a property related to the order of growth $g(N)$ given in the parenthesis of the notation. As usual, we adopt the popular version of the notation in which the symbol "$\in$" is replaced by the symbol "$=$". For example, in $f(N) = O(g(N))$, $f(N)$ belongs to the set $O(g(N))$ because it satisfies a property related to the order of growth of $g(N)$. In particular,

$$\begin{aligned} f(N) &= O(g(N)) \Leftrightarrow \\ O(g(N)) &= \{f(N) | \exists c_0 > 0, N_0 > 0 | f(N) \leq c_0 g(N), \forall N \geq N_0\} \end{aligned} \quad (2.22)$$

The property of the set 2.22 states that $f(N)$ is asymptotic equal or less than

$g(N)$. Informally, this means that it is possible to find out a curve with the same order of growth of $g(N)$ (i.e. $c_0 g(N)$) that remains larger than $f(N)$ from the constant N_0 on the abscissa axis. This rationale applies inversely to the big omega notation, meaning that

$$\begin{aligned} f(N) &= \Omega(g(N)) \Leftrightarrow \\ \Omega(g(N)) &= \{f(N) | \exists c_0 > 0, N_0 > 0 | f(N) \geq c_0 g(N), \forall N \geq N_0\}, \end{aligned} \quad (2.23)$$

and

$$f(N) = O(g(N)) \quad \Leftrightarrow \quad g(N) = \Omega(f(N)) \quad (2.24)$$

Assuming that $f(N)$ and $g(N)$ are monotonically increasing functions and that the limits below do exist, both big O and big Omega notations can be intuitively expressed as follows [Cormen et al., 2009]

$$\begin{aligned} f(N) &= O(g(N)) \Leftrightarrow \\ & \quad O(g(N)) = \{f(N) | \lim_{N \to \infty} f(N)/g(N) > 0\} \quad (2.25) \\ f(N) &= \Omega(g(N)) \Leftrightarrow \\ & \quad \Omega(g(N)) = \{f(N) | \lim_{N \to \infty} g(N)/f(N) > 0\} \quad (2.26) \end{aligned}$$

In the case of $f(N) = o(g(N))$ notation, the property demands that all non-negative increasing functions with the same order of growth of $g(N)$ must be larger than $f(N)$ from their respective constant N_0 on the abscissa axis. This means that the order of growth of $f(N)$ is strictly less than $g(N)$ and can be formalized as

$$\begin{aligned} f(N) &= o(g(N)) \Leftrightarrow \\ o(g(N)) &= \{f(N) | \forall c_0 > 0, \exists N_0 > 0 | f(N) < c_0 g(N), \forall N \geq N_0\} \end{aligned} \quad (2.27)$$

Demonstrating the inequality $f(N) < c_0 g(N)$ for all possible functions with the same order of growth of $g(N)$ may be cumbersome. An alternative way to prove the property of Eq.[1] 2.27 consists in solving the limit $\lim_{N \to \infty} f(N)/g(N)$ (assuming it does exist). In particular,

$$f(N) = o(g(N)) \quad \Leftrightarrow \quad \lim_{N \to \infty} f(N)/g(N) = 0 \quad (2.28)$$

This rationale applies inversely to the little omega notation, meaning that

$$\begin{aligned} f(N) &= \omega(g(N)) \Leftrightarrow \\ \omega(g(N)) &= \{f(N) | \forall c_0 > 0, \exists N_0 > 0 | f(N) > c_0 g(N), \forall N \geq N_0\}, \end{aligned} \quad (2.29)$$

[1] The signal '=' means '$\in$' in asymptotic notation. Thus, the term "Equation" is abuse of term.

Table 2.2: Asymptotic notations: c_0, c_1, N_0 and k are non-negative constants and $f(N)$ and $g(N)$ non-negative increasing functions.

Notation	Property	Description
$f(N) = o(g(N))$	$\lim_{N\to\infty} f(N)/g(N) = 0$	Order of growth of $f(N)$ less than $g(N)$
$f(N) = \omega(g(N))$	$\lim_{N\to\infty} f(N)/g(N) = \infty$	Order of growth of $f(N)$ larger than $g(N)$
$f(N) = O(g(N))$	$\{f(N) \leq c_0 g(N)\ \forall N_0 \geq N\}$	Order of growth of $f(N)$ less than or equal to $g(N)$
$f(N) = \Omega(g(N))$	$\{f(N) \geq c_0 g(N)\ \forall N_0 \geq N\}$	Order of growth of $f(N)$ larger than or equal to $g(N)$
$f(N) = \Theta(g(N))$	$\{c_0 g(N) \geq f(N) \geq c_1 g(N)$ $\forall N_0 \geq N\}$ or $\lim_{N\to\infty} f(N)/g(N) = k$	Order of growth of $f(N)$ equal to $g(N)$

and

$$f(N) = \omega(g(N)) \quad \Leftrightarrow \quad \lim_{N\to\infty} f(N)/g(N) = \infty \tag{2.30}$$

$$f(N) = o(g(N)) \quad \Leftrightarrow \quad g(N) = \omega(f(N)) \tag{2.31}$$

The big theta notation relates functions of the same order of growth. This can be formalized as

$$f(N) = \Theta(g(N)) \quad \Leftrightarrow \quad f(N) = O(g(N)) \wedge f(N) = \Omega(g(N)) \tag{2.32}$$

Considering c as a non-negative constant, the property of the big theta notation can be alternatively written as

$$f(N) = \Theta(g(N)) \quad \Leftrightarrow \quad \lim_{N\to\infty} f(N)/g(N) = c > 0 \tag{2.33}$$

Other useful properties of asymptotic notations are given below considering c as a non-negative constant. In Table 2.2, we summarize the properties and description of the main asymptotic notations.

$$c \cdot O(f(N)) = O(f(N)) \tag{2.34}$$

$$f(N) \pm g(N) = \Theta(\max\{f(N), g(N)\}), \tag{2.35}$$

$\max\{\cdots\}$ gives the largest order of growth among the listed functions.

$$g(N) \cdot f(N) = O(f(N) \cdot g(N)) \tag{2.36}$$

$$\tag{2.37}$$

2.2.2 Useful Definitions

The asymptotic notation is employed in the analysis of algorithms to formalize some basic definitions related to computational complexity such as "optimal algorithm", "complexity lower bound", "tractable algorithm" and "intractable algorithm". These definitions are formalized having computational complexity as the unique performance indicator of the analysis. For the class of communication signal processing algorithms considered in this work, indicators of communication performance such as signal capacity, throughput and spectral efficiency are also as relevant as the signal processing complexity. However, these performance indicators are not considered in the classic asymptotic definitions of the analysis algorithms. To support the specialization of these definitions throughout this thesis proposal, in this subsection we review some key definitions of asymptotic complexity.

Based on the properties of asymptotic notation, one verifies that the asymptotic complexity of a procedure consisted of a sequence of subroutines – as is the case of sequence of DSP algorithms that compose a waveform – is big theta of the most complex subroutine. Such routine is named the *asymptotic dominant algorithm* of the entire routine. Formally, if G subroutines have complexities $T_1(N), \cdots, T_G(N)$, respectively, and $T_i(N)$ $(0 \leq i \leq N)$ is the complexity of the asymptotic dominant algorithm, then the overall asymptotic complexity $T(N)$ is

$$\begin{aligned} T(N) &= T_1(N) + \cdots + T_G(N) \\ &= \Theta(\max\{T_1(N), \cdots, T_G(N)\}) \\ T(N) &= \Theta(T_i(N)) \end{aligned} \tag{2.38}$$

The *asymptotic lower bound* of a computational problem corresponds to the order of growth of the fastest *possible* algorithm for the problem and can be described with the notation Ω. It is the intrinsic minimum complexity holding not only for existing algorithms but also for the ones to be devised. For this reason, a precise lower bound may be hard to identify. In these cases, loose lower bounds can serve as reference by considering that at least N computational instructions are needed to read an N-size input yielding a lower bound of $\Omega(N)$[2].

In other cases, the lower bound of a computational problem can demand a number of instructions that is asymptotic larger than the length of the input. For example, the problem of sorting an N-size array by means of comparisons has a lower bound of $\Omega(N \log_2 N)$ [Cormen et al., 2009]. By contrast, the lower bounds for other problems still remain open in the literature, leading to some conjectures. For example, the "Fast Fourier Transform" (FFT) algorithm popularly assigned to [Cooley and Tukey, 1965][3] remains the fastest procedure to handle

[2]Not all problems demand a minimum of N instructions to read the input. For instance, the problem of finding a key in a given N-node self-balanced tree demands no more than $O(\log_2(N))$ steps.

[3]The current oldest reference to the FFT method is due to Carl F. Gauss [Heideman et al., 1985]. The work due to [Cooley and Tukey, 1965] is recognized as an independent redis-

the Discrete Fourier Transform (DFT)[4] since 1965. This leads some to conjecture that the lower bound of the problem is $\Omega(N \log_2 N)$ [Ailon, 2015].

For other problems, the lower bounds are proved to be exponential (usually denoted as $\Omega(2^N)$ for an N-length input problem). In this case, the problem is defined as *intractable* whereas problems that can be decided under polynomial complexity are classified as *tractable* [Cormen et al., 2009].

In the field of communication signal processing, optimal signal detectors are typical example of computationally intractable problems. This stems from the fact that some optimal detector formulations e.g, [Basar et al., 2012] must compute a maximum likelihood metric between the received signal and each possible signal modulation shape of the system. Since the search space grows exponentially on the spectral bandwidth in those systems, no polynomial algorithm can meet the formal definition of such optimal detection. These situations are usually overcome by means of *heuristics*, that slightly relax optimality on behalf of complexity. In the case of communication signal detectors, several near-optimal polynomial time heuristics have been proposed [Guerreiro et al., 2013], [Ochiai, 2003].

An *asymptotically optimal algorithm* is such that its worst-case computational complexity runs as fast as the lower bound verified for its corresponding computational problem. Note that, in theory, this definition also encompasses intractable problems. However, in practice, the terminology is usually employed only for tractable algorithms. The definition of optimal algorithm considered in this thesis refers to algorithms of tractable problems unless otherwise stated.

2.3 Related Work

In this section, we review the literature on signal communication performance indicators. In subsection 2.3.1, we report some research efforts towards the joint analysis of distinct communication signal processing performance indicators. In subsections 2.3.2 and 2.3.3, we summarize the literature and identify the need for a unified model between computational complexity and indicators of capacity (such as throughput and spectral efficiency), respectively.

2.3.1 Hybrid Signal Performance Indicators

The design of a novel waveform is a complex task that targets several distinct performance indicators. An ideal waveform would score best in all of them. However, in practice, the performance ranking among distinct waveforms varies depending on the assessed indicator. In this context, some research efforts propose analytical methodologies that relate distinct performance indicators through a

covery of that work.

[4]Assuming that the length of the input is a power of two.

single mathematical model. These joint analyses are specially useful to calculate the ideal balance between performance indicators that face a trade-off.

We find out that unified proposals of computational complexity and indicators of communication speed such as capacity, throughput, and spectral efficiency are scarce in the literature. By contrast, the relevance of unified models can be verified through other signal waveform performance indicators. Next, we review and summarize some of these proposals and discuss the need for a joint capacity-complexity model.

2.3.1.1 Fundamental Information Theory Metrics and Derivations

In his classic work that originated the information theory, [Shannon, 1948] establishes the relationship between the bandwidth W of a continuous-time analog Gaussian channel and its maximum capacity in bits per seconds. This imposes a theoretical upper bound for the capacity $C(W)$ bps of a communication signal. For the family of N-subcarrier signals considered throughout this work, the intercarrier space Δf Hz is usually a fixed configuration parameter whereas N varies depending on the channel conditions. Thus, the signal capacity $C(W)$ can be conveniently described as function of N rather than W.

[Nyquist, 1928] identified the foundations for the so-called sampling theorem[5], which relates the bandwidth of a signal to its minimum required sampling rate that ensures a sufficiently precise translation between the analog and digital versions of the signal. According to [Luke, 1999], the fundamental work of [Shannon, 1949] brought the sampling theorem to the broad attention of communication engineers.

Ever since, several other works build upon the works of Shannon and Nyquist. In [Chen et al., 2013], [Chen et al., 2014], for example, authors concern about the maximum achievable analog channel capacity under different sub-Nyquist sampling regimes for constant frequencies with perfect known information. In [Chen et al., 2017], the authors study the relationship between maximum capacity and sub-Nyquist rates for scenarios where the active range of frequencies is not known in advance e.g. cognitive radios.

2.3.1.2 Spatial Area, Energy Efficiency and Deployment Metrics

In [Alouini and Goldsmith, 1999] and [Alouini and Goldsmith, 1997], authors identify a trade-off between channel reuse efficiency – which measures the ability of a cellular system to use the same frequency at spatially separated locations – and link quality per user. Because neighboring base stations may partially overlap coverage area, mobile devices might experience distinct maximum data

[5]The foundations for the sampling theorem was independently reported by several distinct researchers. Throughout this work, we adopt the widely known label "Nyquist sampling theorem". Please, refer to the entry "Nyquist–Shannon sampling theorem " of Wikipedia [Wikipedia, 2020] for a historic overview.

rates depending on their location in the cell, thereby there is a relationship between maximum spectral efficiency and area of coverage. Thus, the authors define the Area Spectral Efficiency (ASE) (in bits/Hertz/meters) as the sum of the maximum average data rates per unit bandwidth per unit area supported by a cell's base station.

ASE is further enhanced to account trade-offs with other performance indicators such as energy efficiency [Lanhua et al., 2017] and delay sensitive networks [Makki et al., 2017]. [Richter et al., 2009] introduce the notion of area power consumption which is given in Watts per square kilometer. The metric is defined as the ratio between the average transmission power consumed in a cell and the corresponding average cell area measured.

[Chen et al., 2011] focus on unifying the study of performance indicators for green networks considering mainly transmission power (Watts) and energy efficiency (bits/Joule). They propose a joint trade-off analysis between the following pairs of metrics: deployment efficiency vs. energy efficiency, spectral efficiency vs. energy efficiency, bandwidth capacity vs. power consumption, and delay vs. power consumption.

Some studies specialize the joint spectral and energy efficiency analyses for particular scenarios of Multiple Input and Multiple Output (MIMO) systems. This is the case of [Salh et al., 2019], [Hei et al., 2019], [Mukherjee and Mohammed, 2015], and [Heliot et al., 2012] for downlink MIMO, massive MIMO, power-constrained MIMO and Rayleigh MIMO channels, respectively.

2.3.1.3 Computational Complexity and Power Consumption

The complexity of an algorithm measures its performance regarding a given metric such as the number of computational instructions, runtime or storage (a.k.a "space"). According to [Fortnow and Homer, 2003], the main definitions for the formal expression of the complexity of algorithms are due to [Hartmanis and Stearns, 1965]. The analysis of an algorithm is the process through which its complexity is obtained. The introduction of the term "analysis of algorithms" is popularly assigned to Donald Knuth that mentions it the 1968's edition of [Knuth, 1997].

Studies concerning computational complexity and energy consumption consider either Very Large-Scale Integration (VLSI) circuits or software implementations that correspond to low and high level implementations of an algorithm, respectively.

[Jain et al., 2005] started the discussion towards an energy complexity model for algorithms inspired by the classic asymptotic analysis of algorithms. The authors present an enhanced version of the Turing machine to account the energy cost to switch between different units of the processor. The proposed machine parameterizes the amount of computation, communication and memory of an algorithm – as well as the trade-offs among them – to measure the energy consumption. The authors also present a case study demonstrating the trade-off

between energy and space memory in the FFT algorithm.

2.3.1.4 Other Studies

Other studies somehow merge communication and complexity aspects but without capturing the asymptotic growth of complexity and throughput of a waveform.

[Thompson, 1979] relate the asymptotic complexity of Discrete Fourier Transform (DFT) algorithms to the asymptotic silicon area required to deploy them on a chip. In [Thompson, 1980], the analysis is applied to derive the asymptotic bounds of other kind of algorithmic problems, such as sorting.

Some theoretical proposals employ the term "complexity" to study aspects of communication other than the amount of consumed computational resources, as is the case of this thesis. This is the case of the communication complexity theory and the Kolmogorov complexity. The communication complexity [Rao and Yehudayoff, 2020] concerns about the minimum number of message exchanges to solve a problem whose input parameters are distributed among entities of a network. Thus, although that theory concerns about communication, the term "complexity" stands for the *number of messages* transmitted in the network.

In turn, the algorithmic information theory [Chaitin, 1987], [Kolmogorov, 1998], [Solomonoff, 1960], also known as Kolmogorov complexity, relates the Shannon's information theory to the Turing's computational model aiming to identify the irreducible form of an information, i.e., the shortest computer program that produces the information. In this case, the term "complexity" stands for the *shortest length of a string* that represents the information. The string can be either the transmission information or the algorithmic source code of a computer program that generates the information. For example, assuming a computer model in which the string "x^y" returns the result of the real number "x" raised to the real number power "y", the 4-length algorithmic string "10^6" shortens the 7-length string representation "1000000" of the decimal number 'one million'.

Therefore, nor the communication complexity theory nor the Kolmogorov complexity concern about the relation between the communication signal throughput and the computational complexity required to process the signal.

2.3.2 Summary of Literature

We categorize the performance analysis metrics of waveforms into two broad categories that we refer to as Channel Performance Indicators (CPIs) and Device Performance Indicators (DPIs), respectively. The choice for this categorization approach reflects the performance indicators we concern throughout this thesis. More precisely, CPIs refer to the performance metrics assessed from or related

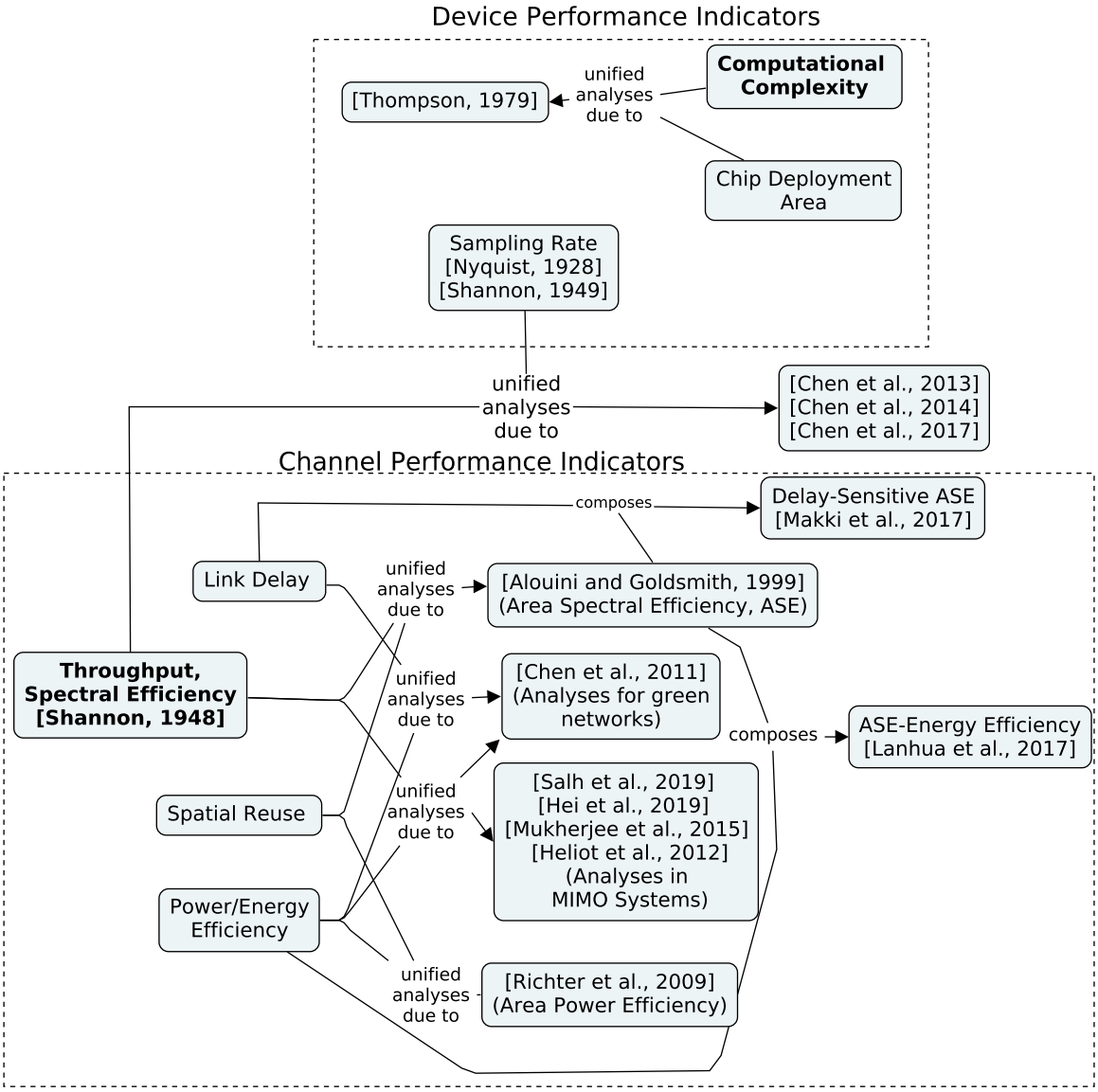

Figure 2.3: Map of research efforts towards joint analysis of distinct signal performance indicators.

to the communication channel. Metrics of this category are link delay, spatial reuse, signal strength and indicators of capacity such as throughput and spectral efficiency. In turn, DPI refer to performance indicators assessed at the communication device. The main metrics of this category are computational complexity and sampling rate which also directly affect the power consumption of the device.

In Fig. 2.3, we present a conceptual map illustrating how the performance analysis proposals derive from CPI and DPI metrics. We dispose DPI and CPI metrics on the left- and right-hand sides of the map, respectively, and the joint performance analysis proposals based on both categories in-between. Such graphical disposal highlights that few works of the reviewed literature concern about a joint analytical model between CPI and DPI metrics. For example, we identified that only [Chen et al., 2013], [Chen et al., 2014], [Chen et al., 2017]

concern about the joint analysis of two performance indicators of distinct categories, namely, sampling rate from DPI and capacity from CPI. In particular, we find no unified model embracing the indicators of performance considered in this thesis, namely, computational complexity and indicators of capacity such as spectral efficiency and throughput.

2.3.3 Why a Joint Throughput-Complexity Model?

The fact that few progress has been achieved towards a model that supports the joint throughput-complexity analysis can also be verified by looking at recent comparative studies about the performance of different waveform proposals.

The expectation for massive channel bandwidths in future millimeter waves and Terahertz wireless networks aims to unleash unprecedented data rates. As a side effect, the augmented complexity required to process extremely wide signals leads to a capacity-complexity trade-off that has gained increasing attention in the communication signal processing literature.

[Letaief et al., 2019], for instance, argue that the scenario of mmWave wireless networks will "significantly affect the transceiver architecture and algorithm design" of future waveforms. The authors argue that the hardware changes required to achieve Terabytes per second data rates will affect the design of signal processing techniques.

[Zaidi et al., 2016] remark that computational complexity imposes a major challenge for small form-factor mobile base stations, in which the energy and computational constraints limit the computational complexity budget for the digital back-end. Thus, complexity should be considered a cost-effective metric in the implementation of waveforms modulated in digital domain.

[Rappaport et al., 2019] argue that the power consumption induced by the processing overheads of future massive channel bandwidth may lead the classic Fast Fourier Transform (FFT) algorithm to be replaced by approximate FFT (AFFT) variants, in which the fidelity of the frequency/time conversion is penalized – causing the impairment of Signal-to-Noise Ratio (SNR) – to save computations. In a sense, this argument envisions scenarios in which computational complexity becomes more relevant than other classic waveform design performance indicators such as Bit Error Rate (BER). [Xiao et al., 2017] opine that "fully digital mmWave MIMO implementations are currently infeasible from a cost-efficiency perspective". They argue that signal processing techniques must be redesigned to enable good trade-off between the spectral efficiency and energy consumption/hardware cost.

Despite the intrinsic connection between capacity and computational complexity for communication signal waveforms, both indicators have been considered aside from each other by current studies [Gerzaguet et al., 2017], [Doré et al., 2017], [Zaidi et al., 2016]. This may reflect the fact that these performance indicators come from heterogeneous fields of knowledge. Besides, with the release

of extremely wide bandwidths, the joint capacity-complexity waveform comparison need to be performed asymptotically on the spectrum. In other words, *comparisons need also to be performed under the assumption of arbitrarily large spectrum rather than on particular limited values of spectrum.*

2.4 Summary

In this chapter, we presented the background and related literature of this thesis. We reviewed the IQ radio architecture model and classic concepts based on which we derive the analytical model proposed and applied throughout this work. From the field of communication signal processing, we reviewed the concepts of symbol throughput, spectral efficiency, channel capacity, signal sampling and band- and power-limited signal regimes. In turn, from the field of computational complexity, we reviewed concepts of computational complexity lower bound, asymptotic optimal algorithm, tractable and intractable algorithms. We also reviewed the basic OFDM waveform to exemplify the analytical model proposed in this thesis. Moreover, the joint throughput-complexity optimizations proposed in chapters 4 and 5 are for variants of OFDM. Besides, we also analyzed the literature in performance evaluation of communication signal waveforms to motivate the need for a joint capacity-complexity model.

Chapter 3

The Spectro-Computational Complexity Analysis

"You can't connect the dots looking forward; you can only connect them looking backwards."

(Steve Jobs)

Contents

This chapter builds on [Queiroz et al., 2019] and [Queiroz et al., 2020] to introduce a mathematical model for the Spectro-Computational complexity (SC) analysis of communication signal algorithms and waveforms. The model considers indicators of performance from the theory of computational complexity (such as number of computational instruction, processing runtime and lower bound complexity) along with indicators of performance from the theory of information such as capacity, throughput and spectral efficiency. Based on that, the model

can capture the intrinsic relation between both classes of indicators thereby enabling one to identify whether the impairment of time complexity does pay off for the improvement of throughput as the signal spectrum gets arbitrarily large. Moreover, the model enables one to calculate the minimum computational complexity required to achieve maximal asymptotic throughput for a given waveform design.

The chapter is organized as follows. Section 3.1 and Section 3.2 present a rationale and the formalization of the SC analysis, respectively. Section 3.3 explain how the presented definitions relate and derive from the definitions of computational complexity and information theory. Section 3.4 presents a step-by-step SC analysis of the basic OFDM waveform and Section 3.5 summarizes the chapter.

3.1 Rationale of the Proposal

Typical communication signal performance indicators such as symbol throughput and capacity capture the number of transported bits per unit of time without considering the necessary signal processing overhead. Usually, signal throughput metrics and computational complexity have traditionally been handled as heterogeneous and uncorrelated performance indicators by signal processing [Proakis and Salehi, 2008] and algorithms textbooks [Cormen et al., 2009], [Knuth, 1997], respectively. This assumption can be verified even in performance models that capture the throughput above the physical layer in which the signal processing computational complexity is assumed as negligible e.g. [Bianchi, 2000], [Queiroz, 2013], [Daneshgaran et al., 2008]. The implicit assumption in those analyses is that radio engineers scale the hardware processing capabilities such that the signal baseband runtime is bounded by a constant value as the symbol throughput grows.

In practice, the overall digital signal processing runtime must not be longer than the symbol period T_{SYM} imposed by the sampling theorem. Formally, if the total amount of computational instructions to assembly an N-subcarrier baseband symbol is $T(N)$ and each instruction takes κ seconds in average, then the radio design must ensure that

$$\kappa T(N) \quad \leq \quad T_{SYM} \tag{3.1}$$

Therefore, based on the sampling theorem [Shannon, 1949] [Nyquist, 1928], classic waveform capacity measures (such as symbol throughput and spectral efficiency) assume that all signal baseband computations take no more than the symbol period, irrespective of the number of performed computational instructions. As channel width gets wider across novel wireless network standards, the number of computational instructions grows, requiring more expensive designs to keep the runtime within the symbol period.

Moreover, by considering computational complexity aside from capacity meas-

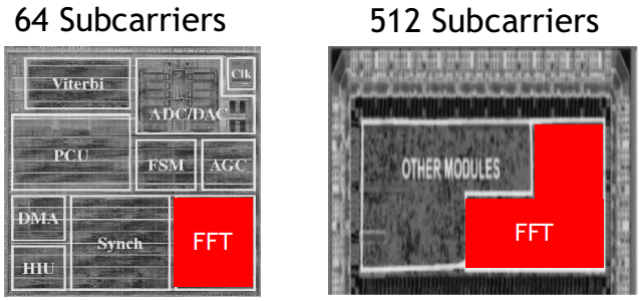

Figure 3.1: Die micrograph comparison of OFDM with 64-point FFT [Thomson et al., 2002] (left-hand side) and 512-point FFT [Davila et al., 2015] (right-hand side). If the transceiver computational complexity does not grow on the number of points then the processing runtime can nullify the signal throughput improvement. This throughput-complexity trade-off is not captured by the classic symbol data rate analysis.

ures, current analytical methodologies are unable to establish a fair cost-benefit comparison among candidate waveforms in the race towards future wireless network standards. Indeed, to outperform a given waveform design from the perspective of the spectral efficiency analysis, a novel proposal must manage to convey more bits in the same amount of spectrum during the same symbol period. In turn, the assignment of more spectrum to a given waveform suffices to cause the channel throughput to increase. In any of these cases, the analyses ignore the side-effect of capacity improvement on computational complexity.

To illustrate the prior explanation, consider the following example. In an IEEE 802.11a radio [IEEE 802.11, 2012], a 64-subcarrier OFDM symbol is processed in up to $T_{SYM} = 3.2\ \mu s$. Under this same symbol period deadline, an IEEE 802.11ac radio finishes the entire baseband computation of a 512-subcarrier OFDM symbol, yielding a gain of eight times from the perspective of the classic symbol throughput analysis. However, such analysis does not capture the extra complexity cost of the IEEE 802.11ac solution. If one considers, for instance, the $O(N \log_2 N)$ complexity of the FFT algorithm, the 512-subcarrier solution needs roughly $(512 \log_2 512)/(64 \log_2 64) = 12\times$ more computational instructions than the 64-subcarrier solution.

With the end of the Moore's law, it is no more possible to keep improving the processing capabilities without penalizing cost and area [Chen et al., 2019], [Haron and Hamdioui, 2008], [Moore, 2003]. Indeed, Fig. 3.1 presents the OFDM radio transceiver die micrograph of a 64-point FFT [Thomson et al., 2002] and a 512-point FFT [Davila et al., 2015], respectively. Clearly, the 64-point FFT solution corresponds to circa one fourth of the chip area whereas the faster 512-point one is nearly half the entire project.

More efficient signal processing algorithms can alleviate the hardware design budget but, in some cases, minimum complexity prevents both the spectral efficiency and the throughput maximization [Queiroz et al., 2020]. Finding the minimum asymptotic complexity for a given waveform setup might be hard to

accomplish if throughput and complexity are handled as uncorrelated performance indicators as usual in comparative studies of future waveforms [Conceição et al., 2020], [Schaich and Wild, 2014].

3.2 Proposed Mathematical Model

In this section, we introduce the fundamental definitions and concepts of the SC model. Since the main goal of the SC model is to support the joint throughput-complexity analysis of communication signal algorithms and waveforms, we also refer to it as "SC analysis" in a reminiscence to the term "asymptotic analysis" in the theory of computational complexity.

3.2.1 Spectro-Computational Throughput, Capacity and Efficiency

In Fig. 3.2, we illustrate the general system model of the SC analysis. In the analog part of the radio, the transmitted N-subcarrier symbol has W Hz of spectrum bandwidth and takes T_{SYM} seconds to carry $B(W)$ bits through the wireless channel. The DAC takes one complex sample every T_{NYQ} seconds following the sampling theorem thereby leading to $T_{SYM} = NT_{NYQ}$ seconds. As reviewed in Section 2.1.3, these variables compose the classic signal performance analysis such as symbol throughput (Eq. 2.9), capacity (Eq. 2.10) and spectral efficiency (Eq. 2.14).

3.2.1.1 Spectro-Computational Throughput

The digital back-end of the radio architecture shown in Fig. 3.2 comprises a sequence of G communication signal processing algorithms. These algorithms work to turn the $B(W)$ transmission bits into the equivalent digital complex baseband signal. The computational complexity of the i-th($1 \leq i \leq G$) algorithm is denoted as $T_i(B(W))$. Both $B(W)$ and $T_i(B(W))$ are assumed as non-null, non-negative monotonically increasing functions[1] of W.

From this, we define the SC throughput of the i-th signal processing algorithm as

$$SC_i(W) = \frac{B(W)}{T_i(B(W))} \quad \text{bits/instructions} \tag{3.2}$$

The SC throughput is reminiscent to the classic symbol throughput $R = B/T_{SYM}$ (Eq. 2.9) with the difference that the B bits "propagates" through the algorithm rather than through the channel. Thus, the time complexity $T_i(B(W))$ replaces the channel symbol duration T_{SYM}.

[1] If $0 < x \leq y$ then $0 < B(x) \leq B(y)$.

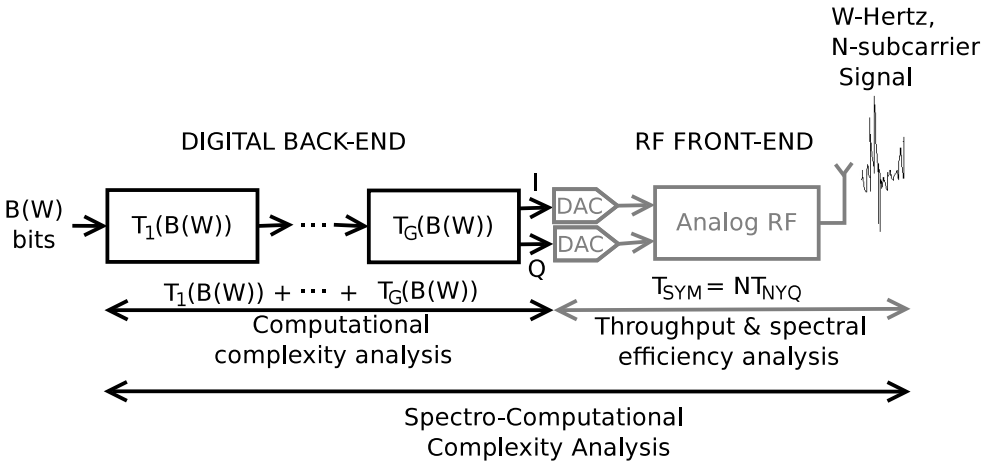

Figure 3.2: General scheme of the spectro-computational complexity analysis.

As in the analysis of algorithms, in the SC analysis the computational complexity $T_i(B(W))$ measures the number of computational instructions demanded by a particular algorithm under an input of length $B(W)$. Hence, the throughput[2] is given in bits per computational instructions. Note, however, that the conversion to bits/seconds is straightforward if the wall-clock time spent by each computational instruction on the particular baseband processor is given. For this reason, we consider both units as interchangeable and the entire *waveform throughput* $SC(W)$ accounts not only the time T_{SYM} spent by the symbol duration but also the computational complexity overhead. Therefore,

$$SC(W) \;=\; \frac{B(W)}{\sum_{i=1}^{G} T_i(B(W)) + T_{SYM}} \quad \text{bits/seconds} \tag{3.3}$$

Note that the Eq. 3.3 is the classic symbol throughput R (Eq. 2.9) with the time duration added by the overhead of the computational complexity.

Eq. 3.3 captures the fact that a signal going through the channel does necessarily need a pre-processing, hence a computational overhead is inevitable. Thus, from the perspective of a layer immediate above the physical layer, there is no difference whether the overall time to transmit/receive the bits is due to signal processing overhead or symbol duration time. This way, the signal processing and the channel transmission time can be seen as a single extended entity. Consequently, if the computational complexity overhead is sufficiently large, the throughput or capacity efficiencies can be nullified. This possibility will be captured by the formalism we introduce next.

The SC study of a waveform is an asymptotic analysis on the variable spectrum bandwidth[3] In other words, *we are concerned about the symbol throughput and the computational complexity of the waveform as* $W \to \infty$. Thus, based

[2]Hereafter, the term "throughput" stands for spectro-computational throughput unless otherwise stated.

[3]Our choice for the term "spectro-computational" analysis comes from the fact that both the spectrum bandwidth is the common element for the symbol's computational complexity and number of modulation bits.

on the properties of the asymptotic notation, the asymptotic dominant signal processing algorithm of the waveform can be denoted as

$$T(B(W)) \quad = \quad O(\sum_{i=1}^{G} T_i(B(W))) \tag{3.4}$$

and the waveform asymptotic throughput results

$$SC(W) \quad = \quad \lim_{W \to \infty} \frac{B(W)}{T(B(W)) + T_{SYM}} \quad \text{bits/seconds} \tag{3.5}$$

To ensure increasing symbol throughput as W grows, the overall symbol duration must not grow on W (as previously discussed in Subsection 3.1) In this context, we assume

$$T_{SYM} \quad = \quad \Theta(1) \quad \text{seconds} \tag{3.6}$$

As usual in asymptotic analysis, constants can be neglected. Thus, differently from the classic symbol throughput analysis, we focus on the computational complexity overhead to define the throughput in the SC analysis. From Eqs. 3.5 and 3.6, in Def. 1, we introduce the throughput of a particular communication signal processing algorithm whereas in Def. 2, we define the throughput of an entire waveform.

Definition 1 (Spectro-Computational Complexity Algorithmic Throughput). Let $T_i(B(W))$ be the computational complexity of the i-th communication signal processing algorithm of a waveform whose digital back-end comprises a sequence of G algorithms ($1 \leq i \leq G$) and the transmission symbol carries $B(W)$ bits on W Hz of spectra. We define its spectro-computational (SC) complexity throughput as

$$SC_i(W) \quad = \quad \frac{B(W)}{T_i(B(W))} \quad \text{bits/seconds} \tag{3.7}$$

and its SC asymptotic throughput as

$$SC_i(W \to \infty) \quad = \quad \lim_{W \to \infty} \frac{B(W)}{T_i(B(W))} \quad \text{bits/seconds} \tag{3.8}$$

Definition 2 (Spectro-Computational Complexity Waveform Throughput). Let $T(B(W))$ (Eq. 3.4) be the asymptotically dominant algorithm of the waveform referred to by Def. 1. Then, we define the spectro-computational complexity throughput of the waveform as

$$SC(W) \quad = \quad \frac{B(W)}{T(B(W))} \quad \text{bits/seconds} \tag{3.9}$$

and its SC asymptotic throughput as

$$SC(W \to \infty) = \lim_{W \to \infty} \frac{B(W)}{T(B(W))} \quad \text{bits/seconds} \tag{3.10}$$

3.2.1.2 Remarks

About the limits of Defs. 1 and 2, it is important to remark that we are not assuming signals of infinite bandwidth. Instead, we are concerned about both the symbols' number of bits and computational complexity as the spectrum bandwidth *tends* to infinity. In this case, assuming the limit $SC(W)$ exists, the SC throughput analysis can reflect whether the increase of the spectrum causes a time complexity bottleneck that nullifies the algorithmic throughput.

One may also remark that the existence of the limit in Eq. 3.5 may conflict with the assumptions about $B(W)$ and $T(B(W))$ (i.e., increasing functions). Indeed, by definition of calculus, the solution of the limit requires the same result for both $W \to +\infty$ and the $W \to -\infty$. From this, one may wonder about a symbol of negative number of bits and computational instructions. This is the same dilemma faced by the computer scientists when classifying the complexity of algorithms with the limit property of the little o, little omega or bit theta notations. Of course, those properties assume neither input problems of negative lengths nor algorithms that perform a negative quantity of computational instructions. Actually, the negative quantities are implicitly assumed only for the sake of the proof of the limit. Alternatively, one may consider only the one-sided left-handed limit under which $W \to +\infty$.

3.2.1.3 Spectro-Computational Efficiency

The spectral efficiency formula (Eq. 2.14) can be enhanced to account the signal processing overhead similarly to Eq. 3.3 for the classic symbol throughput formula. We refer to it as the SC efficiency (SCE) that is given as

$$SCE(W) = \frac{\frac{B(W)}{\sum_{i=1}^{G} T_i(B(W)) + T_{SYM}}}{W} \quad \text{bits/seconds/Hz} \tag{3.11}$$

In the case of waveforms running under the Nyquist sampling theorem, the entire signal processing runtime overhead $\sum_{i=1}^{G} T_i(B(W))$ (Eq. 3.3) must respect the Nyquist time interval T_{NYQ}. Some waveforms requires at least one batch-oriented algorithm whose unit of operation is a set of signal samples. This is the case, for instance, of an N-subcarrier OFDM symbol, in which the FFT algorithm operates on a batch of N samples (i.e., symbols) before feeding the DAC sampler. Since the symbol occupies W Hz of spectrum during $T_{SYM} =$

NT_{NYQ} seconds, then

$$\sum_{i=1}^{G} T_i(B(W)) \quad \leq \quad T_{SYM} = NT_{NYQ} \tag{3.12}$$

In the case of batch-oriented waveforms, the spectral efficiency metric (Eq. 2.14) fails to reflect the time/spectrum performance experienced by a particular symbol because the symbol cannot occupy the spectrum before it finishes being processed. By accounting the signal processing overhead along with the symbol duration, one gets the spectro-computational efficiency (Eq. 3.11). The impact of accounting the computational complexity is specially relevant for implementations of waveforms whose overall processing runtime is nearly as high as the symbol duration, i.e., $\sum_{i=1}^{G} T_i(B(W)) = T_{SYM}$ (e.g. [Tan et al., 2011], [Zacheo et al., 2012]). In that case, the SC efficiency reveals that the complexity overhead impairs the classic spectral efficiency S (Eq. 2.14) by a factor of two, as shown in the ratio

$$\frac{S}{SCE(W)} \quad = \quad \frac{B(W)/WT_{SYM}}{B(W)/(2WT_{SYM})} = 2 \tag{3.13}$$

The Eq. 3.13 implies that the complexity causes the symbol to experience a bandwidth twice narrower. This is the same result obtained by the traditional spectral efficiency analysis when the time occupying spectrum doubles but the number of points remains the same.

3.2.1.4 Spectro-Computational Complexity Capacity

Similarly to the concept of channel capacity, the *SC asymptotic capacity stands for the upper bound SC throughput of a signal processing algorithm or waveform.* The maximum number of bits given by a channel capacity model can be employed to determine the SC capacity of a communication signal algorithm and, consequently, of an entire waveform. However, since the SC throughput also depends on the computational complexity, faster algorithms also translate into better throughput. Therefore, in the SC analysis, the definition of asymptotic capacity depends both on the bits computed from the channel capacity as well as the asymptotic complexity lower bound of the implied waveform algorithms.

Assuming waveform algorithms that work on a symbol-by-symbol basis, one needs to calculate the maximum number of bits $B_{MAX}(W)$ a single T_{SYM}-second W-Hz symbol can convey. Taking as reference the Shannon's channel capacity model [Shannon, 1948], the symbol capacity $C_{SYM}(W)$ is readily obtained from Eq. 2.10, which is

$$C_{SYM}(W) \quad = \quad T_{SYM} W \log_2\left(1 + \frac{\mathcal{P}}{WN_0}\right) \quad \text{bits/seconds} \tag{3.14}$$

Thus, since an algorithm cannot modulate more than the number of bits given by the symbol capacity (Eq. 3.14, assuming the Shannon limit), the maximum number of bits given as input to a waveform is

$$B_{MAX}(W) \;=\; T_{SYM} W \log_2\left(1 + \frac{\mathcal{P}}{W N_0}\right) \quad \text{bits}, \tag{3.15}$$

in the duration of one symbol, i.e., T_{SYM} seconds.

Assuming that the capacity grows linearly under the band-limited regime (Eq. 2.13) and the fact that the symbol duration must remain as W grows (Eq. 3.6), the following asymptotic relationship results

$$B_{MAX}(W) \;=\; O(W) \quad \text{bits} \tag{3.16}$$

From Eq. 3.15, we introduce two different concepts of SC capacity that differ slightly from each other, namely, the SC algorithmic capacity and the SC waveform capacity. These concepts are are formalized in Defs. 3 and 4 and establish bounds for the SC throughput of a communication signal algorithm and a particular implementation of a waveform, respectively. Please, recall that both definitions assume band-limited signals such that the Signal-to-Noise Ratio (SNR) is sufficiently large (Eq. 2.12) to enable the linear growth of the channel capacity.

Definition 3 (Spectro-Computational Algorithmic Capacity). Let $\mathcal{L}_i(B(W))$ be the asymptotic complexity lower bound of the computational problem handled by the i-th signal processing algorithm of a given G-algorithm waveform. Let also $B_{MAX}(W)$ (Eq. 3.15) be the maximum number of bits given as input to the waveform. Then, the SC asymptotic capacity $SC_i(W)$ of the i-th waveform algorithm (Def. 1) is upper bounded as follows

$$SC_i(W) \;=\; O\left(\frac{B_{MAX}(W)}{\mathcal{L}_i(B_{MAX}(W))}\right) \tag{3.17}$$

Based on the Shannon theorem, Def. 3 tells us that a communication signal processing algorithm cannot reach its SC capacity in practice unless i) the asymptotic number of modulated bits grows at least linearly on the bandwidth (Shannon limit) ii) the algorithm runs in optimal complexity, i.e., lower bound complexity. In turn, the spectro-computational complexity capacity of a waveform is obtained from the maximum number of bits supported by a symbol and the most complex lower bound among the computational problems associated to the waveform signal processing.

Definition 4 (Spectro-Computational Waveform Asymptotic Capacity). Let $\mathcal{L}_i(B(W))$ be as in Def. 3 and $\mathcal{L}(B(W)) = \Theta(\sum_{i=1}^{G} \mathcal{L}_i(B(W)))$ be the asymptotic dominant complexity lower bound among the algorithms of a G-algorithm waveform. Then, the SC waveform throughput $SC(W)$ (Def. 2) is upper bounded as

follows

$$SC(W) = O\left(\frac{B_{MAX}(W)}{\mathcal{L}(B_{MAX}(W))}\right) \tag{3.18}$$

3.2.2 Optimal Spectro-Computational Algorithm and Waveform

Based on Def. 3, we specialize the concept of *asymptotically optimal algorithm* for the class of communication signal algorithms. The specialization stems from the fact that our definition is based on the SC capacity (Def. 3) which comprises not only the lower bound time complexity requisite but also the upper bound throughput.

Definition 5 (Asymptotically Optimal Spectro-Computational Algorithm). The i-th communication signal processing algorithm referred to by Def. 3 is SC optimal if, and only if, its SC throughput $SC_i(W)$ is such that

$$SC_i(W) = \Theta\left(\frac{B_{MAX}(W)}{\mathcal{L}_i(B_{MAX}(W))}\right) \tag{3.19}$$

Note that, as the definition of asymptotically optimal algorithms of the theoretical computer science, the definition of asymptotically optimal SC algorithm also comprises exponential time algorithms. This is the case of intractable algorithms whose asymptotic lower bound is exponential on the input length.

In some cases, an exponential complexity may be required to meet a given target of signal communication performance. This is the case, for instance, of the optimal signal detection problem in some waveforms [Basar et al., 2012]. As explained in Subsection 2.2.2, some optimal detectors must compute a maximum likelihood metric between the received signal shape and each possible signal modulation of the system. If the detection search space grows exponentially on a variable of the system (e.g., spectral bandwidth [Mao et al., 2018], number of antennas [Albreem et al., 2019]) then the complexity required by the optimal detection grows accordingly. The exponential complexity of detection can be handled by heuristics that relaxes optimality of the detection. In these cases, very good heuristics reach near-optimal detection while preserving polynomial time complexity and minimum impact on the overall system performance [Sandell et al., 2016].

Other more exotic alternative towards the efficient execution of complex algorithms is the development of beyond-Turing (yet-under-debate) computational models [Deutsch, 1985],[Traversa et al., 2015]. These models inspire computational apparatus that are expected to handle the intrinsic complexity of some signal processing problems (e.g., detection [Botsinis et al., 2013]) in future wireless communications standards [Nawaz et al., 2019]. Def. 6 formalizes the optimal implementation of a waveform in terms of SC throughput.

Definition 6 (Asymptotically Optimal Spectro-Computational Waveform). The waveform implementation referred to by the Def. 4 is SC-optimal if, and only if, its SC waveform throughput $SC(W)$ is such that

$$SC(W) \;=\; \Theta\left(\frac{B_{MAX}(W)}{\mathcal{L}(B_{MAX}(W))}\right) \tag{3.20}$$

This means that a waveform implementation must abide to achieve an asymptotic throughput as fast as SC capacity which also is equivalent to say that the implementation modulates the maximum number of bits of the waveform spending the minimum possible asymptotic computational complexity. This differs from Def. 3 by the fact that the asymptotic throughput of the waveform implementation can grow slower than the SC capacity as the spectrum gets wider.

3.2.3 Computation-Limited Signals

The concepts of throughput and capacity rely on the ratio bits/complexity of the SC throughput. If the computational complexity is asymptotically larger than the number of bits, the computational overhead becomes a bottleneck that nullifies the throughput as spectrum bandwidth W widens. However, the fact that the throughput of a particular algorithm nullifies on W does not necessarily mean that the waveform throughput nullifies as well. Indeed, if a more efficient algorithm or modulation technique is found, a better throughput can be achieved. Conversely, if the SC capacity nullifies on W then no algorithm is able to achieve better SC throughput. In this case, the waveform need to be redesigned to rely on less complex computational problems or to modulate an asymptotically larger number of bits per spectrum.

The fact that the asymptotic capacity of some signal algorithms and waveforms can be null as W grows gives room for a novel category of waveforms that complements the classic band- and power-limited classes of signals. We refer to this novel class of waveform as *comp-limited signal* (from computational complexity-limited signals) whose description is given in Def. 8 based on the Def. 7.

Definition 7 (Comp-Limited Signal Algorithm). Let $SC_i(W)$ be the throughput of an optimal SC algorithm (i.e., $SC_i(W)$ is as efficient as the SC algorithmic capacity). Then, such communication signal algorithm is limited by computation (i.e., comp-limited signal algorithm) if

$$SC_i(W) = \lim_{W\to\infty} \frac{B(W)}{T_i(B(W))} \;\leq\; 0, \tag{3.21}$$

where T_i is the computational complexity of the i-th communication signal processing algorithm of the waveform.

Recalling that the throughput of an optimal SC algorithm is as efficient as its

corresponding upper bound throughput (i.e., it is as fast as the SC algorithmic capacity, Def. 3), Eq. 3.21 can be alternatively written as

$$\lim_{W\to\infty} \frac{B_{MAX}(W)}{\mathcal{L}_i(B_{MAX}(W))} \leq 0, \tag{3.22}$$

where $\mathcal{L}_i(B_{MAX}(W))$ is the computational complexity lower bound of the computational problem handled by the i-th communication signal processing algorithm of the waveform.

Definition 8 (Comp-Limited Signal Waveform). A waveform is limited by computation (i.e., comp-limited) if at least one of its algorithms is comp-limited (Def. 7).

From the properties of asymptotic notation, a comp-limited signal whose optimal asymptotic dominant algorithm is as complex as $T(W)$ can be alternatively expressed as

$$B(W) = o(T_i(B(W)), \tag{3.23}$$

i.e., the number of bits $B(W)$ modulated in a W-Hz symbol grows slower than the symbol processing complexity $T_i(B(W))$ as the spectrum bandwidth W gets wider.

3.2.4 Condition for the Scalability of Throughput

In a comp-limited signal waveform, the complexity constitutes a bottleneck for the throughput because it grows faster than the number of modulated bits. To prevent the throughput nullification, an asymptotic higher number of bits should be modulated in the signal or less complex algorithms should be devised. This leads to the condition of throughput scalability given by the *Proposition 1*.

Proposition 1 (Condition for Scalable Throughput). The asymptotic throughput $SC(W)$ of a signal waveform does not scale unless it meets Ineq. 3.24.

$$SC(W) = \lim_{W\to\infty} \frac{B(W)}{T(B(W))} > 0 \tag{3.24}$$

Proof. In essence, the above proposition concerns about which quantity grows asymptotically faster on the spectrum bandwidth W towards infinity, namely, the number of modulated bits $B(W)$ or the computational complexity $T(B(W))$ required to process the bits. If $T(B(W))$ grows asymptotically faster than $B(W)$ (i.e., $B(W) = o(T(B(W)))$ then increasing W does not translate into larger throughput as usually expected. Indeed, if $B(W) = o(T(B(W))$ then $B(W)/T(B(W)) = 0$ as $W \to \infty$ (Eq. 2.28) meaning that the SC throughput nullifies on W. By contrast, if $B(W)$ grows faster or as fast as $T(B(W))$ (i.e.,

$B(W) = \Omega(T(B(W)))$, from Eq. 2.26, it follows that the SC throughput does not nullify on W. ■

Proposition 1 can constitute a practical design target for designers of on-demand spectrum waveforms. In other words, the proposition can formally identify the best throughput/complexity cost-benefit among distinct candidate waveforms of standards that aim to support very fast data rate applications such as the enhanced Mobile Broadband (eMBB) traffic service of 5G [Yu et al., 2017].

3.3 Relation to Complexity and Information Theory

In Fig. 3.3, we present a conceptual map that illustrates how the novel definitions (rectangles) of the SC analysis relate to (links) the basic concepts of computational complexity and information theory and communication signal analysis. The basic concepts from computational complexity are disposed on the left-hand side of the map and are algorithm (for communication signal), asymptotic complexity, problem complexity lower bound and optimal complexity algorithm. In turn, the basic concepts from the communication signal field are disposed at the right-hand side of the map and are waveform (given by a sequence of algorithms), spectral bandwidth, symbol throughput, channel capacity and both the channel capacity regimes, namely, band-limited and power limited regimes.

The definitions introduced by the SC analysis are placed in-between the concepts of computational complexity and communication signal processing. The central definition of the SC analysis is the SC throughput (in bold) that can be employed as a performance indicator for a particular communication signal processing algorithm or a sequence of communication signal processing algorithms (link 0). The SC throughput is built on the concept of asymptotic complexity from the field of computational complexity and on the concepts of spectral bandwidth and symbol throughput from the field of signal processing (link 1). The SC throughput is bounded by the SC capacity (link 2), which is the ratio between the maximum number of bits given by the channel capacity and the problem complexity lower bound (link 3). The SC capacity can be employed to characterize the comp-limited regime (link 4) which stands for the class of algorithms whose throughput nullifies as the spectrum bandwidth grows. Besides, the SC capacity also does stand for the SC throughput of an an optimal SC algorithm (link 5).

The map of Fig. 3.3 also identifies some homologous concepts between the SC analysis and its reference fields. The comp-limited signal regime introduced by the SC analysis is homologous to the band- and power-limited signal regimes of the information theory and communication signal processing field. The definition of an optimal SC algorithm is a specialization of the optimal complexity algorithm of the computational complexity theory. Finally, the SC capacity is reminiscent to the concept of channel capacity.

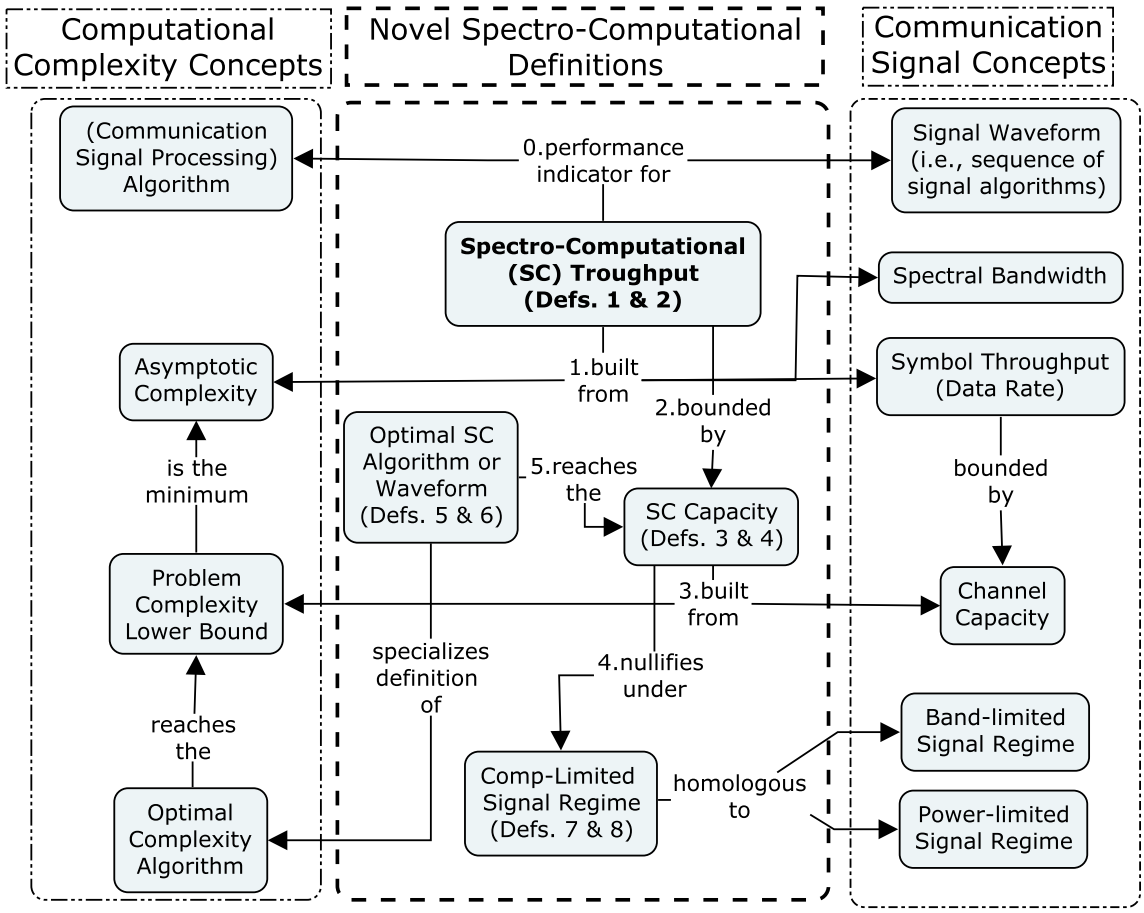

Figure 3.3: How novel definitions of the SC analysis derive from and relate to basic concepts of computational complexity and communication signal processing fields.

3.4 Step-by-Step SC Analysis of OFDM

In this section, we illustrate the application of the SC asymptotic analysis through a step-by-step example based on the basic OFDM transmitter.

3.4.1 Asymptotic Growth of Basic OFDM Parameters

The SC asymptotic study of a waveform is performed having the signal bandwidth W as variable. In the family of OFDM waveforms, the bandwidth W_{OFDM} is given by $N\Delta f$ Hz, in which Δf Hz is the inter-carrier space. Letting $W \to \infty$ for the sake of the asymptotic analysis, it follows that

$$\lim_{W_{OFDM}\to\infty} W_{OFDM} \quad = \quad \lim_{N\Delta f\to\infty} N\Delta f \quad \text{Hz} \tag{3.25}$$

To ensure that an increasing number N of subcarriers translates into larger symbol throughput, the system must produce more time samples per OFDM symbol without enlarging the symbol duration. This means that the inter-sample time interval T_{NYQ} decreases on N whereas N is kept constant. In asymptotic notation, this means

$$T_{NYQ} = \Theta(1/N) \tag{3.26}$$

$$T_{SYM} = \Theta(1) \tag{3.27}$$

In OFDM and variants that keep subcarrier orthogonality, it is known that the symbol duration is inverse to the inter-carrier space, i.e., $\Delta f = 1/T_{SYM}$. Therefore, from Eq. 3.27, one gets,

$$\Delta f \quad = \quad \Theta(1) \tag{3.28}$$

Thus, by considering that both Δf (Eq. 3.28) and T_{SYM} (Eq. 3.27) are $\Theta(1)$ with relation to the number N of subcarriers, the asymptotic bandwidth of OFDM rewrites as

$$\lim_{W_{OFDM}\to\infty} W_{OFDM} \quad = \quad \Delta f \lim_{N\to\infty} N \quad \text{Hz} \tag{3.29}$$

$$W_{OFDM} \quad = \quad \Theta(N) \tag{3.30}$$

In other words, the adoption of N as the variable of the asymptotic analysis is equivalently to W.

To determine the number of bits per symbol $B(N)$, we refer to the band-limited regime in which the growth of capacity is dominated by bandwidth rather than SNR. In particular, SNR is bounded by a constant (Eq. 2.12)

$$SNR \quad = \quad \frac{\mathcal{P}}{N\Delta_f \mathcal{N}_0} = \Theta(1) \tag{3.31}$$

otherwise either the Shannon capacity (Eq. 2.10) nullifies or the regime switches to power-limited. This means that the linear growth of the OFDM capacity in the band-limited regime is due to the raise of N rather than the number of bits per subcarrier. Thus, the size of the constellation diagram $M = 2^p$ $(p \geq 0)$ that modulates each subcarriers is such that

$$M = \Theta(1), \tag{3.32}$$

from which the number of bits per subcarrier follows,

$$\begin{aligned} B(1) &= \log_2 M \\ B(1) &= \Theta(1) \end{aligned} \tag{3.33}$$

Therefore, the total number of bits in a N-subcarrier OFDM symbol is such that

$$B(N) = \Theta(N) \tag{3.34}$$

Let $T_{MAP}(N)$, $T_{DFT}(N)$ and $T_{CP}(N)$ denote the complexities of the OFDM mapper, IDFT and the CP adder, respectively (see Section 2.1.2). Then, the overall spectro-computational throughput of the OFDM waveform is

$$SC(N) = \frac{B(N)}{T_{MAP}(N) + T_{DFT}(N) + T_{CP}(N) + T_{SYM}} \quad \text{bits/instructions} \tag{3.35}$$

One may wish to enhance Eq. 3.35 to account the computational complexity overhead in order to assess the point-to-point SC analysis. This would double the overall time computational complexity. However, our focus goes to an asymptotic analysis on N aiming to understand the SC limit of the waveform as bandwidth grows across novel generation of wireless networks. In this case, constants can be neglected as usual in asymptotic analysis. Denoting $T(N)$ as the asymptotic dominant algorithm of OFDM, the SC asymptotic throughput of OFDM finally rewrites as

$$\begin{aligned} T(N) &= O(T_{MAP}(N) + T_{DFT}(N) + T_{CP}(N) + T_{SYM}) \quad \text{instructions} \\ SC(N) &= \lim_{N \to \infty} \frac{B(N)}{T(N)} \quad \text{bits/instructions} \end{aligned} \tag{3.36}$$

Table 3.1 summarizes the asymptotic growth of the OFDM parameters with relation to the spectral bandwidth W.

3.4.2 Spectro-Computational Complexity Capacity of OFDM

To determine the maximum asymptotic throughput of an OFDM transmitter one may refer both to the maximum number of bits per symbol and the asymptotic complexity lower bound associated to the computational problems handled by

Table 3.1: Asymptotic growth of OFDM parameters with relation to the number of subcarriers N.

OFDM Variable	Asymptotic Relation to N
W_{OFDM}	$\Theta(N)$
Δf	$\Theta(1)$
T_{NYQ}	$O(1/N)$
T_{SYM}	$\Theta(1)$
SNR	$\Theta(1)$
M	$\Theta(1)$
$B(N)$	$\Theta(N)$

OFDM. Both performance indicators are respectively analyzed next. Then, we discuss the conditions to classify OFDM either as a comp-limited or a non comp-limited signal.

3.4.2.1 Maximum Asymptotic Number of Bits of OFDM

The maximum asymptotic number of bits B_{MAX} can be given by the number of bits of the Shannon capacity. Under the band-limited regime, it is $B_{MAX} = O(W_{OFDM})$ (Eq. 3.16). Recalling that $W_{OFDM} = N\Delta f$ and $\Delta f = \Theta(1)$ (Eq. 3.28), N is asymptotic equivalent to W, then,

$$B_{MAX} \;=\; O(N) \quad \text{bits} \tag{3.37}$$

3.4.2.2 Asymptotic Complexity Lower Bound of OFDM

The asymptotic lower bound of OFDM is readily obtained from the asymptotic lower bound of each computational problem it handles with, namely, mapping, Fourier transform and CP addition. Of these, we found only discussions about the Fourier transform problem lower bound. This may reflect the fact that the Fourier transform problem covers a broad range of applications of distinct input lengths, whereas symbol mapping and CP addition are particular to OFDM. Besides, OFDM algorithms have usually standardized to operate on inputs of small fixed lengths, which dispenses the need for asymptotic studies such as the derivation of their asymptotic lower bounds. Conversely, we discuss the Ω classes of these problems having in mind the unprecedented growth of their inputs in future terahertz wide waveforms.

- **Symbol mapping problem lower bound**: By operational definition, any OFDM mapper must take N sequences of $\log_2 M$ bits as input and must give N complex baseband frequency domain samples (from an M-point constellation diagram) as output measuring $O(\log_2 M)$ bits each. Thus, at least $N \log_2 M$ bits must be read at the input and $NO(\log_2 M)$ bits are written at the output, yielding a complexity lower bound of

$\Omega(N \log_2 M)$. Under the band-limited regime, one gets $M = \Theta(1)$ (Eq. 3.32), yielding a final complexity lower bound of $\Omega(N)$ for the OFDM symbol mapping problem;

- **Fourier transform problem lower-bound**: The FFT algorithm [Cooley and Tukey, 1965] is currently the fastest known algorithm for the Fourier transform problem. It outperforms the basic Fourier algorithm from $O(N^2)$ to $O(N \log_2 N)$ if N is a power of two. That is the reason why communication standards adopt a power of two for the number of OFDM subcarriers [IEEE 802.11, 2012]. Since at least $O(N)$ computational instructions must be performed, a natural question is whether any to-be-invented algorithm is able to operate on $O(N)$ complexity in practice. Because there is no proof that such an algorithm is impossible to devise, whether the exact asymptotic lower bound of the Fourier problem is $\Omega(N)$ or $\Omega(N \log_2 N)$ remains an open question in the literature [Lokam, 2009].
- **CP Addition problem lower-bound**: by operational definition, the CP addition read a fraction N/c (for a constant $c > 0$) of an N-point symbol as input and gives $N + N/c$ points as output. Since $N/c = O(N)$, the complexity lower bound of any implementation is $\Omega(N)$.

From the prior analysis, the asymptotic complexity lower bound of OFDM $\mathcal{L}_{OFDM}(N)$ is

$$\mathcal{L}_{OFDM}(N) = \Omega(N) + \Omega(FT) + \Omega(N), \tag{3.38}$$

in which $\Omega(FT)$ is the yet unknown asymptotic lower bound of the Fourier transform problem. Considering the maximum asymptotic number of bits in the OFDM symbol (Eq. 3.37), the SC capacity that bounds the SC throughput $SC(N)$ of OFDM is such that

$$SC(N) = O\left(\frac{B_{MAX}(N)}{\mathcal{L}_{OFDM}(N)}\right) \quad \text{bits}, \tag{3.39}$$

i.e., the asymptotic SC throughput of the N-subcarrier OFDM waveform grows slower or, at most, as fast as the ratio between the maximum asymptotic number of bits per symbol $B_{MAX}(N)$ and the computational complexity lower bound $\mathcal{L}_{OFDM}(N)$ required to process the bits.

3.4.3 Is OFDM a Comp-Limited Signal?

Because the asymptotic complexity lower bound $\Omega(FT)$ of the Fourier problem remains unknown, so does the asymptotic growth of $\mathcal{L}_{OFDM}(N)$ and, therefore, it is still not possible to determine whether the OFDM throughput is limited by computation as N grows. However, because the hypothesis for $\Omega(FT)$ are either $\Omega(N)$ (i.e., faster or as fast as linearly on N) or $\omega(N)$, (i.e., faster than linearly on N), the lower bound of OFDM is restricted either to $\Omega(N)$ or $\omega(N)$.

If, for instance, FFT is confirmed as the asymptotically fastest algorithm ever, then $\Omega(FT) = \Omega(N \log_2 N)$. Based on the unique mutually exclusive hypothesis for $\Omega(FT)$, we formulate the Proposition 2.

Proposition 2 (Condition for Non Comp-limited OFDM Signal). The basic OFDM waveform is limited by computation (i.e., comp-limited signal, Def. 8) unless the asymptotic lower bound of the Fourier transform algorithm verifies as $\Omega(N)$, i.e., the complexity of the fastest possible Fourier transform algorithm grows linearly on N.

Proof. Let us assume that FFT is confirmed as the fastest Fourier transform algorithm ever. In that case, $\Omega(FT)$ verifies as $N \log_2 N = \omega(N)$ and the SC asymptotic capacity bounding the OFDM throughput is given by a limit that nullifies as N grows, namely,

$$SC(N) \quad = \quad \lim_{N \to \infty} \frac{N}{N + N \log_2 N + N} = 0 \tag{3.40}$$

Otherwise, the minimum possible order of growth of any is $\Omega(N)$. In that case, the SC capacity of OFDM does not nullify as N gets arbitrarily large, being bounded by a non null constant c as follows

$$SC(N) \quad = \quad \lim_{N \to \infty} \frac{N}{N + N + N} = c > 0 \tag{3.41}$$

Therefore, the OFDM waveform is a comp-limited signal unless the asymptotic lower bound of the Fourier transform problem verifies as $\Omega(N)$. ■

Proposition 2 tells us that one might devise a faster-than-FFT algorithm to enable the scalability of OFDM SC throughput. As a workaround for that, one may concern on re-designing the OFDM waveform in a way to pack more bits per symbol – as pursued by OFDM with Index Modulation (OFDM-IM) [Basar et al., 2013] – or requiring less complex algorithms – as is the case of the Vector OFDM waveform (V-OFDM) [Xiang-Gen Xia, 2001].

In this sense, in chapters 4 and 5, we perform the SC analysis of OFDM-IM and V-OFDM, respectively. In each chapter, we demonstrate that the SC throughput of each waveform nullifies on N and show the conditions to turn them into non comp-limited signals.

3.5 Summary

In this chapter, we introduced the spectro-computational (SC) complexity analysis for wireless communications waveforms. In the SC analysis, we defined the SC throughput of an N-subcarrier waveform and their communication signal algorithms as the ratio of the number of bits carried by the symbol and the computational complexity to process the symbol. Based on that, we derived

novel definitions from (and homologous to) concepts of computational complexity and information theory.

We defined the asymptotic capacity of a communication signal algorithm as the ratio between the maximum number of bits it can modulate – taken from the channel capacity – and the asymptotic complexity lower bound of its corresponding computational problem. From that, we classified an algorithm as SC-optimal if its asymptotic throughput grows as fast as its asymptotic capacity. From these novel concepts, we also identified a peculiar class of signal waveforms in which the complexity lower bound grows asymptotically faster than the number of bits in the symbol. In this case, capacity nullifies as bandwidth grows. We referred to this novel category of signals as *comp-limited signals* in a reminiscence to the classic capacity regimes of band- and power-limited signals.

This way, to pursue novel non comp-limited signal waveforms is synonym of scalable SC throughput. Finally, we presented a step-by-step SC analysis of the basic OFDM waveform and demonstrated it is a comp-limited signal unless the N-point Fourier transform problem verifies as $\Omega(N)$, which remains an open conjecture in theoretical computer science.

Chapter 4

Optimal Mapper for OFDM with Index Modulation

"Everyone knew it was impossible, until a fool who didn't know came along and did it."

(Albert Einstein)

Contents

In this chapter, the SC analysis is applied for the design of an optimal mapper for OFDM with Index Modulation (OFDM-IM). The ideal setup of OFDM-IM outperforms the basic OFDM in terms of spectral efficiency but the resulting complexity of mapping has been considered computationally intractable by the specialized literature. The SC analysis is employed to find out the minimum complexity that maximizes the spectral efficiency gain of OFDM-IM over OFDM and for the design of an optimal mapper. This chapter is organized as follows. Section 4.2 presents the system model and the underlying assumptions. Section 4.3 calculates the complexity scaling laws of the OFDM-IM mapper. Section 4.4 analyzes the SC throughput of the original OFDM-IM mapper. Section 4.5 presents two mappers for OFDM-IM. Both are asymptotically optimal in terms of time complexity but only one is also optimal in terms of asymptotic storage. Section 4.6 validates the reported theoretical findings by the implementation and evaluation through an open source library that was developed. Finally, Section 4.7 summarizes the chapter.

4.1 Introduction to the Index Modulation Mapping

Index Modulation (IM) is a physical layer technique that can improve the spectral efficiency (SE) of OFDM. IM's basic idea for OFDM consists in activating $k \in [1, N]$ out of N subcarriers of the symbol to enable extra $C(N,k) = \binom{N}{k} = N!/(k!(N-k)!)$ waveforms [Frenger and Svensson, 1999], [Basar et al., 2012]. Of these waveforms, $2^{\lfloor \log_2 C(N,k) \rfloor}$ are employed by OFDM-IM to map $P_1 = \lfloor \log_2 \binom{N}{k} \rfloor$ bits. Besides by modulating the k active subcarriers with an M-ary constellation diagram as in the classic OFDM, the OFDM-IM symbol can transmit more $P_2 = \log_2 M$ bits along with P_1. Thus, the OFDM-IM mapper takes a total of $m = P_1 + P_2$ bits as input and gives k complex baseband samples as output for the modulation of the k subcarriers.

The distinct idea of OFDM-IM is illustrated in Table 4.1 for $k = 4$ active subcarriers out of $N = 6$. The setup yields a total of $C(6,4) = 15$ waveform patterns out of which only 8 patterns are employed to modulated all possible binary values of $P_1 = \lfloor \log_2(6,4) \rfloor = 3$ bits. In each row of the table, active and deactive subcarriers are denoted as $\times$ and ✓, respectively. In the example, the active subcarriers are BPSK-modulated, hence each of them carries one bit and the number of bits carried by the demodulation of active subcarriers is $P_2 = 4$ bits. Thus, in the example, the OFDM-IM symbol modulates a total of $m = P_1 + P_2 = 3 + 4 = 7$ bits on six subcarriers against six bits carried by a typical OFDM symbol in the same spectrum. Besides this spectral efficiency gain, the deactivation of the $N - k = 6 - 4 = 2$ subcarriers decreases the average symbol energy in comparison to OFDM symbol and can be exploited for the implementation of energy-constrained wireless networks [Salah et al., 2019].

Table 4.1: Example of index modulation mapping for $k = 4$ BPSK-modulated active subcarriers out of $N = 6$ subcarriers. Active and deactive subcarriers are denoted as × and ✓, respectively.

P_1 Bits		Subcarrier Indexes					
Decimal	Binary	1	2	3	4	5	6
0	000	×	×	✓	✓	✓	✓
1	001	×	✓	×	✓	✓	✓
2	010	×	✓	✓	×	✓	✓
3	011	×	✓	✓	✓	×	✓
4	100	×	✓	✓	✓	✓	×
5	101	✓	×	×	✓	✓	✓
6	110	✓	×	✓	×	✓	✓
7	111	✓	×	✓	✓	×	✓

In the OFDM-IM block diagram (Fig. 4.1a), the index selector (IxS) algorithm determines the k-size list of indexes – out of 2^{P_1} possibles – from the P_1-bit input (more details about the OFDM-IM diagram are given in Section 4.2.1). The other DSP steps follow as usual in OFDM, except for the signal detector at the receiver. In this sense, several research efforts have been done to improve the receiver's bit error rate at low computational complexity [Hu et al., 2018; Siddiq, 2016; Zheng et al., 2015; Basar et al., 2013]. Since our focus is on the OFDM-IM mapper, we refer the reader to the survey works [Mao et al., 2018; Basar et al., 2017; Sugiura et al., 2017; Ishikawa et al., 2016] for other aspects of the index modulation technique.

4.1.1 Problem

In this chapter, we concern about whether the OFDM-IM mapper can reach the maximal SE gain over its OFDM counterpart keeping the same computational complexity (CC) asymptotic constraints. The SE maximization of OFDM-IM over OFDM happens when the IM technique is applied on all N subcarriers of the symbol with $k = N/2$ and the active subcarriers are BPSK-modulated, i.e., $M = 2$ [Fan et al., 2014, 2015]. We refer to this setup as the optimal OFDM-IM configuration.

The computational complexity of the OFDM-IM mapper under the optimal SE configuration has been considered an "impossible task" up to date [Lu et al., 2018], [Basar et al., 2017]. This belief comes from the fact that the number of OFDM-IM waveforms that can be mapped grows as fast as $O(\binom{N}{k})$, which becomes exponential if the optimal SE configuration is allowed. Indeed, according to the theory of computation, a problem of size N is computationally intractable if its time complexity lower bound is $\Omega(2^N)$. Despite that, as far as we know, *the CC lower bound required to sustain the maximal SE gain of OFDM-IM remains an open question across the literature*. Consequently, no prior work can answer whether the OFDM-IM mapper indeed needs more asymptotic computational

resources than its OFDM counterpart to sustain the maximal SE gain.

4.1.2 Related Work

In this subsection, we review the literature related to the design and computational complexity of the OFDM-IM mapper.

4.1.2.1 Early Attempt

The earliest mapper for OFDM-IM we find is due to [Frenger and Svensson, 1999]. The authors suggest a Look-Up Table (LUT) to map P_1 bits into one out of 2^{P_1} unique waveforms for relatively small P_1. To avoid the exponential increase in storage implied by the optimal SE configuration, the authors employ a Johnson association scheme [MacWilliams and Sloane, 1978] to map P_1 based on the recursive matrix $A_{N,k} = [[1\ 0]^T[A_{N-1,k-1}\ A_{N-1,k}]^T]$, in which Z^T is the transpose of a given matrix Z. Those authors remark that the matrix indexes decrease linearly with N towards the base case of recursion. However, we remark that the overall CC to write all rows of $A_{N,k}$ is exponential under the optimal SE configuration. To verify that, consider firstly that $A_{N,k}$ can be lower-bounded by $A_{k,k}$, since $k \leq N$. To build $A_{k,k}$, one needs at least two computational instructions to write the numbers 1 and 0 and two other independent and distinct recursive calls $A_{k-1,k-1}$ and $A_{k-1,k}$. In the worst-case analysis, the number of computational steps T to write all entries of $A_{k,k}$ can be captured by the recurrence $T(k) = 2 + 2T(k-1)$, which is trivially verified as $\Omega(2^k)$. Under the optimal SE setup, the proposed recursive scheme is $\Omega(2^N)$.

4.1.2.2 Sub-block Partitioning

To handle the OFDM-IM mapping overhead, Basar et al. [Basar et al., 2013, 2012] propose the subblock partitioning (SP) approach. According to the survey work of [Basar et al., 2017], SP and the IxS algorithm presented by [Basar et al., 2013, 2012] were (along with a low complexity detector) the distinctive methods responsible to release the true potential of the IM scheme, thereby shaping the family of index modulation waveforms as we know today. The key idea of SP is to attenuate the mapper CC by restricting the application of the IM technique to smaller portions of the symbol called "subblocks". The length $n = \lfloor N/g \rfloor$ of each subblock depends on the number g of subblocks, which is a configuration parameter of OFDM-IM. Increasing g, decreases n, which causes the complexity of the IxS algorithm to decrease too. This way, SP introduces a trade-off between SE and CC, since the number of OFDM-IM waveforms increases for lower g [Basar et al., 2013, 2012]. Thus, setting $g = 1$ (i.e., deactivating SP) means maximizing the SE efficiency. SP has represented the state of the art approach to balance SE and CC across the family of IM-based multi-carrier waveforms [Yoon et al., 2019], [Li et al., 2019b], [Li et al., 2019a], [Kim and Park, 2019], [Shi et al., 2019], [Jaradat et al., 2018], [Mao

et al., 2018], [Lu et al., 2018], [Aldirmaz et al., 2018], [Wen et al., 2018], [Wen et al., 2018], [Mao et al., 2017b], [Wen et al., 2017], [Ozturk et al., 2017], [Zhang et al., 2017], [Mao et al., 2017a], [Gokceli et al., 2017], [Basar et al., 2017; Fan et al., 2016], [Fan et al., 2014], [Fan et al., 2015].

4.1.2.3 (Un)Ranking Algorithms

The IxS algorithm is a mandatory part for the asymptotic analysis of the OFDM-IM mapper. As observed by authors in [Basar et al., 2013, 2012], the IxS task at the OFDM-IM transmitter (receiver) can be implemented as an unranking (ranking) algorithm. By reviewing the literature in combinatorics, one can find out several different (un)ranking algorithms, running at different time complexities [Parque and Miyasita, 2018; Shimizu et al., 2014; McCaffrey, 2004; Martínez and Molinero, 2001; Kreher and Stinson, 1999; Kokosiński, 1995; H. Chen and Chern, 1986; Er, 1985; Buckles and Lybanon, 1977]. At a first glance, building the optimal OFDM-IM mapper may just be a matter of adopting the IxS algorithm that establishes the complexity upper-bound for the (un)ranking problem, i.e., the fastest currently known algorithm. However, in the particular domain of OFDM-IM, *k represents a trade-off between SE and CC*. Thus, because the literature in pure combinatorics does not concern about SE as a performance indicator, it does not suffice to guide the design of an optimal OFDM-IM mapper. Therefore, to the best of our knowledge, *no prior analysis concerns about the OFDM-IM mapper complexity minimization under the constraint of SE maximization.*

4.1.2.4 Novel SP-Free OFDM-IM Mappers

In [Salah et al., 2019], the authors propose the concept of sparsely indexing modulation to improve the trade-off between SE and energy efficiency of OFDM-IM. Because this concept imposes k to be much less than N, the authors rely on [Kokosiński, 1995] to perform IxS in $O(k \log N)$ time. With the achieved time complexity reduction, the authors present the first SP-free OFDM-IM mapper. However, the constraint on the value of k prevents the SE maximization. we refer to the SC analysis to identify the largest tolerable computational complexity to enable the maximal SE. We define the SC throughput of an N-subcarrier mapper as the ratio $m(N)/T(N)$ (in bits per computational instructions[1]), where $T(N)$ is the mapper's asymptotic complexity to map $m(N)$ bits into an N-subcarrier complex OFDM symbol. From this, the largest computational complexity $T(N)$ must satisfy $\lim_{N\to\infty} m(N)/T(N) > 0$, i.e., the SC throughput must not nullify as the system is assigned an arbitrarily large amount of spectrum.

This chapter builds on the practical case studies of [Queiroz et al., 2020] and [Queiroz et al., 2020] to present the first asymptotically optimal OFDM-IM

[1] or seconds, given the time each instruction takes in a particular computational apparatus e.g. FPGA, ASIC.

mapper. By optimal, we mean our mapper enables all $2^{\lfloor \log_2 \binom{N}{N/2} \rfloor}$ waveforms of OFDM-IM under the same asymptotic time and space complexities of the classic OFDM mapper. In summary, we report the following contributions:

- We derive the general OFDM-IM mapper lower-bound $\Omega(k \log_2 M + \log_2 \binom{N}{k} + k)$ and show it becomes the same of the classic OFDM mapper under the optimal configuration (i.e., $g = 1$, $k = N/2$, $M = 2$). *This formally proves that enabling all OFDM-IM waveforms is not computationally intractable, as previously conjectured [Lu et al., 2018], [Basar et al., 2017]*;
- We show that the optimal OFDM-IM mapper must run in exact $\Theta(N)$ asymptotic complexity. An implementation running above this complexity (i.e. $T(N) = \omega(N)$) nullifies the SC throughput for arbitrarily large N, whereas one running below that (i.e., $T(N) = o(N)$) prevents the SE maximization;
- We present an OFDM-IM mapper that runs in $\Theta(N)$ time in the same asymptotic storage required by the classic OFDM waveform. Based on that, we show that if OFDM is a non comp-limited signal then OFDM-IM is non comp-limited too;
- We implement an open-source C++ library that supports all steps to map/demap an N-subcarrier complex frequency-domain OFDM-IM symbol.

4.2 System Model and Assumptions

In this section, we review the OFDM-IM mapper (Subsection 4.2.1) and present its required design for SE maximization (Subsection 4.2.2). The symbols and notation adopted throughout this Chapter are presented in Table 4.2.

4.2.1 OFDM-IM Background

The SP mapping approach [Basar et al., 2012], [Basar et al., 2013] is responsible for the main changes OFDM-IM causes to the classic OFDM transmitter block diagram (as illustrated in Fig. 4.1a). SP is characterized by the configuration parameter $g \geq 1$, which stands for the number of subblocks within the N-subcarrier OFDM-IM symbol. Each subblock has $n = \lfloor N/g \rfloor$ subcarriers out of which k must be active. Considering an M-point modulator for the active subcarriers, each subblock maps $p = p_1 + p_2 = k \log_2 M + \lfloor \log_2 \binom{n}{k} \rfloor$ bits and the entire symbol has gp bits. The IxS algorithm of the β-th subblock ($\beta = 1, \ldots, g$) is fed with $p_1 = \lfloor \log_2 \binom{n}{k} \rfloor$ bits and outputs vector I_β, the k-size vector containing the indexes of the subcarriers that must be active in the β-th subblock. To modulate the k active subcarriers, the "M-ary modulator" step takes the remainder $p_2 = k \log_2 M$ bits as input and outputs the vector $\mathbf{s}_\beta$, which consists of k complex baseband signals taken from an M constellation diagram. Then,

Table 4.2: Notation and symbols of the chapter.

Symbol	Description
c_i	Index of the i-th active subcarrier in the symbol
g	Number of subblocks per symbol
N	Number of subcarriers per symbol
M	Constellation size of the modulation diagram
k	Number of active subcarriers
m	Total number of bits per symbol
$m(N)$	Asymptotic number of bits per symbol as function of N
n	Number of subcarriers per subblock
p	Total number of bits per subblock
p_1	Number of index modulation bits per subblock
p_2	Number of bits per active subcarriers in a subblock
P_1	Number of index modulation bits per symbol
P_2	Number of bits per active subcarriers in a symbol
δ	Half-width of the confidence interval
x	Number of samples of the steady-state mean
$\mathbf{s}$	List of baseband samples per symbol
$\mathbf{s}_\beta$	List of baseband samples in the β-th subblock
$A_{N,k}$	$N \times k$ Johnson association scheme
I	List of active subcarrier indexes per symbol
I_β	List of active subcarrier indexes in the β-th subblock
X	Decimal representation of the P_1-bit mapper input
$T(N)$	(De)Mapper computational complexity as function of N
$m(N)/T(N)$	(De)Mapper spectro-computational throughput
$\binom{N}{k}$	$N!/(k!(N-k)!)$
κ	Wall-clock runtime of a computational instruction
$o(f)$	Order of growth asymptotically smaller than f
$\omega(f)$	Order of growth asymptotically larger than f
$O(f)$	Order of growth asymptotically equal or smaller than f
$\Omega(f)$	Order of growth asymptotically equal or larger than f
$\Theta(f)$	Order of growth asymptotically equal to f
Z^T	Transpose of the matrix Z

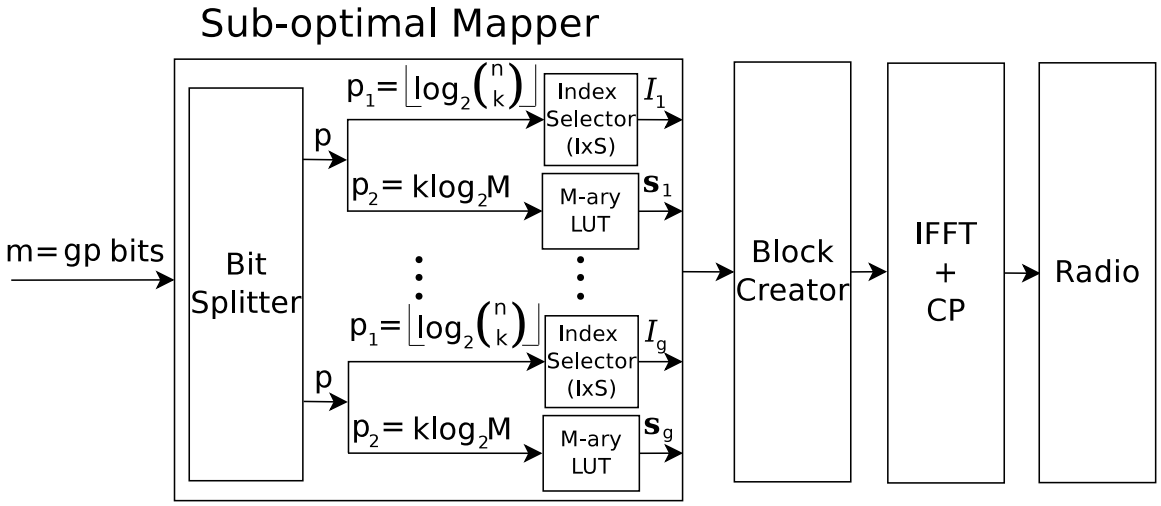

(a) OFDM-IM Waveform.

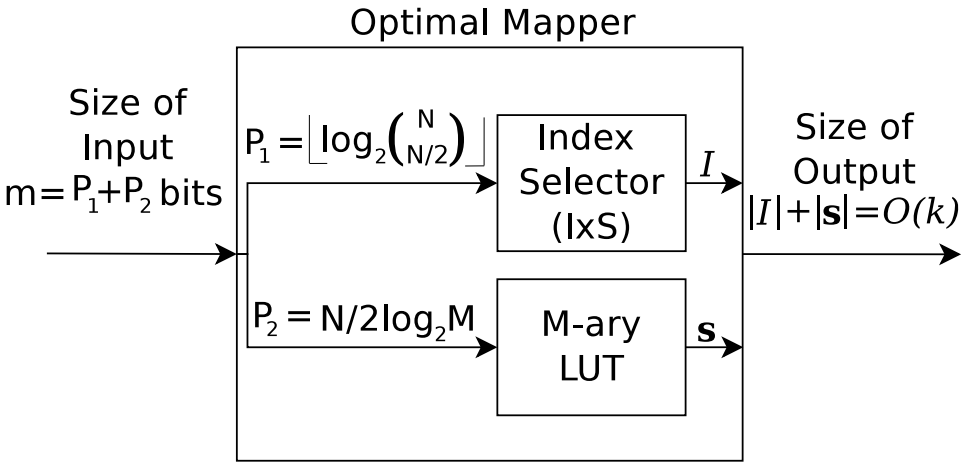

(b) Optimal Mapper: $k = N/2$ and $g = 1$.

Figure 4.1: The OFDM-IM block diagram (Fig. 4.1a) mitigates the mapping computational complexity by subdividing the symbol into g small subblocks. To maximize the spectral efficiency (SE) gain over OFDM, the mapper has to set $g = 1$ and $k = N/2$ (Fig. 4.1b). We prove such optimal mapper can be implemented under the same time and space asymptotic complexities of the classic OFDM mapper.

each subblock forwards $2k$ values (i.e., $|\mathbf{s}_\beta| + |I_\beta|$) to the "OFDM block creator", which refers to $\mathbf{s}_\beta$ and I_β to modulate the k active subcarriers in each subblock and build the full N-subcarrier frequency domain OFDM-IM symbol. The remaining steps proceed as usual in OFDM [Proakis and Salehi, 2008].

4.2.2 SE Optimal OFDM-IM Mapper Design

A requirement to maximize the OFDM-IM SE is to deactivate SP (i.e., set g to 1) and k to $N/2$ [Basar et al., 2013]. In theory, achieving the maximal

SE is just a matter of setting OFDM-IM with the proper parameters. Indeed, by setting g to 1 (i.e., deactivating SP) and k to $N/2$, the resulting mapper (Fig. 4.1b) enables all 2^{P_1} waveforms of OFDM-IM [Basar et al., 2013]. However, the authors of the original OFDM-IM waveform recommend avoiding the ideal setup because of the resulting computational complexity (compared with the classic OFDM mapper). In fact, by looking at Fig. 4.1b, one may observe that the ideal OFDM-IM mapper can be seen as a classic OFDM mapper with the addition of the IxS step. Because of this extra-step, the optimal OFDM-IM mapper requires more computational steps than its OFDM counterpart. However, our rationale is that, *if one can design an OFDM-IM mapper under the same asymptotic computational complexity of the classic OFDM mapper, then the extra computational operations required by the OFDM-IM mapper (compared to OFDM's) are bounded by a constant even for arbitrarily large N.* Since the IxS complexity is not affected by M, without loss of generality, in this chapter we adopt $M = 2$ to achieve the largest gain in comparison to the OFDM counterpart [Fan et al., 2014, 2015]. We refer to this as the optimal OFDM-IM setup.

We study the scaling laws of the OFDM-IM mapper as a function of the number N of subcarriers. In particular, for an N-subcarrier OFDM-IM symbol, we study the number $m(N)$ of bits per symbol and the mapper's computational complexity $T(N)$ to map these bits into N complex baseband samples. We concern about the minimum and maximum asymptotic number of computational instructions required by any OFDM-IM mapper implementation.

4.3 Index Modulation Mapping Complexity Bounds

In this section, we derive the CC lower and upper bounds for an OFDM-IM mapper implementation through asymptotic analysis as a function of the number of subcarriers N.

4.3.1 Lower and Upper Bound Complexities

To derive the general asymptotic lower bound for any OFDM-IM implementation, we refer to Fig. 4.1b. Recall we are considering an SP-free mapper design (i.e., $g = 1$) to enable the IM principle on the entire N-subcarrier OFDM-IM symbol. In this case, the lower bound is readily derived by observing that any implementation needs at least m basic computational steps to read the binary input to be mapped. Also, $O(k)$ basic computational steps are required to write the baseband samples in the mapper's output. Based on this, we derive the general CC lower bound for any OFDM-IM mapper implementation as follows.

Lemma 1 (OFDM-IM Mapper General CC Lower Bound). The minimum number of computational steps of any OFDM-IM mapper implementation is $\Omega(k \log_2 M + \lfloor \log_2 \binom{N}{k} \rfloor + k)$.

Proof. In the optimal OFDM-IM mapper, $g = 1$. Thus, the minimum number of computational steps to read the input is $m = P_1 + P_2 = \lfloor \log_2 \binom{N}{k} \rfloor + k \log_2 M$. Further, the OFDM-IM mapper must feed the "OFDM block creator" DSP step with the vectors of the active subcarriers indexes I_β and their corresponding baseband samples $\mathbf{s}_\beta$ ($\beta = 1, \ldots, g$). Since the optimal mapper requires $g = 1$, there is only a single k-size vector I_1 and another k-size vector $\mathbf{s}_1$, yielding to the total output size of $2k = O(k)$. Thus, any OFDM-IM mapper implementation must write at least $O(k)$ units of data in its output. Therefore, because of the computational effort to read (input) and write (output) units of data, any OFDM-IM mapper solution will demand at least $\Omega(k \log_2 M + \lfloor \log_2 \binom{N}{k} \rfloor + k)$ computational steps.

When the optimal OFDM-IM setup is allowed, the general asymptotic lower bound of Lemma 1 becomes $\Omega(N)$, as shown next.

Corollary 1 (OFDM-IM Mapper CC Lower Bound under Maximal Spectral Efficiency). Under the optimal spectral efficiency setup, the general mapping CC lower bound of OFDM-IM (Lemma 1) becomes $\Omega(N + P_1)$, which is the same of OFDM, i.e., $\Omega(N)$.

Proof. Since P_1 approaches $N - \log_2 \sqrt{N} = O(N)$ for arbitrarily large N (Lemma 2), the general asymptotic lower-bound $\Omega(N + P_1)$ becomes $\Omega(N)$, which is the minimum asymptotic number of computational steps performed by the classic OFDM mapper.

Corollary 1 stems from the fact that the number of index modulated bits P_1 approaches $N - \log_2 \sqrt{N}$ as $N \to \infty$, as one can verify in the following lemma.

Lemma 2 (Maximum Number P_1 of Index Modulation Bits). The maximum number of index modulated bits P_1 approaches $N - \log_2 \sqrt{N}$ for arbitrarily large N.

Proof. By definition, $P_1 = \lfloor \log_2 \binom{N}{k} \rfloor$. If the maximum SE gain of OFDM-IM over OFDM is allowed, $\binom{N}{k}$ becomes the so-called central binomial coefficient $\binom{N}{N/2}$, whose well-known asymptotic growth is $O(2^N/\sqrt{N})$ [OEIS Foundation Inc., 2018]. From this, it follows that P_1 approaches $\log_2(2^N N^{-0.5}) = N - \log_2 \sqrt{N} = O(N)$ as $N \to \infty$.

Therefore, although the number of waveforms of the optimal OFDM-IM setup grows exponentially on N, the CC of the IM mapping problem is not intractable (i.e., $\Omega(2^N)$) as previously conjectured [Lu et al., 2018], [Basar et al., 2017].

Lemma 1 and Corollary 1 imply that it is not possible to implement an OFDM-IM mapper with less than $\Omega(N)$ computational steps without sacrificing the SE optimality (Corollary 2). This conclusion is summarized in the following corollary.

Corollary 2 (OFDM-IM Mapper Spectro-Computational Lower-Bound Trade-Off). No OFDM-IM mapper implementation can maximize the spectral

efficiency (SE) gain over OFDM while running in $o(N)$ computational steps.

Proof. The asymptotic number of steps of any OFDM-IM mapper is subject to the general lower bound of $\Omega(k \log_2 M + \lfloor \log_2 \binom{N}{k} \rfloor + k)$ (Lemma 1). Thus, the only way to improve that bound consists of changing the OFDM-IM configuration parameters M and k. Out of all possible values of M and k, the *maximum* SE gain of OFDM-IM over OFDM is achieved *only* when $M = 2$ and $k = N/2$ [Fan et al., 2014, 2015]. Also, under such optimal SE configuration, the general CC lower bound becomes $\Omega(N)$ (Corollary 1). Therefore, an OFDM-IM implementation cannot run bellow this bound (i.e., in sub-linear time) unless a non-optimal SE configuration is adopted for k.

In essence, Corollary 2 states that any OFDM-IM mapper running in sub-linear complexity, i.e., $k = o(N)$ (which excludes the ideal $k = N/2$), prevents the maximal SE gain over OFDM. However, sub-optimal SE setups can be useful for sparse OFDM-IM systems, in which one gives up the maximal throughput on behalf of energy consumption minimization [Salah et al., 2019].

The CC upper bound of a problem is usually defined as the complexity of the fastest currently known algorithm that solves it [Harel, 1987]. This definition does not suffice to our study because our asymptotic analysis is further constrained by the SE maximization. In fact, if the fastest known algorithm does not suffice to avoid an increasing bottleneck in the mapping throughput as N grows, then its complexity cannot be considered suitable to scale the mapper throughput on N. From this, we define the spectro-computational mapper throughput (Def. 9) and, based on its condition of scalability (Def. 10), we derive the required computational complexity upper bound for any OFDM-IM mapper implementation (Lemma 3).

Definition 9 (The Spectro-Computational (SC) Throughput). Let $T(N)$ be the computational complexity (CC) to map $m(N)$ input bits into an N-subcarrier OFDM-IM symbol. We define $m(N)/T(N)$ in bits per computational steps (or seconds), as the spectro-computational (SC) throughput of the mapper.

As a side note about our Def. 10, we call attention to the fact that it consists of the asymptotic analysis. As such, "time complexity" means "amount of computational instructions" which can be translated to (but does not necessarily mean) wall clock runtime. That said, we recognize that a radio implementation that does not meet our Def. 10 can achieve the same wall clock runtime of another one that does. However, in this case, the CC $T(N)$ will translate into other relevant radio's design performance indicators. For example, suppose that the largest complexity $T(N)$ to satisfy our Def. 10 in a particular DSP study is $O(N)$. A design that violates such a requirement by employing a more complex algorithm, let us say $O(N^2)$, can still reach the same wall clock runtime of a design that does not. However, since the overall number of performed computational instructions depends on the algorithm's CC rather than the hardware technology, the average wall clock time to run a single computational instruction must be (much) lower in the $O(N^2)$ solution in comparison to the $O(N)$ counterpart. This pushes the algorithm's CC to

the hardware design rather than to the wall clock runtime. Therefore, the SC throughput of a radio design that violates our Def. 10 can scale with N but at the expense of impairing other relevant design performance indicators, such as the number of hardware components (e.g., logic gates), circuit area, energy consumption and manufacturing cost [Blume et al., 2002].

Definition 10 (Spectro-Computational Throughput Scalability). The SC throughput $m(N)/T(N)$ of a mapper is not scalable unless the inequality (4.1) does hold.

$$\lim_{N\to\infty} \frac{m(N)}{T(N)} \;>\; 0 \tag{4.1}$$

4.3.2 Required Complexity for Maximal SE

Based on Def. 10, in Lemma 3 we show that the upper bound complexity any OFDM-IM mapper implementation must meet to ensure the optimal SE configuration is $O(N)$.

Lemma 3 (OFDM-IM Mapper Upper Bound under Optimal SE Configuration). Under the optimal SE configuration, the OFDM-IM mapper CC must be upper bounded by $O(N)$.

Proof. To meet the inequality 4.1 of Def. 10, $T(N)$ must be asymptotically less or equal than $m(N)$, i.e., $T(N) = O(m(N)) = O(P_1+P_2)$. Under the optimal SE configuration, $k = N/2$ and $P_1 = \log_2 \binom{N}{N/2} = O(N)$ bits (Lemma 2). Therefore, $T(N)$ must be $O(N)$.

Based on the fact that the required OFDM-IM mapper upper bound complexity matches its lower bound in the optimal SE configuration, Theorem 1 tells us that *the OFDM-IM mapper must run in* $\Theta(N)$ *time complexity.*

Theorem 1 (Required OFDM-IM Mapping Complexity). If the configuration that maximizes the OFDM-IM spectral efficiency gain over OFDM is allowed (i.e., $g = 1$, $k = N/2$, $M = 2$), the OFDM-IM mapper block of [Basar et al., 2012, 2013] must run in $\Theta(N)$ computational steps.

Proof. Corollaries 1 and 2 show that any OFDM-IM mapper implementation running with less than $\Omega(N)$ computational steps cannot achieve the optimal SE gain over OFDM. In turn, Lemma 3 tells us that the mapper throughput nullifies for arbitrarily large N if its complexity requires more than $O(N)$ steps. Therefore, the exact asymptotic number of computational steps for any OFDM-IM mapper implementation under the optimal SE configuration must be $\Theta(N)$.

A solution running asymptotically slower than the complexity of Theorem 1 (i.e., $\omega(N)$) nullifies the mapper throughput as N grows, whereas one running faster (i.e., $o(N)$) prevents the SE gain maximization, as shown in Corollary 2.

Although the OFDM-IM symbol can carry more bits than OFDM's under the ideal setup, Lemma 2 shows that the the number of bits grows linearly in both cases. In terms of signal processing, OFDM-IM has the IxS algorithm as an extra step at the transmitter and a more complex signal detector at the receiver. Considering that optimal detectors such as maximum likelihood are computationally intractable, heuristics are necessary in practice to balance BER and complexity. [Hu et al., 2018], for instance, evaluates the performance of the max-log detector [Sandell et al., 2016] in the context of OFDM-IM getting a complexity of $O(M)$.

Thus, under the SNR required by low complexity detection heuristics, OFDM-IM has the same overall asymptotic computational complexity of OFDM unless by the IxS algorithm. Therefore, the classification of OFDM-IM as a comp-limited signal is conditioned to the classification of OFDM as a comp-limited signal and to the implementation of an OFDM-IM mapper that runs in $\Theta(N)$ time complexity. As discussed in Section 3.4.3, the characterization of OFDM as a comp-limited signal is conditioned to the existence of an $O(N)$ time algorithm for the N-point Fourier transform, which remains an open question in theoretical computer science.

4.4 Throughput Analysis of the OFDM-IM Mapper

The original OFDM-IM mapper (and its variants) refer to the (un)ranking algorithm named "Combinadic" [Buckles and Lybanon, 1977; McCaffrey, 2004][2].

The Combinadic algorithm relies on the fact that each decimal number X in the integer range $[0, \binom{N}{k} - 1]$ has an unique representation $(c_k, \cdots, c_2, c_1)$ in the combinatorial number system[Knuth, 2011] (Eq. 4.2). For OFDM-IM, X represents the P_1-bit input (in base-10) and the coefficients $c_k > \cdots > c_2 > c_1 \geq 0$ represent the indexes of the k subcarriers that must be active in the subblock.

$$X = \binom{c_k}{k} + \cdots + \binom{c_2}{2} + \binom{c_1}{1} \tag{4.2}$$

Combinadic may refer to two distinct tasks, namely, unranking and ranking. The Combinadic unranking (shown in Alg. 4.1) consists in computing the array of coefficients c_i, $i \in [1, k]$, of Eq. (4.2) from the input X (along with N and k). The Combinadic unranking takes place in the IxS of the OFDM-IM transmitter. The reverse process, i.e., computing X given all k coefficients c_i, $i \in [1, k]$, is known as ranking and is performed by the IxS of the OFDM-IM receiver (Alg. 4.2).

[2] In [Crouse, 2007], the author points a fix to the algorithm of [Buckles and Lybanon, 1977].

Algorithm 4.1. Combinadic Unranking (OFDM-IM IxS Transmitter).

1: {Inputs: X, N, and $k \in [1, N]$}
2: {Output: Array c_i ($i \in [1, k]$) such that $X = \sum_{i=1}^{k} \binom{c_i}{i}$ (Eq. 4.2)}
3: $cc \leftarrow N$;{the current next candidate for c_i};
4: **for** i **from** k **downto** 1 **do**
5: **repeat**
6: $cc \leftarrow cc - 1$; {the first candidate for c_k is $N - 1$};
7: $ccBinCoef \leftarrow \binom{cc}{i}$;
8: **until** $ccBinCoef \leq X$
9: $c_i \leftarrow cc$;
10: $X \leftarrow X - ccBinCoef$;
11: **end for**
12: **return** array c;

Algorithm 4.2. Combinadic Ranking (OFDM-IM IxS Receiver).

1: {Inputs: Array $c_k > \cdots > c_2 > c_1 \geq 0$, $N > c_k$, and $k \in [1, N]$}
2: {Output: $X = \sum_{i=1}^{k} \binom{c_i}{i}$ (Eq. 4.2)};
3: $X \leftarrow 0$;
4: **for** i **from** 1 **to** k **do**
5: $X \leftarrow X + \binom{c_i}{i}$;
6: **end for**
7: **return** X;

Combinadic unranking and ranking algorithms referred to by the IxS block of original OFDM-IM mapper. In the maximal spectral efficiency OFDM-IM mapper (Fig. 4.1b), these algorithms run in $O(N^2)$, surpassing the computational complexity of the Fourier transform algorithm.

4.4.1 Combinadic (Un)ranking Algorithm

The Combinadic unranking is shown in Alg. 4.1. It takes N, k and X as input parameters and outputs the array c_i, $i \in [1, k]$ such that $X = \sum_{i=1}^{k} \binom{c_i}{i}$ (Eq. 4.2). The *candidate* values for the coefficients c_i considered by the algorithm are $0, 1, \cdots, N-1$, which represent the indexes of the N subcarriers. The coefficients are determined from c_k until c_1 and the variable cc (line 3) stores the next candidate value for the current coefficient being computed. The first coefficient to be computed is c_k and its first candidate is $N - 1$. This is the value of cc in the very first execution of line 6. For every candidate value cc, the corresponding binomial coefficient $\binom{cc}{i}$ is computed and stored in the variable $ccBinCoef$ (line 7). If condition $ccBinCoef \leq X$ is satisfied (line 8), then the candidate value cc is confirmed as the value of c_i (line 9) and X is updated accordingly (line 10). This entire process repeats until all the remainder $k - 1$ coefficients are determined.

In a particular *worst-case* instance of Combinadic unranking (Alg. 4.1), the logic test of the inner loop (line 8) fails for $cc = N-1, N-2, \cdots, k$ in the first iteration of the outer loop, i.e. when the first coefficient c_k is being determined. Thus, c_k is assigned to $k-1$. This narrows the list of candidates (for the remainder $k-1$ coefficients) to the values $k-2, k-3, \cdots, 1, 0$. Since the combinatorial number

system ensures that all k coefficients are distinct and that c_k is the largest one, a candidate value that fails for c_k can be discarded for c_{k-1} and so on. Thus, after c_k is determined, there must be at least $k-1$ candidate values for the remainder $k-1$ coefficients. Because of this, there is only one logic test per candidate value in the inner loop regardless of the number of coefficients. Since there are N candidate values, the inner loop takes $O(N)$ time regardless of the outer loop. In each test of the inner loop, Combinadic relies on the multiplicative identity (Eq. 4.3) to compute the binomial coefficient value in $O(k)$ time.

$$\binom{N}{k} = \prod_{i=1}^{k} \frac{N-i+1}{i} \tag{4.3}$$

Therefore, the overall CC of the Combinadic unranking algorithm is $O(Nk)$. Considering the optimal SE configuration, $k = N/2$ and the complexity becomes $O(N^2)$, which is asymptotically higher than the $O(N \log N)$ complexity of the FFT block.

The Combinadic ranking is shown in Alg. 4.2. It takes the array of coefficients c_i, $i \in [1, k]$ from the OFDM-IM detector and performs a summation of the k binomial coefficients $\binom{c_1}{1} + \binom{c_2}{2} + \cdots + \binom{c_k}{k}$ (Eq. 4.2). Since each binomial coefficient $\binom{c_i}{i}$ can be calculated in $O(i)$ time by the multiplicative formula (Eq. 4.3), and i ranges from 1 to k, the total number of multiplications performed by the algorithm is $1 + 2 + \cdots + k = k(k+1)/2 = O(k^2)$. Considering the optimal OFDM-IM setup, $k = N/2$, the overall complexity becomes $O(N^2)$ as with Combinadic unranking.

4.4.2 OFDM-IM Mapper Throughput with Combinadic

We now analyze the SC throughput of the OFDM-IM mapper assuming the IxS block is implemented by the Combinadic algorithm [McCaffrey, 2004; Buckles and Lybanon, 1977] as in the original OFDM-IM design [Basar et al., 2013]. Considering the optimal OFDM-IM setup, the total number of bits per symbol is $N/2 + \lfloor \log_2 \binom{N}{N/2} \rfloor$, whereas the IxS complexity is $O(N^2)$, as previously analyzed. Thus, according to Def. 10, the resulting SC throughput must satisfy Ineq. (4.4) as follows, otherwise it nullifies over N.

$$\lim_{N \to \infty} \frac{N/2 + \lfloor \log_2 \binom{N}{N/2} \rfloor}{O(N^2)} \stackrel{?}{>} 0 \tag{4.4}$$

According to the theory of computational complexity, the wall-clock time taken by a particular implementation of a $O(N^2)$ algorithm is bounded by the function κN^2, in which the constant $\kappa > 0$ captures the wall-clock runtime taken by the asymptotic dominant instruction of the algorithm[3] on a real machine. In

[3]The instruction we choose to count in the analysis. Mostly, real or complex arithmetic

turn, the number of index modulated bits tends to $N - \log_2 \sqrt{N}$ as N grows (Lemma 2). With basic calculus, one can verify that the limit in Ineq. (4.4) tends to zero for arbitrarily large N regardless of the value of κ, as follows.

$$\lim_{N\to\infty} \frac{N/2 + N - \log_2 \sqrt{N}}{\kappa \cdot N^2} \quad = \quad 0 \tag{4.5}$$

Therefore, referring to the original Combinadic algorithm to implement the IxS block in the optimal SE configuration causes the SC throughput of the OFDM-IM mapper to nullify as N grows.

4.5 Optimal OFDM-IM Mapper

Our theoretical findings summarized in Theorem 1, disclose the conditions for the computational feasibility of the optimal OFDM-IM mapper. The theorem requires exactly $\Theta(N)$ steps for the mapper. Since the M-ary LUT block of the OFDM-IM mapper (Fig. 4.1b) already runs in $N/2 = O(N)$ computational steps, to meet the theorem we just need to demonstrate the IxS block can be implemented with $\Theta(N)$ computational steps.

In this subsection, we demonstrate two distinct designs for an SC optimal OFDM-IM mapper. The first design reported in [Queiroz et al., 2020] and discussed in Subsection 4.5.1, solves the trade-off between time complexity and storage faced by current LUT-based OFDM-IM mappers. It meets optimality without requiring an exponential amount of LUT entries. Yet, that mapper design still requires more table entries than OFDM's. Then, in Subsection 4.5.2, we show how the original OFDM-IM mapper can run in the same time and storage complexity of OFDM. This design is published in [Queiroz et al., 2020]. Based on that, in Subsection 4.5.3, we demonstrate that the OFDM-IM transmitter is comp-limited.

4.5.1 Optimal Mapper under Polynomial Storage Complexity

Theorem 1 points the OFDM-IM mapper must be as fast as OFDM's. In Lemma 4, we show that a LUTs can provide OFDM-IM mappers with the same asymptotic complexity efficiency of OFDM's. However, up to date designs LUTs require an exponential amount of entries under the maximal SE. For this reason, the literature recommends LUTs only for 'small' N [Lu et al., 2018],[Basar et al., 2017]. We calculate the order of growth of LUT entries for the optimal setup in Lemma 5.

Lemma 4 (LUT-Based OFDM-IM Mapper Complexity). A 2^{P_1}-entry LUT enables the OFDM-IM IxS to run in $O(N)$.

instructions for DSP algorithms.

Proof. Let $0 \leq X \leq 2^{P_1} - 1$ be the decimal representation of the P_1-bit input given to the IxS DSP block. If the IxS is a 2^{P_1}-entry LUT indexed from 0 to $2^{P_1} - 1$, then the k-list of active indexes corresponding to X is stored in the X-th entry of the table. Since LUTs are based on random access storage technology, any data can be retrieved in $O(1)$ time *after* the LUT index is read (which is X, in this case). Therefore, the time complexity of a LUT-based IxS is determined by the time to read X, which is $O(P_1) = O(\log_2 C(N, N/2)) = O(N - \log_2 \sqrt{N}) = O(N)$ (Lemma 2). Also, since the modulation of the $k = N/2$ active subcarriers follows as in the classic OFDM for $M = 2$, more $O(N/2)$ computations are required. Thus, if the IxS is implemented as a 2^{P_1}-entry LUT, the overall OFDM-IM mapper runs in $O(N) + O(N/2) = O(N)$ time.

Lemma 5 (OFDM-IM LUT Size Under Maximal SE). Under the ideal OFDM-IM setup, a LUT-based OFDM-IM mapper requires $\Theta(2^N/\sqrt{N})$ entries.

Proof. A LUT-based OFDM-IM mapper has one entry per each one of all possible $2^{P_1} = 2^{\lfloor \log_2 C(N,k) \rfloor}$ symbol waveforms. Since P_1 approaches $N - \log_2 \sqrt{N}$ as N grows (Lemma 2), the number of LUT entries approaches $\Theta(2^{N - \log_2 \sqrt{N}}) = \Theta(2^N/\sqrt{N})$.

In other words, the OFDM-IM mapping literature faces a trade-off between computational time and space complexities. Conversely, we note that the time-storage trade-off faced by current OFDM-IM mappers can be improved if the OFDM-IM mapper is assisted by the so-called Pascal's triangle (PT) instead of being implemented as a 2^{P_1}-entry LUT. Based on that, we propose the SC optimal mapper illustrated in Fig. 4.2. It consists of the original OFDM-IM mapper set to a single subblock and having the IxS algorithm assisted by a PT table. The PT table can be viewed as an $N \times k$ matrix that stores the result of $C(c_i, i)$ in row c_i and column i (Table 4.3). This way, the $O(i)$ iterations required to compute a single binomial coefficient $C(c_i, i)$ is replaced by a single query to the PT table. Therefore, the $O(k^2)$ iterations performed by the IxS algorithm to compute the k binomial coefficients $C(c_k, k), \cdots, C(c_1, 1)$ can be replaced by $O(k)$ queries to the PT table.

Note that the time complexity improvement achieved by the PT table does not change the k binomial coefficients selected by the IxS algorithm. Hence, both the vector of active indexes and the vector of complex baseband samples (denoted as I and $\mathbf{s}$ in Fig. 4.2, respectively) remain the same as in the original OFDM-IM mapper. In Lemma 6, we show that the number of binomial coefficient entries of the PT table grows polynomially on N even if all 2^{P_1} OFDM-IM waveforms are enabled.

Lemma 6 (Binomial Coefficients under Maximal SE). Under the ideal SE setup, the OFDM-IM Index Selector algorithm computes $O(N^2)$ distinct binomial coefficients. Thus, a $\Theta(N^2)$-entry PT table can be employed to reduce the IxS time complexity from $O(N^2)$ to $O(N)$.

Proof. Under the ideal OFDM-IM setup, the variables c_i and i of Combinadic

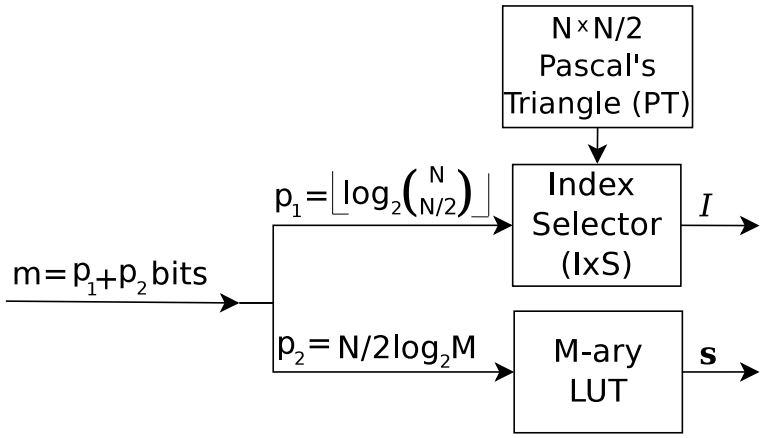

Figure 4.2: First proposed OFDM-IM mapper. Under maximal spectral efficiency, the value of any binomial coefficient $C(c_i, i)$ required in line 7 of the IxS block (Algorithm 4.1) matches an entry of the PT table shown in Table 4.3. By querying the table for each $C(c_i, i)$ instead of calculating them from scratch, the mapper achieves the same time complexity of the $\Theta(2^N/\sqrt{N})$-entry OFDM-IM look-up table but requiring only $\Theta(N^2)$ entries.

(Algorithm 4.1) decrease by 1 starting from $N-1$ and $k = N/2$, respectively. Hence, the algorithm needs to compute no binomial coefficient other than $C(c_i, i)$, $0 \leq c_i \leq N-1$ and $1 \leq i \leq N/2$. Therefore, the $\Theta(N^2)$-entry PT of Table 4.3 enables any binomial coefficient required by the IxS algorithm to be returned in $O(1)$ time. Thus, the inner loop of Combinadic reduces from $O(k) \times O(i)$ to $O(k) \times O(1)$, yielding to an overall complexity of $O(k) = O(N)$ in the ideal OFDM-IM setup.

Next, the Theorem 2 builds on Lemma 6 to show that the PT table can enable all 2^{P_1} OFDM-IM waveforms at the same time complexity of the OFDM mapper.

Theorem 2 (OFDM-IM Mapper under Polynomial Space). All 2^{P_1} OFDM-IM waveforms can be mapped at the same asymptotic time of an OFDM mapper at the expense of polynomial space complexity.

Proof. From Lemma 6, a PT table storing $\Theta(N^2)$ binomial coefficients enables the IxS algorithm to run in $O(N)$ time. This is the same asymptotic number of steps performed by the OFDM mapper. To achieve such time complexity keeping the ideal setup, a traditional LUT-based OFDM-IM mapper requires $\Theta(2^N/\sqrt{N})$ entries (Lemma 5). Thus, by replacing a LUT with an IxS algorithm assisted by the PT table, one enables the OFDM-IM mapper to achieve its ideal SE setup in $O(N)$ time at the expense of polynomial (rather than exponential) space.

It is worthy to remark that the PT table dates back from ancient times, even before Blaise Pascal[4]. Thus, the improvement it provides for the calculation of binomial coefficients is not a novelty for the field of combinatorial algorithms.

[4]for works prior to Blaise Pascal please, refer to en.wikipedia.org/wiki/Pascal's_triangle#History.

Table 4.3: Pascal's triangle of the Proposed OFDM-IM mapper (Fig. 4.2).

$c_i \vert i$	1	2	3	$\cdots$	$N/2$
0	0	0	0	$\cdots$	0
1	1	0	0	$\cdots$	0
2	2	1	0	$\cdots$	0
3	3	3	1	$\cdots$	0
4	4	6	4	$\cdots$	0
$\vdots$	$\vdots$	$\vdots$	$\vdots$	$\ddots$	$\vdots$
$N-1$	$\binom{N-1}{1}$	$\binom{N-1}{2}$	$\binom{N-1}{3}$	$\cdots$	$\binom{N-1}{N/2}$

Nonetheless, how this result turns out to affect the comparative SE performance of OFDM-IM and OFDM is beyond the scope of that literature.

4.5.2 Linear-time Combinadic (Un)ranking

In this subsection, we concern about improving Combinadic to $\Theta(N)$ time complexity under the same storage complexity of OFDM. It is worthy to remark that the literature in combinatorics report algorithms faster than the complexity required by our Theorem 1 e.g., [Parque and Miyasita, 2018], [Shimizu et al., 2014]. Such a performance, however, demands the number of active subcarriers k to be bounded by $o(N)$. Translated to the OFDM-IM domain, this means that such algorithms prevent the SE maximization (Corollary 2). Besides, In [Kokosiński, 1995], the author presents four unranking algorithms, out of which one (called "unranking-comb-D") can meet that requirement. Therefore, one can consider that algorithm to validate our theoretical findings. However, we remark that the Combinadic algorithm (referred to by the original OFDM-IM design) can benefit from the same properties of unranking-comb-D to run in $\Theta(N)$ rather than $O(N^2)$. Similarly, the ranking algorithm (not discussed in [Kokosiński, 1995]) can also run in $\Theta(N)$ as well. Next, we explain how to adapt Combinadic to enable the minimum possible CC when the maximal SE is allowed.

The main bottleneck in the time complexity of Combinadic (un)ranking (Alg. 4.1) is the inner loop. As previously explained, the inner loop takes k iterations, each of which demands further $O(i)$ iterations to compute the binomial coefficients $\binom{c_i}{i}$. Since i ranges from k to 1 and the optimal OFDM-IM setup imposes $k = O(N)$, this yields $k \cdot O(i) = N/2 \times O(N/2) = O(N^2)$. To improve this complexity without extra $O(N^2)$ storage, note that only the first candidate binomial coefficient $\binom{c_k}{k} = \binom{N-1}{N/2}$ needs to be computed from scratch (in $O(k)$ time). Thus, such computation can be performed outside both loops of Combinadic (Alg. 4.1) and stored in a variable we refer to as $ccBinCoef$.

The resulting modification is shown in line 4 of the Linear-time Combinadic unranking (Alg. 4.3). In this algorithm, the variables cc and $ccBinCoef$ denote the candidate values for c_i and $\binom{c_i}{i}$, respectively. Following $ccBinCoef = \binom{c_k}{k}$, the

next candidate binomial coefficient, either $\binom{N-1}{N/2-1}$ or $\binom{N-2}{N/2-1}$, can be computed from *ccBinCoef* itself in $O(1)$ time. In general, one can calculate $\binom{c_i-1}{i}$ and $\binom{c_i-1}{i-1}$ from $\binom{c_i}{i}$ by relying on the following respective equations [Kokosiński, 1995]:

$$\binom{c_i-1}{i} = ((c_i-i)*\binom{c_i}{i})/c_i \tag{4.6}$$

$$\binom{c_i-1}{i-1} = (i*\binom{c_i}{i})/c_i \tag{4.7}$$

The Eqs. (4.6) and (4.7) are exploited by lines 9 and 18 of Alg. 4.3, respectively. Thus, all remainder binomial coefficients within the logic test of the inner loop are computed in $O(1)$ time. Therefore, the complexity of Combinadic unranking improves from $k \cdot O(i) = N/2 \times O(N/2) = O(N^2)$ to $O(k) + k \cdot O(1)$, yielding $N/2 + N/2 \times O(1) = O(N)$ in the optimal OFDM-IM configuration.

As with the Combinadic unranking, one can also reduce the time complexity of the Combinadic ranking (Alg. 4.2) from $O(N^2)$ to $O(N)$ by computing $\binom{c_i+1}{i}$ and $\binom{c_i+1}{i+1}$ from $\binom{c_i}{i}$ in $O(1)$ time rather than from scratch in $O(i)$ time with the multiplicative formula (Eq. 4.3). However, these $O(1)$-time properties require the values in the array c to be consecutive, which can not be the case of OFDM-IM because these values depend on the data the user transmits. One can avoid calculating all k binomial coefficients from scratch by relying on the fact that the values $c_k > \cdots > c_2 > c_1$ are restricted to the integer range $[0, N-1]$.

Based on this, the linear-time Combinadic ranking (Alg. 4.4) computes from scratch only one binomial coefficient (we refer to as *ccBinCoef*, line 10) from which at most $N-1$ other coefficients can be computed sequentially in $O(1)$ time each. Since the value of all other coefficients is computed from *ccBinCoef*, this variable cannot be initialized with null binomial coefficients i.e., $\binom{c_i}{i}$ such that $c_i < i$. Thus, from lines 4 to 9, Alg. 4.4 looks for the largest i in the range $[0, \cdots, i, \cdots, N-1]$ such that $c_i \geq i$. These lines take $O(k)$ iterations. In line 10, *ccBinCoef* is initialized as $\binom{c_i}{i}$ in $O(i)$ time, yielding a cumulative complexity of $O(k) + O(k) = O(k)$. From this, any consecutive binomial coefficient (either $\binom{c_i+1}{i}$ or $\binom{c_i+1}{i+1}$) can be computed in $O(1)$ time from $ccBinCoef = \binom{c_i}{i}$ as in the linear-time unranking algorithm. Since the total number of remainder binomial coefficients ranges from i to $N-1$, the loop in line 11 computes all of them in $O(N-i) = O(N)$ time. Therefore, the overall complexity is $O(k)+O(k)+O(N)$ which becomes $O(N)$ under the optimal OFDM-IM setup (i.e., $k = N/2$).

4.5.3 OFDM-IM as Non Comp-Limited Signal

We now proceed with the SC analysis of the optimal OFDM-IM mapper (Fig. 4.1b) considering an IxS implementation that meets our Theorem 1. The analysis is as in Subsection 4.4.2, except for the fact that the IxS algorithm runs

Algorithm 4.3. Linear-time Combinadic Unranking (OFDM-IM Index Selector Transmitter).

1: {Inputs: X, N, and $k \in [1, N]$}
2: {Output: Array c_i ($i \in [1, k]$) such that $X = \sum_{i=1}^{k} \binom{c_i}{i}$ (Eq. 4.2)}
3: $cc \leftarrow N - 1$; {largest candidate for c_i};
4: $ccBinCoef \leftarrow \binom{cc}{k}$; {candidate value for $\binom{c_k}{k}$};
5: **for** i **from** k **downto** 1 **do**
6: $c_i \leftarrow cc$;
7: **while** $ccBinCoef > X$ **do**
8: {Below, $\binom{c_i-1}{i}$ is computed from $\binom{c_i}{i}$ in $O(1)$};
9: $ccBinCoef \leftarrow ((c_i - i) * ccBinCoef)/c_i$;
10: $c_i \leftarrow c_i - 1$;
11: **end while**
12: $X \leftarrow X - ccBinCoef$;
13: {Below, $\binom{c_i-1}{i-1}$ is computed from $\binom{c_i}{i}$ in $O(1)$};
14: $cc \leftarrow c_i - 1$;
15: **if** $cc = 0$ **then**
16: **return** array c
17: **end if**
18: $ccBinCoef \leftarrow (i * ccBinCoef)/c_i$;
19: **end for**
20: **return** array c

Algorithm 4.4. Linear-time Combinadic Ranking (OFDM-IM Index Selector Receiver).

1: {Inputs: Array $c_k > \cdots > c_2 > c_1 \geq 0$, $N > c_k$, and $k \in [1, N]$}
2: {Output: $X = \sum_{i=1}^{k} \binom{c_i}{i}$ (Eq. 4.2)};
3: $i \leftarrow 1$;
4: **while** $i \leq k$ **and** $c_i < i$ **do**
5: $i \leftarrow i + 1$;
6: **end while**
7: **if** $i > k$ **then**
8: **return** 0;
9: **end if**
10: $ccBinCoef \leftarrow \binom{c_i}{i}$; $X \leftarrow 0$;
11: **for** cc **from** c_i **to** $N - 1$ **do**
12: **if** $c_i = cc$ **then**
13: $X \leftarrow X + ccBinCoef$;
14: $ccBinCoef \leftarrow (ccBinCoef * (c_i + 1))/(i + 1)$;
15: $i \leftarrow i + 1$;
16: **else**
17: $ccBinCoef \leftarrow (ccBinCoef * (cc + 1))/(cc + 1 - i)$;
18: **end if**
19: **end for**
20: **return** X;

Adaptation of the Combinadic algorithms (unranking 4.1 and ranking 4.2) referred to by the original OFDM-IM mapper to run in $O(N)$ time. We prove these adaptations enable the overall OFDM-IM mapper to maximize the spectral efficiency gain over OFDM while consuming the same time and space computational complexities of the classic OFDM mapper.

in $\Theta(N)$ time complexity. Thus, the SC throughput is given by

$$\lim_{N \to \infty} \frac{N/2 + N - \log_2 \sqrt{N}}{\kappa \cdot N} \tag{4.8}$$

As N grows, the time complexity is bounded by κN for some constant $\kappa > 0$.

Similarly, the SC throughput of the mapper results in a non-null constant $\kappa > 0$, meeting the Def. 10. As explained in the Subsection 4.4.2, $\kappa > 0$ is constant that depends on the computational apparatus running the algorithm. Under the linear-time IxS complexity, the throughput of the OFDM-IM mapper does not nullify for arbitrarily large N,

$$\lim_{N\to\infty} \frac{N/2 + N - \log_2 \sqrt{N}}{\kappa \cdot N} = \frac{3}{2\kappa} > 0 \tag{4.9}$$

Note also that the throughput can increase with N if one achieves a $o(N)$ mapper. However, as demonstrated in Corollary 2, this conflicts with the optimal SE setup, thereby preventing the SE maximization.

The scalability of the IxS algorithm as shown in Eq. 4.9, also brings implication about the classification of the optimal OFDM-IM as a non comp-limited signal waveform, i.e. a waveform whose throughput is not nullified by the computational complexity overhead as the spectrum bandwidth gets arbitrarily large (Subsection 3.2.3).

The classification of a signal waveform as non comp-limited is conditioned to the asymptotic growth of its SC asymptotic capacity (Section 3.2.1). In turn, the SC capacity is the ratio between the maximum number of bits a waveform can modulate per symbol and the asymptotic complexity lower bound required to process these bits. As we explained in Subsection 4.3.2, although the ideal OFDM-IM setup outperforms OFDM in terms of SE, the number of bits per symbol grows at the same order on N for both waveforms. Regarding computational complexity, it is important to note that OFDM-IM has the same processing steps of OFDM unless by the IxS algorithm and the signal detection. Therefore, if those extra steps can be performed without increasing the complexity order of growth of OFDM, the classification of OFDM-IM as a non comp-limited signal is conditioned to the classification of OFDM non comp-limited signal. Based on that, we present the Lemma 7.

Lemma 7 (Condition for Non Comp-limited OFDM-IM Signal). If the basic OFDM waveform is a non comp-limited signal then the OFDM-IM waveform is a non comp-limited signal.

Proof. The classification of OFDM as a non comp-limited signal with constant number of bits per subcarrier (i.e., $M = \Theta(1)$) demands a $\Omega(N)$ overall asymptotic complexity (Proposition 2 of Subsection 3.4.3). OFDM-IM and OFDM have the same asymptotic complexity unless by the signal detector and the IxS algorithms. Assuming the employment of signal detection heuristics that run in $O(M)$ time complexity (e.g., [Hu et al., 2018], [Sandell et al., 2016]) and the $\Theta(N)$ time complexity of the IxS Algorithm 4.3) OFDM-IM does not increase the overall asymptotic complexity of OFDM. If OFDM verifies as a non comp-limited signal, it runs in $O(N)$ complexity. Since the extra complexity OFDM-IM adds to OFDM can be at most linear on N, OFDM-IM is non comp-limited too. Therefore, if the basic OFDM waveform is non comp-limited then the OFDM-IM waveform is non comp-limited too.

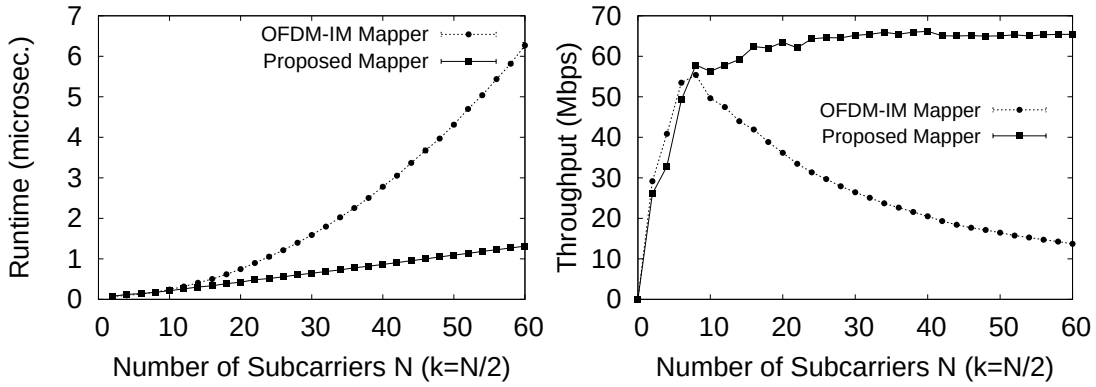

(a) Runtime.

(b) Throughput.

Figure 4.3: Mapper performance: Proposed vs. OFDM-IM.

4.6 Implementation and Evaluation

In this section, we present a practical case study to validate our theoretical findings. In Subsection 4.6.1, we introduce the open-source library we develop for the case study. In Subsection 4.6.2, we describe the methodology to assess and reproduce the empirical values of our experiments. Finally, in Subsection 4.6.3, we present the results of our practical case study that validate our theoretical findings.

4.6.1 Open-source OFDM-IM Mapper Library

We wrote a C++ library that implements all OFDM-IM steps to map/demap an N-subcarrier complex frequency-domain symbol. We implement the IxS block with C++ *callbacks* to enable flexible addition of novel (un)ranking algorithms. In the released version, we implement the original IxS algorithm [Basar et al., 2013] and all the algorithms presented in this chapter (Algs. 4.3 and 4.4). We do not implement (un)ranking algorithms that can reach a complexity that is asymptotically faster than required by our Theorem 1 e.g.[Parque and Miyasita, 2018; Shimizu et al., 2014]. As previously explained (Corollary 2), performing (un)ranking faster than $\Theta(N)$ would require $k \neq N/2$, thereby preventing the SE maximization (Corollary 2). However, future works may implement IxS algorithms that improve the original OFDM-IM using other criteria (e.g. BER [Yoon et al., 2019], [Wen et al., 2016].) than CC and SE. These and other IxS algorithms can also be included/evaluated in our library. The entire source code of our library, as well as detailed instructions on how to enhance it with novel IxS algorithms, are publicly available under the GPLv2 license in [Queiroz, 2020].

4.6.2 Performance Assessment Methodology

We assess the runtime $T(N)$ (in secs.) and the throughput $m(N)/T(N)$ (in megabits per seconds, Def. 9) for both the original OFDM-IM mapper and our proposed mapper under the optimal SE configuration (i.e., $g = 1$, $k = N/2$ and $M = 2$). For each mapper, we assess the performance indicators at both the transmitter (mapper) and the receiver (demapper) on a 3.5-GHz Intel i7-3770K processor.

We sampled the wall-clock runtime $T(N)$ of each mapper with the standard C++ `timespace` library [team, 2018] under the profile `CLOCK_MONOTONIC`. In each execution, we assigned our process with the largest real-time priority and employed the `isolcpus` Linux kernel directive to allocate one physical CPU core exclusively for each process. We generate the input for the mappers with the standard C++ 64-bit version of the Mersenne Twistter (MT) 19937 pseudo-random number generator [Matsumoto and Nishimura, 1998]. We set up three independent instances of MT19937_64 with seeds 1973272912, 1822174485 and 1998078925 [Hechenleitner and Entacher, 2002]. Every iteration, three sampled $T(N)$ are forwarded to the Akaroa-2 tool [McNickle et al., 2010] for statistical treatment. Akaroa-2 determines the minimum number of samples required to reach the steady-state mean estimation of a given precision. In our experiments, this precision corresponds to a relative error below 5% and a confidence interval of 95%. Besides, in all experiments the highest observed variance was below 10^{-3} and the average number of samples in the transient state was about 300.

Table 4.4 reports all assessed results for both the original OFDM-IM mapper and the proposed mapper at the transmitter (mapper). The table 4.5 reports the analogous results assessed at the receiver (demapper). From left to right, the tables present the following columns: the number N of symbol's subcarriers, the number $m(N)$ of bits per symbol, the SE gain of the original OFDM-IM waveform against the classic OFDM mapper[5], the assessed (de)mapper, the assessed runtime $T(N)$, the half-width of the confidence interval δ for $T(N)$, the achieved (de)mapping throughput, and the number x of samples needed to achieve the required precision. The source-code of all our experiments is publicly available under GPLv2 license in [Queiroz, 2020].

4.6.3 Results

In Fig. 4.3a and Fig. 4.3b, we respectively plot the runtime and the throughput performances of the compared mappers for $N = 2, 4, \ldots, 62$. Although only particular values of N verify in industry standards (e.g. $N = 48$ [IEEE 802.11, 2012], $N = 52$ [802.11, 2013]), we range it from small to large values to illustrate the asymptotic shape predicted by our throughput analysis. Detailed information about these plots are reported on the Table 4.4. As predicted by our theoretical analysis (Subsections 4.4.2 and 4.2.2), in the ideal setup, the runtime order of growth of the original OFDM-IM mapper is asymptotically larger than

[5]The maximum SE gain is $m(N)/N$ [Fan et al., 2015].

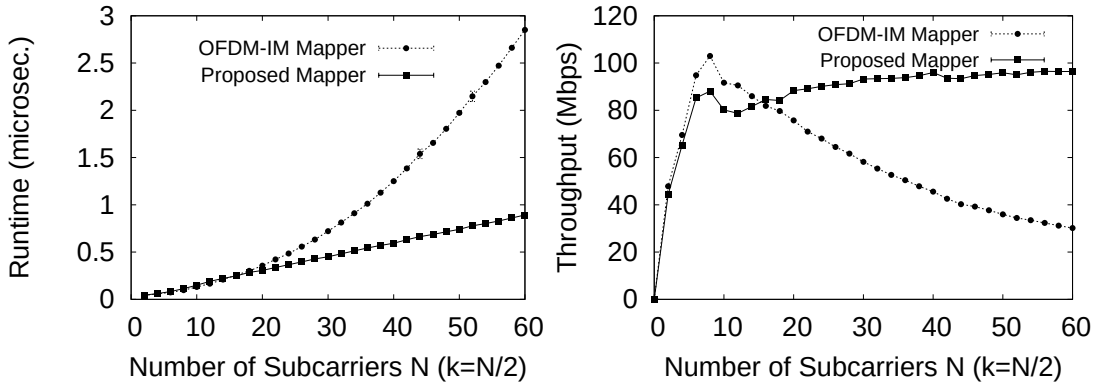

(a) Runtime. (b) Throughput.

Figure 4.4: Demapper performance: Proposed vs. OFDM-IM.

our proposed mapper (Fig. 4.3a). From the theoretical analysis, we know these complexities are $O(N^2)$ and $O(N)$, respectively. Naturally, the runtime curves of both mappers increase monotonically towards infinite as the number N of subcarriers grows. However, because the runtime order of growth of the original OFDM-IM mapper is larger than the number $m(N) = N/2 + \log_2 \binom{N}{N/2} = O(N)$ of bits per symbol, the throughput $m(N)/T(N)$ of this mapper nullifies as N grows (Fig. 4.3b). This validates the theoretical analysis we show in Subsection 4.4.2.

By contrast, when our proposed mapper takes place, both the resulting computational complexity $T(N)$ and the total of bits $m(N)$ per symbol increases in the same order of growth. Thus, the throughput $m(N)/T(N)$ tends to a non-null constant. In particular, according to our theoretical analysis in Subsection 4.5.3, this is $m(N)/T(N) = 3/(2\kappa)$. Recall that the constant $\kappa > 0$ captures the wall-clock runtime taken by the asymptotic dominant instruction of the algorithm on a real machine. However, in our practical case study, the assessed runtime $T(N)$ encompasses all computational instructions performed by each (de)mapper. Thus, κ represents an average of the runtime taken by each kind of instruction on the machine of our testbed i.e., the Intel i7-3770K processor. From the assessed throughput $m(N)/T(N)$, the average value of κ can be computed based on Eq. (4.9), which is $\kappa = 3/2 \cdot 1/(m(N)/T(N))$. In our testbed, the average runtime per computational instruction was 0.02 μs.

In Fig. 4.4a and Fig. 4.4b, we respectively plot the runtime and the throughput performances of the compared demappers for different values of N. Detailed informations of these plots are reported on the Table 4.5. As in the mapper analysis, the throughput of the original OFDM-IM demapper tends to zero as N grows whereas the throughput of our proposed demapper tends to a non-null constant under the same conditions. If compared against its corresponding mapper, we verify that our proposed demapper presents larger throughput. This means that, although both our mapper and demapper have the same $O(N)$ asymptotic complexity, the demapper implementation is less complex concerning the constant κ. Indeed, we verify an average $\kappa = 0.015$ μs for the demapper in

contrast with the 0.02 μs for the mapper.

4.7 Summary

In this chapter, we studied the trade-off between spectral efficiency (SE) and computational complexity (CC) $T(N)$ of an N-subcarrier OFDM with Index Modulation (OFDM-IM) mapper. We identified that the CC lower bound to map any of all $2^{\lfloor \log_2 \binom{N}{N/2} \rfloor}$ OFDM-IM waveforms is $\Omega(N)$. With this, we formally proved that enabling all OFDM-IM waveforms is not computationally intractable, as previously conjectured [Lu et al., 2018], [Basar et al., 2017]. Besides, we showed that any algorithm running faster than this lower bound prevents the OFDM-IM SE maximization. Based on the SC analysis, we proved that the worst tolerable CC for the mapper is $O(N)$ otherwise, the mapper's throughput nullifies as the system is assigned more and more subcarriers. We showed that this is the case of the original OFDM-IM mapper [Basar et al., 2013], in which the $O(N^2)$ CC surpasses the $O(N \log_2 N)$ CC of the FFT algorithm. Then, we presented an OFDM-IM mapper that enables the largest SE under the minimum possible CC.

We demonstrate our theoretical findings by implementing an open-source library that supports all DSP steps to map/demap an N-subcarrier complex frequency-domain OFDM-IM symbol. Our implementation supports different index selector algorithms and is the first to enable the SE maximization while preserving the same time and space asymptotic complexities of the classic OFDM mapper. With our library, *we showed that the OFDM-IM mapper does not need compromise approaches that prevail in the OFDM-IM literature such as subblock partitioning (SP) [Mao et al., 2018; Mao et al., 2017b; Basar et al., 2017; Fan et al., 2015; Basar et al., 2013] or adoption of few active subcarriers [Salah et al., 2019].*

Table 4.4: Mapper performance: Proposed ('Prop.') vs. OFDM-IM ('Orig.')

N	$m(N)$ bits	IM Gain	IM Mapper	**Runtime** (μs)	$\pm\delta$ (μs)	**Through put (Mbps)**	x
4	4	1.00	Prop.	**0.12**	0.001	**32.81**	1854
			Orig.	**0.10**	0.002	**40.86**	1710
6	7	1.17	Prop.	**0.14**	0.003	**49.23**	1704
			Orig.	**0.13**	0.003	**53.48**	1656
8	10	1.25	Prop.	**0.17**	0.001	**57.84**	1686
			Orig.	**0.18**	0.001	**55.40**	1602
10	12	1.20	Prop.	**0.21**	0.001	**56.29**	1536
			Orig.	**0.24**	0.002	**49.65**	2208
12	15	1.25	Prop.	**0.26**	0.002	**57.78**	1614
			Orig.	**0.32**	0.003	**47.47**	1872
14	18	1.28	Prop.	**0.30**	0.002	**59.21**	1524
			Orig.	**0.41**	0.003	**43.99**	1542
16	21	1.31	Prop.	**0.34**	0.002	**62.39**	1728
			Orig.	**0.50**	0.004	**41.92**	1476
18	24	1.33	Prop.	**0.39**	0.002	**62.03**	1596
			Orig.	**0.62**	0.005	**38.85**	1494
20	27	1.35	Prop.	**0.43**	0.002	**63.45**	1524
			Orig.	**0.75**	0.007	**36.18**	1554
22	30	1.36	Prop.	**0.48**	0.002	**62.10**	1884
			Orig.	**0.90**	0.008	**33.46**	1518
24	33	1.38	Prop.	**0.51**	0.002	**64.31**	1554
			Orig.	**1.05**	0.043	**31.35**	1512
26	36	1.38	Prop.	**0.56**	0.001	**64.61**	1560
			Orig.	**1.21**	0.007	**29.70**	1470
28	39	1.39	Prop.	**0.60**	0.002	**64.55**	1536
			Orig.	**1.40**	0.012	**27.92**	1512
30	42	1.40	Prop.	**0.64**	0.003	**65.19**	1518
			Orig.	**1.59**	0.016	**26.43**	1476
32	45	1.41	Prop.	**0.69**	0.010	**65.43**	1524
			Orig.	**1.79**	0.012	**25.07**	1548
34	48	1.41	Prop.	**0.73**	0.003	**65.93**	1560
			Orig.	**2.03**	0.018	**23.70**	1518
36	51	1.42	Prop.	**0.78**	0.008	**65.47**	1500
			Orig.	**2.25**	0.015	**22.63**	1482
38	54	1.42	Prop.	**0.82**	0.002	**65.96**	1608
			Orig.	**2.50**	0.017	**21.57**	1776
40	57	1.42	Prop.	**0.86**	0.002	**66.16**	1524
			Orig.	**2.78**	0.027	**20.51**	1530
42	59	1.40	Prop.	**0.91**	0.003	**65.06**	1620
			Orig.	**3.05**	0.019	**19.33**	1458
44	62	1.41	Prop.	**0.95**	0.003	**65.02**	1686
			Orig.	**3.37**	0.027	**18.41**	1518
46	65	1.41	Prop.	**1.00**	0.002	**65.10**	2118
			Orig.	**3.68**	0.055	**17.68**	1548
48	68	1.42	Prop.	**1.05**	0.002	**64.98**	1536
			Orig.	**3.97**	0.022	**17.13**	1476
50	71	1.42	Prop.	**1.09**	0.010	**65.04**	1530
			Orig.	**4.31**	0.035	**16.47**	1494
52	74	1.42	Prop.	**1.13**	0.002	**65.31**	1578
			Orig.	**4.70**	0.022	**15.75**	1494
54	77	1.42	Prop.	**1.18**	0.002	**65.03**	1470
			Orig.	**5.04**	0.025	**15.28**	1500
56	80	1.43	Prop.	**1.23**	0.002	**65.31**	1440
			Orig.	**5.44**	0.026	**14.71**	1536
58	83	1.43	Prop.	**1.27**	0.004	**65.42**	2064
			Orig.	**5.82**	0.035	**14.27**	1512
60	86	1.43	Prop.	**1.31**	0.003	**65.42**	1614
			Orig.	**6.27**	0.073	**13.72**	1476
⋮	⋮	⋮	⋮	⋮	⋮	⋮	⋮
∞	$\Theta(N)$	1.5	Prop.	$\Theta(N)$	0	$3/(2\kappa)$	∞
			Orig.	$\Theta(N^2)$	0	0	∞

Table 4.5: Demapper performance: Proposed ('Prop.') vs. OFDM-IM ('Orig.').

N	$m(N)$ bits	IM Gain	IM Mapper	**Runtime** (μs)	$\pm\delta$ (μs)	**Through put (Mbps)**	x
4	4	1.00	Prop.	**0.06**	0.001	**65.25**	1674
			Orig.	**0.06**	0.000	**69.57**	1620
6	7	1.17	Prop.	**0.08**	0.001	**85.26**	1758
			Orig.	**0.07**	0.001	**94.85**	1746
8	10	1.25	Prop.	**0.11**	0.001	**88.11**	2208
			Orig.	**0.10**	0.001	**102.99**	1626
10	12	1.20	Prop.	**0.15**	0.002	**80.16**	1518
			Orig.	**0.13**	0.001	**91.67**	1704
12	15	1.25	Prop.	**0.19**	0.002	**78.70**	1524
			Orig.	**0.17**	0.002	**90.53**	1536
14	18	1.28	Prop.	**0.22**	0.001	**81.63**	1536
			Orig.	**0.21**	0.001	**86.00**	1614
16	21	1.31	Prop.	**0.25**	0.002	**84.58**	1512
			Orig.	**0.26**	0.001	**81.87**	1758
18	24	1.33	Prop.	**0.29**	0.003	**84.18**	1536
			Orig.	**0.30**	0.002	**79.68**	1524
20	27	1.35	Prop.	**0.31**	0.002	**88.32**	1542
			Orig.	**0.36**	0.001	**75.74**	1614
22	30	1.36	Prop.	**0.34**	0.004	**89.13**	1596
			Orig.	**0.42**	0.002	**70.99**	1542
24	33	1.38	Prop.	**0.37**	0.003	**90.11**	1488
			Orig.	**0.49**	0.007	**68.03**	1704
26	36	1.38	Prop.	**0.40**	0.003	**90.86**	1500
			Orig.	**0.56**	0.001	**64.49**	1530
28	39	1.39	Prop.	**0.43**	0.008	**91.23**	1482
			Orig.	**0.63**	0.003	**61.69**	1626
30	42	1.40	Prop.	**0.45**	0.002	**93.23**	1566
			Orig.	**0.72**	0.001	**58.20**	1548
32	45	1.41	Prop.	**0.48**	0.007	**93.38**	1464
			Orig.	**0.81**	0.002	**55.35**	1476
34	48	1.41	Prop.	**0.51**	0.003	**93.51**	1602
			Orig.	**0.91**	0.001	**52.67**	1560
36	51	1.42	Prop.	**0.54**	0.011	**93.82**	1548
			Orig.	**1.01**	0.002	**50.42**	1878
38	54	1.42	Prop.	**0.57**	0.002	**94.62**	1500
			Orig.	**1.13**	0.002	**47.85**	1512
40	57	1.42	Prop.	**0.59**	0.003	**95.99**	1464
			Orig.	**1.25**	0.003	**45.58**	1548
42	59	1.40	Prop.	**0.63**	0.003	**93.58**	1548
			Orig.	**1.39**	0.014	**42.58**	1722
44	62	1.41	Prop.	**0.66**	0.002	**93.37**	1464
			Orig.	**1.54**	0.051	**40.27**	2259
46	65	1.41	Prop.	**0.69**	0.001	**94.68**	1512
			Orig.	**1.66**	0.002	**39.27**	1656
48	68	1.42	Prop.	**0.71**	0.006	**95.18**	1554
			Orig.	**1.80**	0.006	**37.68**	1548
50	71	1.42	Prop.	**0.74**	0.002	**95.88**	1458
			Orig.	**1.97**	0.013	**35.98**	1488
52	74	1.42	Prop.	**0.78**	0.009	**95.05**	1530
			Orig.	**2.15**	0.055	**34.45**	1506
54	77	1.42	Prop.	**0.80**	0.002	**96.08**	1542
			Orig.	**2.30**	0.002	**33.49**	1548
56	80	1.43	Prop.	**0.83**	0.002	**96.50**	1572
			Orig.	**2.47**	0.003	**32.35**	1512
58	83	1.43	Prop.	**0.86**	0.003	**96.42**	1566
			Orig.	**2.66**	0.002	**31.19**	1524
60	86	1.43	Prop.	**0.89**	0.003	**96.41**	1482
			Orig.	**2.85**	0.002	**30.16**	1506
⋮	⋮	⋮	⋮	⋮	⋮	⋮	⋮
∞	$\Theta(N)$	1.5	Prop.	$\Theta(N)$	0	$3/(2\kappa)$	∞
			Orig.	$\Theta(N^2)$	0	0	∞

Chapter 5

Is FFT Fast Enough for Beyond 5G Communications?

"Vote for me, it can't get worse than this."

(Tiririca)

Contents

Chapter 3 demonstrates that the FFT algorithm does not enable OFDM as a non comp-limited signal, i.e., FFT causes the throughput of the OFDM to nullify as spectrum grows. This chapter presents a broader SC analysis of the Discrete Fourier Transform (DFT) computational problem in the context of OFDM waveforms. The analysis is generalized for all DFT

algorithms and considers the implications of constraining the DFT complexity with the runtime deadline imposed by the Nyquist sampling theorem. The chapter pursues a non comp-limited alternative for the FFT-OFDM solution. This chapter is organized as follows.

Section 5.1 reviews the historical roots of the DFT problem and the OFDM waveform. Besides, it discusses how the future scenario of wireless communications introduces a case for the joint analysis of the DFT complexity and the OFDM throughput. Section 5.2 presents a joint throughput-complexity analysis of the DFT problem and the FFT algorithm. It also states the sampling-complexity (Nyquist-Fourier) trade-off. Section 5.3 presents the parameterized DFT (PDFT) algorithm as a more efficient alternative to the FFT-OFDM status-quo waveform. Section 5.4 presents a comparative performance among FFT and the PDFT algorithms and validate the theoretical results. Section 5.5 summarizes the chapter.

5.1 FFT Complexity and OFDM Throughput: Trade-Off and Related Work

The Fast Fourier Transform (FFT) algorithm [Cooley and Tukey, 1965] is among the top-ten most relevant algorithm of the 20th century [Madey et al., 2005]. FFT outperforms the classic $O(N^2)$ DFT algorithm by running in $O(N \log_2 N)$ time complexity. Particularly for signal communication processing, FFT revolutionized the OFDM design by replacing a bank of expensive synchronized analog oscillators by a single digital chip that requires a single oscillator. Ever since, FFT has been employed as frequency/time transform algorithm by several multicarrier and single carrier waveforms [Gerzaguet et al., 2017].

However, in recent discussions, scholars have doubted the performance abilities of FFT to modulate signals in the so-called future sixth generation (6G) of wireless networks [Madanayake et al., 2020a], [Rappaport et al., 2019]. They point that 6G waveforms are expected to leverage symbol throughput to the order of Terabit per second (Tbit/s), which envisions signals operating in the so-called Terahertz (THz) frequency band of the electromagnetic spectrum i.e., 0.1-10 $\times 10^{12}$ Hz [Zhao et al., 2019]. To alleviate the power consumption implied by the FFT complexity in such massive channel bandwidths, Rappaport et al. [Rappaport et al., 2019] suggest to give up the "perfect fidelity" of the DFT computation on behalf of (slightly) more error-prone approximation algorithms [Madanayake et al., 2020b]. This suggests that waveform designers should consider computational complexity as a performance indicator as relevant as Bit-Error Rate (BER) for the post-5G generation of wireless networks.

As novel standards adopt wider and wider bandwidths to reach faster data rates, the number of DFT points increases, causing the number of computational instructions to grow regardless of the chosen algorithm. As starting point of this work, we wonder about the computational complexity limits of the exact

DFT, particularly the FFT algorithm. In other words, *does the FFT complexity nullify its throughput as the number of input points N grows?* To the best of our knowledge, a comprehensive formal answer to that question lacks in the literature.

Usually, signal processing literature refers to the classic asymptotic analysis of algorithms to calculate the number of computational instructions (usually, complex multiplications) required to perform DFT for a given value of N. However, predicting the number of complex multiplications for a given N cannot answer whether the $O(N \log_2 N)$ complexity of FFT is sufficiently fast to process larger and larger signals. To fill this gap, the current complexity analysis model need to handle certain limitations, as we explain next.

First, in the field of computational complexity, the presentation of a polynomial-time algorithm (as is the case of FFT) suffices to assert the computational tractability of a the problem it copes with. However, that class of algorithms may fail to meet specific runtime constraints of the signal communication field. When operating in the context of multicarrier waveforms such as Orthogonal Frequency Division Multiplexing (OFDM) and variants, FFT typically must feed a Digital-to-Analog / Analog-to-Digital (DAC/ADC) sampler within the symbol period to ensure unmistakable discrete to/from analog conversion.

As N grows, the inter-sample time interval (hence, the N time samples that compose the symbol period) is given by the Nyquist sampling theorem. Because the DFT computation is constrained by the symbol period, there is a natural relationship between asymptotic lower bound of the DFT computational problem and the Nyquist theorem. However, as far as we know, such relationship remains uncaptured by both the signal processing and computational complexity literature.

Second, differently from the theory of computational complexity, in the field digital communication signals the algorithm input length is also a relevant indicator of performance because it is a measure of signal throughput. However, neither the field of analysis of algorithms concerns about the input length maximization as a performance target nor the communication signal theory considers the relationship between asymptotic complexity and throughput. In fact, the classic symbol throughput formula taught by signal processing textbooks e.g., [Proakis and Salehi, 2008] measures the number of bits per symbol (over-the-air) period of time, thereby assuming the hardware budget scales on the computational complexity such that signal processing wall-clock runtime becomes totally negligible. In baseband processors where such assumption is reasonable, computational complexity impact other indicators. For instance, [Thompson, 1979], [Thompson, 1980] present asymptotic lower bounds relating the DFT complexity to the silicon area required to implement DFT on a single chip and [Ailon, 2015] present evidences that the FFT complexity is hard to beat. However, these studies do not cover the DFT complexity limits considering the symbol throughput. The need for such joint analysis has been pointed as relevant for beyond-5G wireless networks [Zhao et al., 2019] but it still lacks in the literature.

This chapter builds on [Queiroz et al., 2020]. We study the capacity and complexity limits of the DFT problem hence its feasibility for future extremely wide bandwidth signals. We investigate the condition of scalability of different DFT algorithms and enhance the SC analysis to account the Nyquist deadline constraint on the minimum required complexity of DFT algorithms. We identify that the throughput of FFT nullifies on N and its power of two $N = 2^i$ $(i > 0)$ constraint causes the complexity to grow exponentially as spectrum widens. This result is generalized to show that no exact DFT algorithm scales its throughput on N (for a specific value of M) unless the asymptotic complexity lower bound of the DFT problem verifies as $\Omega(N)$. Currently, this DFT lower bound remains an open "fascinating" question in field of computational complexity [Lokam, 2009]. To overcome the FFT scalability issues we found out, we consider the alternative formulation of frequency-time transform employed in Vector OFDM (V-OFDM) [Xiang-Gen Xia, 2001], a waveform that replaces an N-point FFT by N/n $(n = 2^j > 0)$ smaller FFTs to mitigate the cyclic prefix overhead of OFDM. Based on that, we report the following contributions:

- We present a joint throughput-complexity study of the frequency-time transform of the V-OFDM waveform. In this context, we replace FFT by DFT to relax the power of two constraint on N and to provide V-OFDM with flexible numerology (e.g. $n = 3$, $N = 156$). Besides, we apply the parameterized complexity technique [Downey and Fellows, 2012] on the DFT algorithm, getting what we refer to as the Parameterized DFT (PDFT) algorithm. By setting $n = \Theta(1)$, PDFT runs linearly on N rather than exponentially on i (as is the case of FFT);
- We identify a particular setup in which PDFT becomes multiplierless requiring only $O(N)$ complex sums. Although this does not solve the Nyquist-Fourier trade-off – because $\Theta(N)$ additions are still necessary – the solution dispenses complex multiplications, which is the most expensive computational instruction of a typical DFT circuit design. This way, we believe our results constitute a relevant step towards the practical deployment of the digital baseband part of multicarrier Terahertz signals.

5.2 DFT Spectro-Computational Asymptotic Analysis

In this section, we analyze the SC throughput of the DFT problem and some of its algorithms. In Subsection 5.2.1, we study the joint throughput-complexity asymptotic limit of the DFT problem. Then, in Subsection 5.2.2, we analyze the SC throughput of the FFT algorithm to respond whether it is sufficiently fast to process signals of increasing throughput. Finally, in Subsection 5.2.3, we relate the DFT complexity with the Nyquist sampling interval and introduce what we refer to as the sampling-complexity (Nyquist-Fourier) trade-off. The notation and symbols used throughout the paper are summarized in Table 5.1.

Table 5.1: Notation and symbols of the chapter.

Symbol	Usage
N	Number of subcarriers (DFT points)
Δf	Intercarrier space (Hz)
W	Symbol bandwidth (Hz)
M	Size of modulation points
$B(N)$	Bits per N-subcarrier symbol
$T(N)$	Complexity of an algorithm under an N-size input
$SC(N)$	Throughput of an algorithm under an N-size input
$\mathcal{L}_{DFT}(N)$	Complexity lower bound of the N-point DFT problem
$\mathcal{L}_{DFT}(N)$	Complexity lower bound of the d-bit multiplication problem
T_{NYQ}	Inter sample time interval (seconds)
j	Imaginary unity
$\mathbf{X}$	Complex frequency domain symbol
$\mathbf{Y}$	Complex time domain symbol
X_k	k-th complex frequency domain sample
Y_t	t-th complex time domain sample
$\mathbf{x}_l$	l-th frequency domain vector block
$\mathbf{y}_q$	q-th time domain vector block
L	Number of vector blocks and DFT size
M	Length of vector blocks
$\Omega(f)$	Order of growth asymptotically equal or larger than f
$O(f)$	Order of growth asymptotically equal or smaller than f
$\Theta(f)$	Order of growth asymptotically equal to f
$[\cdot]^T$	transpose of the matrix $[\cdot]$

5.2.1 Throughput-Complexity Limits of the DFT Computation

The IDFT at an OFDM transmitter consists in computing the complex discrete time samples Y_t, $t = 0, 1, \cdots, N-1$ of a symbol given the complex samples X_k that modulate the baseband frequencies $k = 0, 1, \cdots, N-1$. According to the Fourier analysis, such relationship is given by $Y_t = \sum_{k=0}^{N-1} X_k e^{j2\pi kt/N}$, $t = 0, 1, \cdots, N-1$, in which $i = \sqrt{-1}$ and $e = \lim_{x\to\infty}(1+1/x)^x = 2.718281\ldots$. At the receiver, a DFT algorithm takes the signal back from time to the frequency domain by performing $X_k = \sum_{t=0}^{N-1} Y_t e^{-j2\pi kt/N}$, $k = 0, 1, \cdots, N-1$. Since in each transform both k and t vary from 0 to $N-1$, it is easy to see that the resulting asymptotic complexity $T_{DFT}(N)$ is $O(N^2)$. The FFT algorithm improves this complexity to $O(N \log_2 N)$ at the constraint of $N = 2^i$, for some $i > 0$. For this reason, the number of FFT points (hence, channel width) at least doubles across novel wireless network standards targeting faster data rates, e.g., IEEE 802.11ax [IEEE, 2019]. For other details about DFT and FFT, please refer to [Kumar et al., 2019].

The SC analysis described in chapter 3 defines the SC throughput $SC(N)$ of an N-subcarrier signal processing algorithm as the ratio between the amount of useful transmission bits $B(N)$ carried by the symbol and computational complexity $T(N)$ taken to build the symbol. Also, the asymptotic growth of $SC(N)$ is bounded by a corresponding SC capacity which results from the ratio between the maximum number of bits $B_{MAX}(N)$ of the symbol and the asymptotic complexity lower bound $\mathcal{L}(N)$ of the computational problem. Next, we discuss $B_{MAX}(N)$ and $\mathcal{L}(N)$ for the DFT problem in the context of the OFDM waveform.

The SC capacity of the N-point DFT problem is built as follows. The quantity $B_{MAX}(N)$ results from the maximum number of bits modulated by an OFDM symbol. Denoting $M = 2^p$ (for some $p > 0$) as the length of the constellation diagram, it is given by

$$B_{MAX}(N) \;=\; N \log_2 M \tag{5.1}$$

As usual in the analysis of algorithms, the complexity accounts for the most recurrent and expensive computational instruction. For the DFT problem, this is the number of complex multiplications. Then, without loss of generality, $\mathcal{L}_{DFT}(N)$ captures the minimum asymptotic number of complex multiplications required by any existing or to-be-invented DFT algorithm. Now, let $\mathcal{L}_{MULT}(d)$ denote the asymptotic lower bond to perform a single complex multiplication between two d-bit complex numbers. In the case of OFDM,

$$d \;=\; \Theta(\log_2 M) \tag{5.2}$$

Therefore, the general capacity of OFDM is given in Def. 11.

Definition 11 (General Spectro-Computational Capacity of OFDM). Let $\mathcal{L}_{DFT}(N)$ be the minimum asymptotic number of complex multiplications required by the N-point DFT problem and $\mathcal{L}_{MULT}(d)$ be the complexity lower

bound of the d-bit multiplication problem. Let also $\log_2 M$ be the number of modulated bits per subcarrier. Since $\mathcal{L}_{DFT}(N)$ is not less complex than the remainder computational problems of the basic OFDM waveform (i.e., mapping and addition of cyclic prefix) the asymptotic throughput $SC_{DFT}(N)$ of the DFT algorithm defines the asymptotic throughput of the OFDM waveform. The SC capacity bounding this throughput is given as follows

$$SC_{DFT}(N) = O\left(\frac{N \log_2 M}{\mathcal{L}_{MULT}(d)\mathcal{L}_{DFT}(N)}\right) \tag{5.3}$$

Def. 11 establishes the foundations to determine whether OFDM is a comp-limited or a non comp-limited signal. Recall that the throughput of a comp-limited signal nullifies as N grows thereby the design of non comp-limited signals should be pursued by waveform designers. Since N is the variable of the SC asymptotic analysis, we need to discuss the asymptotic growth of M and d with relation to N.

Let us firstly assume a band-limited channel regime whose Signal-to-Noise ratio (SNR) does not grow arbitrarily on N. In this case, capacity grows linearly on the bandwidth and both the length of the constellation diagram and the number of bits per subcarrier are bounded by a constant. Under these conditions, the number of bits grows linearly on the bandwidth. This gives the condition to turn OFDM into a non comp-limited signal waveform as shown by Lemma 8.
Lemma 8 (Condition for Non Comp-Limited OFDM Signal with Bounded SNR). The N-subcarrier OFDM signal with a constant number of bits per subcarrier is comp-limited unless the N-point DFT problem lower bound $\mathcal{L}_{DFT}(N)$ verifies as $\Omega(N)$.

Proof. Consider Def. 11 under a band-limit channel with constant SNR, i.e.,

$$B_{MAX}(N) = Nd \tag{5.4}$$
$$M = \Theta(1) \tag{5.5}$$
$$d = \Theta(\log_2 M) = \Theta(1) \tag{5.6}$$

Neglecting all constants for the sake of the asymptotic analysis and considering the Eqs. 5.4, 5.5 and 5.6, the general SC capacity that bounds the throughput of OFDM (Eq. 5.3) turns into the following limit

$$SC_{DFT}(N) = \lim_{N\to\infty} \frac{N}{\mathcal{L}_{DFT}(N)} \tag{5.7}$$

If the minimum conjectured complexity for the N-point DFT problem (i.e., $\mathcal{L}_{DFT}(N) = \Omega(N)$ [Lokam, 2009]) does not verify as true, the SC capacity captured by the limit in Eq. 5.7 nullifies causing OFDM to be a comp-limited signal. Otherwise, the OFDM capacity does not nullify on N. Therefore, the OFDM waveform is comp-limited unless $\mathcal{L}_{DFT}(N) = \Omega(N)$. ■

If one relaxes the assumption $M = \Theta(1)$ by considering M can grow faster or as

fast as N (i.e., SNR grows on N), the Shannon channel capacity grows linearly on N and logarithmically on the SNR. If $M = \Theta(N)$, for example, then the number of bits per subcarrier grows as fast as $\log_2 N$. However, the complexity to multiply two d-bit binary numbers grows accordingly. Based on that, we present the Lemma 9.

Lemma 9 (Comp-Limited OFDM Signal under Unbounded SNR). The N-subcarrier OFDM signal waveform with $\Omega(N)$ bits per subcarrier is comp-limited unless the N-point DFT problem lower bound $\mathcal{L}_{DFT}(N)$ verifies as $\Omega(N)$ and the d-bit multiplication problem lower bound $\mathcal{L}_{MULT}(d)$ verifies as $\Omega(d)$.

Proof. Consider Def. 11 under a band-limit channel with a SNR such that

$$M \;=\; \Omega(N) \tag{5.8}$$

Then, the minimum asymptotic number of bits per subcarrier is such that

$$d \;=\; \Theta(\log_2 M) = \Theta(\log_2 N) \tag{5.9}$$

and the general SC capacity that bounds the throughput of OFDM (Eq. 5.3) turns into the following limit

$$SC_{DFT}(N) \;=\; \lim_{N\to\infty} \frac{N \log_2 N}{\mathcal{L}_{MULT}(\log_2 N)\mathcal{L}_{DFT}(N)} \tag{5.10}$$

Assuming the best-case scenario for the OFDM throughput, $\mathcal{L}_{DFT}(N)$ is linear on N and the OFDM capacity rewrites as

$$SC_{DFT}(N) \;=\; \lim_{N\to\infty} \frac{\log_2 N}{\mathcal{L}_{MULT}(\log_2 N)} \tag{5.11}$$

The SC capacity of OFDM captured by limit in Eq. 5.11 nullifies on N unless the lower bound $\mathcal{L}_{MULT}(d)$ verifies as $\Omega(d)$. ■

The complexity of the current fastest known algorithm for the d-bit multiplication problem is $O(d \log_2 d)$ [Harvey and Hoeven, 2020]. Although the exact lower bound of the problem remains unknown, evidences have strongly suggested that it is $\Omega(d \log_2 d)$ [Afshani et al., 2019], [Schonhage and Strassen, 1971]. Based on that, *we conjecture that the basic OFDM turns into a comp-limited signal if the number of bits per subcarrier grows as fast N at least.* For the remainder of this work, we assume Lemma 8 in which the number of bits per subcarrier is constant on N.

5.2.2 Spectro-Computational Analysis of the FFT Algorithm

The FFT algorithm [Cooley and Tukey, 1965] outperforms the classic $O(N^2)$ DFT algorithm by running in $O(N \log_2 N)$ time complexity. FFT performs $O(N)$ computational instructions to decrease an N-point DFT problem into two $N/2$-DFTs per iteration (or recursive calling). This is possible by noting that

the frequency samples X_k and $X_{k+N/2}$ ($k = 0, 1, \cdots, N/2-1$) can be computed from the same following $N/2$-point DFTs:

$$E_k = \sum_{t=0}^{N/2-1} Y_{2t} e^{\frac{-j2\pi tk}{N/2}} \tag{5.12}$$

$$O_k = e^{-j2\pi k/N} \sum_{t=0}^{N/2-1} Y_{2t+1} e^{\frac{-j2\pi tk}{N/2}} \tag{5.13}$$

In other words, E_k (Eq. 5.12) and O_k (Eq. 5.13) are the $N/2$-point DFT taken from the even-indexed and odd-indexed time samples of the N-point input array, respectively. Based on them, the Danielson–Lanczos lemma shows that,

$$X_k = E_k + e^{-j2\pi k/N} O_k \tag{5.14}$$

$$X_{k+N/2} = E_k - e^{-j2\pi k/N} O_k \tag{5.15}$$

This way, $N/2$ iterations are necessary to compute X_k and $X_{k+N/2}$, yielding a total of $O(N)$ computations. Each of these iterations needs to solve both the $N/2$-point DFTs E_k and O_k. Denoting $T(N)$ as the complexity of an N-point DFT and applying the Danielson–Lanczos lemma recursively, the overall complexity can be given by the recurrence relation $T(N) = O(N) + 2T(N/2)$ which is trivially verified as $O(N \log_2 N)$. Note, however, that FFT demands $N = 2^i$ ($i > 1$), yielding an exponential complexity of $O(2^i i)$ on i. The Corollary 3 follows from the $O(N \log_2 N)$ complexity of FFT.

Corollary 3 (Asymptotic Null FFT Throughput). The spectro-computational throughput of the FFT algorithm does nullify as N grows.

Proof. Let $T_{MULT}(d)$ be the computational complexity to multiply two d-bit numbers and and $T_{DFT}(N)$ the computational complexity of the N-point FFT algorithm. Following Def. 11, the FFT asymptotic throughput in OFDM is readily obtained

$$SC_{FFT} = \lim_{N\to\infty} \frac{Nd}{T_{MULT}(d) N \log_2 N} \tag{5.16}$$

If the SNR channel can get arbitrarily large such that the constellation diagram length M grows on N then $d = \Omega(\log_2 N)$. Recall that the complexity to multiply two d-bit numbers grows at least linearly on d. Thus, the asymptotic throughput of FFT is given by Eq. 5.17 at best.

$$SC_{FFT} = \lim_{N\to\infty} \frac{N \log_2 N}{N \log_2^2 N} = 0 \tag{5.17}$$

If the number of bits per subcarrier is constant, i.e., $d = \Theta(1)$, then $T_{MULT}(d) = \Theta(1)$ and the resulting FFT throughput in OFDM $1/\log_2 N$ nullifies in the same way. Therefore, the FFT throughput nullifies as N grows. ■

Fig. 5.1 illustrates the asymptotic growth of the FFT throughput for different

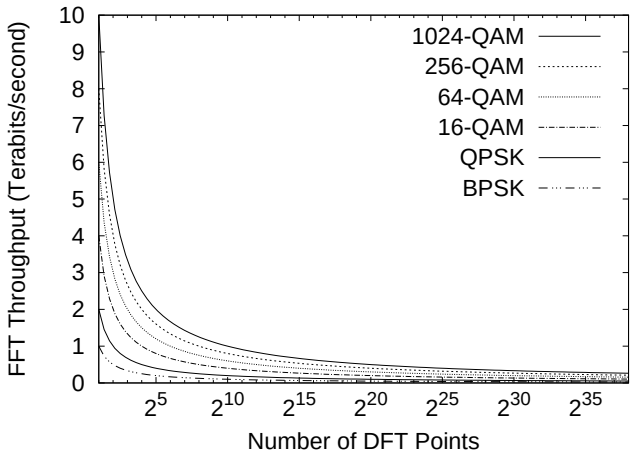

Figure 5.1: Asymptotic throughput of the FFT algorithm over distinct OFDM signal mappers. As the number of points increases, complexity grows faster than the number of modulated bits irrespective of the chosen mapper.

subcarrier signal mappers assuming a total of $T_{DFT} = N \log_2 N$ complex multiplications, each lasting 1 picosecond. Note that, in all cases, widening symbol spectrum by increasing the number of subcarriers causes the FFT throughput to decrease rather than increasing. The reason is that computational complexity grows asymptotically faster than the number of modulated bits on N. To overcome this bottleneck in practice, the hardware processing capability must scale on N.

We also note that the massive regime of subcarriers of future wireless networks can cause FFT to become unfeasible in practice. The reason is that FFT demands $N = 2^i$, leading to an exponential complexity of $O(2^i i)$. For nowadays narrow-width wireless networks, this complexity does not constitute a serious concern. However, as telecommunication standards evolve towards THz bands and beyond, such exponential complexity on i can become intractable.

5.2.3 The Sampling-Complexity Nyquist-Fourier Trade-Off

DFT algorithms face two particular issues in the context multicarrier waveforms such as OFDM. The first comes from a mismatch between the unit of processing of DFT algorithms and the other algorithms along the processing block diagram. Although blocks such as “signal mapping” and “cyclic prefix insertion” process a total of N signal samples, they can process them in a sample-by-sample basis. Thus, the processing of a particular sample does not depend on the value of other samples in those blocks.

By contrast, DFT algorithms can not start running before all N samples are loaded in the input because they operate in a symbol (i.e., batch-of-samples) basis. Hence, the unit of processing of DFT algorithms is N times higher than their preceding and succeeding processing blocks. As N grows, such mismatch

turns a DFT algorithm to become a bottleneck along the OFDM block diagram. This problem has been described by the digital radio design literature as a runtime deadline to be met by signal processing algorithms [Hessar et al., 2020], [Liu et al., 2019], [Hellstrom et al., 2019], [Drozdenko et al., 2018], [Tan et al., 2011]. By formalizing the problem as a trade-off between sampling and computational overhead, we can calculate the required asymptotic complexity to meet the sampling interval.

Second, DFT algorithms are responsible to feed the DAC in a classic OFDM transmitter. To avoid signal aliasing at the receiver, the transmitter must sample the time-domain signals produced by the IDFT algorithm within a specific time interval. This interval is calculated from the Nyquist sampling theorem which states that the largest time interval between two equally spaced (time-domain) samples of a signal band-limited to W Hz must be $T_{NYQ} = 1/(2W)$ seconds. In the case of complex IQ modulators where the real and imaginary dimensions of the signal are independently and simultaneously sampled by two parallel samplers, $T_{NYQ} = 1/W$ seconds.

In IQ systems, *at least* W samples must feed the DAC every second – which is known as the Nyquist sampling rate – otherwise the signal frequency can suffer from aliasing thereby preventing its correct identification at the receiver. For an inter-subcarrier space of Δf Hz, the width of an N-subcarrier OFDM signal is $W_{OFDM} = N\Delta f$, so a complex time-domain OFDM sample must feed the DAC every,

$$T_{NYQ} \quad = \quad \frac{1}{N\Delta f} \quad \text{seconds} \tag{5.18}$$

Based on Eq. 5.18, we relate the asymptotic complexity of DFT algorithms with the Nyquist interval. As result, we introduce the sampling-complexity (Nyquist-Fourier) trade-Off in Def. 12.

Definition 12 (The Sampling-Complexity Nyquist-Fourier Trade-Off). In OFDM radios with Δf Hz of inter-subcarrier space, the N-point DFT computational complexity $T_{DFT}(N)$ increases as the Nyquist period $1/(N\Delta f)$ decreases to improve symbol throughput.

The sequence of discrete time samples output by the IDFT algorithm corresponds to the time-domain version of the OFDM symbol that lasts $T_{SYM} = 1/\Delta f$ seconds. In the design of a real-time OFDM radio the entire digital signal processing must take no more T_{SYM}, otherwise the system either suffers from sample losses or misses the real-time communication capability [Hessar et al., 2020], [Liu et al., 2019], [Hellstrom et al., 2019], [Drozdenko et al., 2018; Tan et al., 2011]. We capture this condition in terms of asymptotic complexity in Lemma 10.

Lemma 10 (DFT Upper Bound for OFDM Waveforms). The computational complexity upper bound required to solve the DFT problem under the Nyquist interval constraint on radios with finite processing capabilities is $O(1)$.

Proof. Considering that a DFT algorithm is the asymptotically most complex procedure of the basic OFDM waveform, its complexity must satisfy

$$T_{DFT}(N) \leq T_{SYM} = NT_{NYQ} \tag{5.19}$$

To ensure that larger N translates into faster signals, the symbol period T_{SYM} must remain constant as N grows. From this, it does result

$$\lim_{N\to\infty} T_{DFT}(N) \leq T_{SYM} \tag{5.20}$$

$$T_{DFT}(N) = O(1) \tag{5.21}$$

■

Note that one can relax the complexity lower bound predicted by Lemma 10 if the radio digital baseband processing capabilities can grow arbitrarily on the number of subcarriers. However, with the end of the so-called "Moore's law" [Moore, 2003], higher processing capability translates into higher manufacturing cost, power consumption and hardware area, bringing doubts to the feasibility of portable multicarrier Terahertz radios.

The Corollary 4 follows from Lemma 10.
Corollary 4 (Unfeasible Nyquist-Constrained DFT). Given that the minimum possible lower bound complexity of the DFT problem is $\Omega(N)$ [Lokam, 2009] and the Nyquist interval imposes an upper bound of $O(1)$ (Lemma 10), *no DFT algorithm can meet the Nyquist interval as N grows.*

To face the result of the Corollary 4, one may relax the Nyquist constraint which results in the so-called compressive sensing systems [Qaisar et al., 2013]. However, high accuracy signal frequency prediction in such systems has been proved to be a NP-hard problem [Mousavi et al., 2019] which turns out to much more complex systems because only exponential time algorithms are known for that class of problems.

Note that the sampling-complexity trade-off does not restrict to multicarrier waveforms such as OFDM and its variants but also to single carrier signals that rely on DFT to mitigate the peak-to-average power ratio of uplink transmissions in wireless cellular networks [Zaidi et al., 2016]. The single carrier Frequency Division Multiple Access (FDMA, aka DFT-s-OFDM) [Myung et al., 2006], for example, mitigates PAPR by performing an extra DFT step before following the typical steps of an OFDM transmitter (i.e., precode). In turn, the single carrier Frequency Domain Equalization (FDE) waveform [Pancaldi et al., 2008] moves the IDFT computation from the transmitter to the receiver giving support for lower PAPR and mitigation of inter-symbol interference. Of course, the sampling-complexity trade-off is likely to be more critical in waveforms of broadband services since they pursue wider spectrum as wireless communication standards evolve. In any case, the entire DFT computation is batch-oriented and must be finished within the symbol period for samplers operating under the Nyquist sampling theorem.

5.3 Pushing the Throughput-Complexity Limits of DFT

In this section, we consider methods to overcome the throughput bottleneck faced by N-point DFT algorithms such as FFT (Section 5.2) and discuss a solution to mitigate the sampling-complexity trade-off described in Subsection 5.2.3.

5.3.1 Parameterized Complexity and Signal Vectorization

To mitigate the Nyquist-Fourier trade-off in practice, we apply an algorithm design technique inspired in the parameterized complexity [Downey and Fellows, 2012]. The parameterized complexity was originally proposed to enable the polynomial time solution of multi-parameter NP-complete problems. The idea consists in bounding one or more parameters of the problem such that the complexity of the solution becomes a polynomial function of the non-bounded parameters. For example, the vertex cover of an undirected graph G consisted of V vertices and E edges is a subset V' of V in which every edge of E has at least one of its vertices in V'. Finding out the minimum vertex cover of length $|V'|$ of a given $|V|$-vertex graph is a classic NP-complete problem [Karp, 1972], meaning that polynomial time algorithms are still unknown for the problem.

The parameterized complexity exploits scenarios in which $|V'|$ can be assumed much less than $|V|$ and bounded by some value (the parameter) g. Then, a parameterized algorithm for the problem is polynomial on $|V|$ and exponential only on g. This is the case of [Chen et al., 2006], whose $O(g|V| + 1.274^g)$ algorithm performs much better than $O(2^{|V|})$ for scenarios of bounded g and increasing $|V|$. For a comprehensive study about the parameterized complexity please, refer to [Downey and Fellows, 2012].

We consider an alternative formulation of frequency-time transform in which parameterization can enable faster-than FFT computations. In a typical OFDM transmitter, the IDFT operation associates N input frequency samples X_k ($k = 0, \cdots, N-1$) to N respective baseband frequencies k Hz at the time instant t by the complex multiplication $X_k e^{j2\pi kt/N}$. The direct IDFT algorithm repeats these N multiplications to compute N time samples, which yields a total of $O(N^2)$ operations. To cut this complexity, we parameterize the number $g \leq N$ of frequency samples associated to a given baseband frequency, as illustrated in Fig. 5.2. In the parameterized DFT scheme, all the N frequency samples are equally divided across g baseband frequencies k, leading to $n = N/g$ groups (solid rectangles) of g frequency samples each. An n-point IDFT across frequency samples of distinct groups (dashed rectangles), yields one g-sample time domain group per time instant $t = 0, 1, \cdots, n-1$, resulting in a total of $ng = N$ time domain samples.

We identify that the waveform resulting from the parameterized DFT computation we have just described is not new. Indeed, it exactly matches OFDM in its vectorized form (i.e., V-OFDM), a waveform originally proposed to reduce

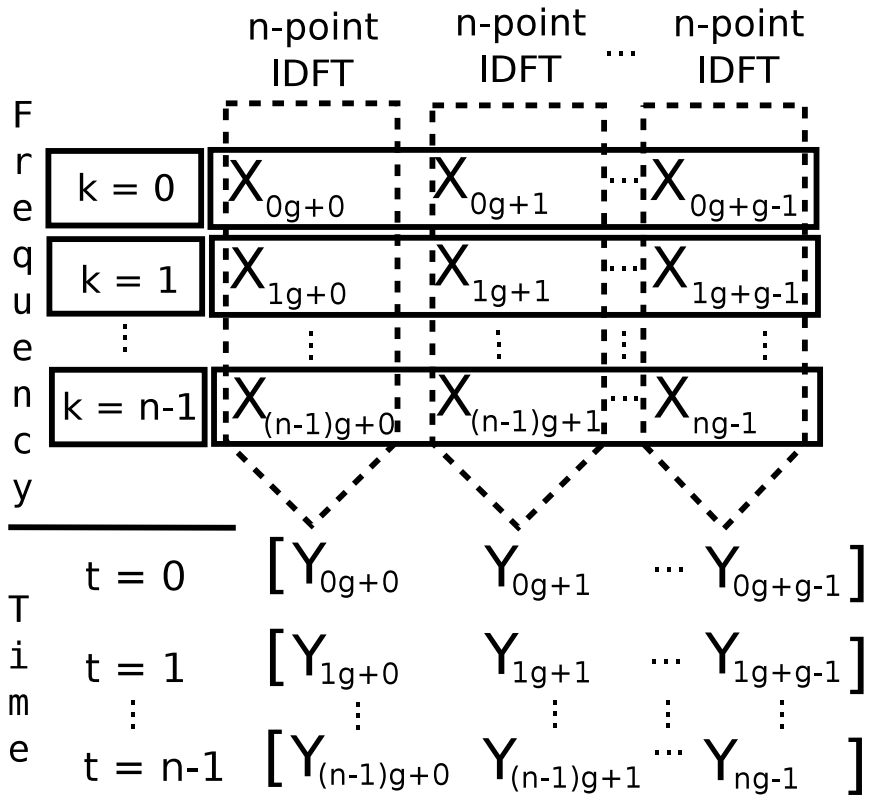

Figure 5.2: Frequency-time transform scheme of Vector OFDM. The N-size frequency domain input is arranged into n groups (solid rectangles) of frequency k and length $g = N/n$ each. We rely on the classic DFT algorithm (rather than FFT) to relax the power of two constraint on N and n and to parameterize n to $\Theta(1)$. This way, we achieve a flexible frequency-time transform whose complexity is effectively linear on N rather than exponential on i.

the cyclic prefix overhead of OFDM [Xiang-Gen Xia, 2001]. Prior works have investigated V-OFDM with respect to different aspects. Cheng et al. [Cheng et al., 2011] study the BER performance in Rayleigh channels and Li et al. [Li et al., 2012] identify setups in which the V-OFDM BER performs similarly or better than OFDM for different low-complexity receivers. More recently, V-OFDM has been merged with other signal processing techniques such as index modulation [Liu et al., 2017] and MIMO [Zhang et al., 2020].

Despite the valuable contributions of prior V-OFDM works, we identify that they impose the $N = 2^i$ constraint of OFDM on V-OFDM to benefit from the $O(N \log_2 N)$ complexity of FFT. That assumption was popularized by the basic OFDM waveform in which the employment of DFT (instead of FFT) does necessarily impair the asymptotic complexity. Thus, the spectrum numerology flexibility is sacrificed on behalf computational complexity. Our point is that, differently from OFDM, replacing FFT by the basic DFT in V-OFDM does not necessarily impair the resulting asymptotic complexity as it does in OFDM. In this sense, in Subsections 5.3.2 and 5.3.3, we review the V-OFDM signal and discuss how to relax the $N = 2^i$ constraint of V-OFDM keeping a complexity

that does not nullify throughput on N, respectively.

5.3.2 The Vector OFDM Signal

The V-OFDM transmitter arranges the N-sample complex frequency domain symbol $\{X_i\}_{i=0}^{N-1}$ into L complex Vectors Blocks (VBs) $\mathbf{x}_l$ $(l = 0, 1, \cdots, L-1)$ having $\mathsf{M} = N/L$ samples each. Denoting $[\cdot]^T$ as the transpose of the matrix $[\cdot]$, the samples of $\{X_i\}_{i=0}^{N-1}$ within the l-th VB $\mathbf{x}_l$ is given by

$$\mathbf{x}_l = [X_{l\mathsf{M}+\mathsf{m}}]^T \quad \mathsf{m} = 0, 1, \cdots, \mathsf{M}-1 \tag{5.22}$$

The sequence of complex frequency domain samples is

$$\mathbf{X} = [X_0, X_1, \cdots, X_{N-1}] \;=\; [{\mathbf{x}_0}^T, {\mathbf{x}_1}^T, \cdots, {\mathbf{x}_{L-1}}^T] \tag{5.23}$$

The q-th time domain VB $(q = 0, 1, \cdots, L-1)$ is denoted as

$$\mathbf{y}_q \;=\; [Y_{q\cdot\mathsf{M}+\mathsf{m}}]^T \quad \mathsf{m} = 0, 1, \cdots, \mathsf{M}-1 \tag{5.24}$$

The V-OFDM literature [Zhang et al., 2020][Liu et al., 2017][Xiang-Gen Xia, 2001][Cheng et al., 2011][Li et al., 2012] perform M inverse L-point FFTs to calculate each time domain VB. Since this contrasts to a single N-point FFT of OFDM, we refer to it as the Parameterized FFT (PFFT). The resulting samples within the q-th time domain VB is therefore

$$\mathbf{y}_q \;=\; \begin{bmatrix} Y_{q\cdot\mathsf{M}+0} \\ Y_{q\cdot\mathsf{M}+1} \\ \vdots \\ Y_{q\cdot\mathsf{M}+(\mathsf{M}-1)} \end{bmatrix} = \begin{bmatrix} X_{0\cdot\mathsf{M}+0} \\ X_{0\cdot\mathsf{M}+1} \\ \vdots \\ X_{0\cdot\mathsf{M}+\mathsf{M}-1} \end{bmatrix} e^{j2\pi q 0/L} + \cdots + \begin{bmatrix} X_{(L-1)\mathsf{M}+0} \\ X_{(L-1)\mathsf{M}+1} \\ \vdots \\ X_{(L-1)\mathsf{M}+\mathsf{M}-1} \end{bmatrix} e^{j2\pi q(L-1)/L} \tag{5.25}$$

The time domain transmitting sequence is

$$\mathbf{Y} = [Y_0, Y_1, \cdots, Y_{N-1}] \;=\; [{\mathbf{y}_0}^T, {\mathbf{y}_1}^T, \cdots, {\mathbf{y}_{L-1}}^T] \tag{5.26}$$

Both the normalized inverse DFT and DFT signals are respectively summarized as follows

$$\mathbf{y}_q \;=\; \frac{1}{L}\sum_{l=0}^{L-1} \mathbf{x}_l e^{j2\pi ql/L} \quad q = 0, 1, \cdots, L \tag{5.27}$$

$$\mathbf{x}_l \;=\; \frac{1}{L}\sum_{q=0}^{L-1} \mathbf{y}_q e^{-j2\pi ql/L} \quad l = 0, 1, \cdots, L \tag{5.28}$$

After the inverse DFT transform, the signal undergoes the same processing as usual in the classic OFDM waveform. For more details about signal detection

in V-OFDM receivers, please refer to [Xiang-Gen Xia, 2001], [Li et al., 2012]. In what follows, we adopt the notation $L\mathsf{M}$ (instead of ng) that is usual across the V-OFDM literature.

5.3.3 Parameterized DFT Algorithm for V-OFDM

In order to relax the power of two constraint on the spectrum parameters of V-OFDM, we replace FFT by the basic DFT algorithm. Since V-OFDM performs M L-point frequency-time transforms, the DFT and FFT complexities in V-OFDM are $O(\mathsf{M}L^2)$ and $O(\mathsf{M}L\log_2 L)$, respectively. However, differently from OFDM in which the asymptotic complexity of DFT cannot be as efficient as FFT's, one can exploit the vectorization feature of V-OFDM to refrain the DFT complexity.

We achieve that by parameterizing L to $\Theta(1)$, getting what we refer to as the Parameterized DFT (PDFT) algorithm (Algorithm 5.1). The parameterization provides DFT with non-null throughput on N as demonstrated in Lemma 11.

Lemma 11 (Scalable Throughput of the Parameterized DFT Algorithm). By setting the number of points L to $\Theta(1)$, the Parameterized DFT (PDFT) algorithm (Algorithm 5.1) achieves non-null throughput as the number of subcarriers N gets arbitrarily large.

Proof. Since $N = ML$, setting $L = \Theta(1)$ leads the $O(L^2\mathsf{M})$ complexity of PDFT to become $O(\mathsf{M}) = O(N)$. Thus, assuming the channel conditions does not enable arbitrarily large constellation diagrams, the total number of bits per V-OFDM symbol is $N \times d = N \times \log_2 M = O(N)$ and the computational complexity to perform a single complex multiplication is $\Theta(1)$. Therefore, the throughput of the PDFT algorithm does not nullify on N, as demonstrated below:

$$\lim_{N\to\infty} \frac{Nd}{L^2 M} = \lim_{N\to\infty} \frac{Nd}{N} = c > 0 \tag{5.29}$$

■

If $N = \mathsf{M}L$ is set to grow as a power of two 2^i, setting L to $\Theta(1)$ leads both FFT and PDFT to run in $O(\mathsf{M}) = O(2^i/L)$ time complexity. However, if that constraint is relaxed, PDFT can provide V-OFDM with flexible numerology (e.g. $n = 3$, $N = 156$, $n = 2$, $N = 40$) while running linearly on N rather than exponentially on i. The flexible numerology of PDFT, turns V-OFDM a competitive waveform for spectrum allocation in fragmented frequency bands. Besides, the reduced complexity is a step towards the enhancement of current broadband-driven services such as the enhanced mobile broadband service of 5G [3GPP, 2018] and the very high throughput service of IEEE 802.11ac [802.11, 2013].

Algorithm 5.1. The Parameterized inverse DFT algorithm for Vector OFDM. We show PDFT *i*) can perform $O(N)$ complex multiplications while relaxing the $N = 2^i$ constraint that causes FFT to run in $O(2^i i)$ exponential complexity and *ii*) becomes multiplierless performing only $O(N)$ complex sums for $M = 2$.

1: $\{X_i(i = 0, 1, \cdots, N-1)$ is the frequency domain input$\}$
2: $\{Y_i(i = 0, 1, \cdots, N-1)$ is the time domain output$\}$
3: $\{L$ is the number of points per vector block$\}$;
4: $\{\mathsf{M}$ is the number of vectors such that $N = L\mathsf{M}\}$;
5: **for** $(i = 0; i < N; ++i)$ **do**
6: $\quad Y_i \leftarrow 0$; {initialization of the entire time-domain array};
7: **end for**
8: **for** $(q = 0; q < L; ++q)$ **do**
9: $\quad$ **for** $(\mathsf{m} = 0; \mathsf{m} < \mathsf{M}; ++\mathsf{m})$ **do**
10: $\quad\quad$ **for** $(l = 0; l < L; ++l)$ **do**
11: $\quad\quad\quad Y_{q\cdot\mathsf{M}+\mathsf{m}} = Y_{q\cdot\mathsf{M}+\mathsf{m}} + X_{l\cdot\mathsf{M}+\mathsf{m}} \cdot e^{j2\pi ql/L}$;
12: $\quad\quad$ **end for**
13: $\quad$ **end for**
14: **end for**

5.3.4 Multiplierless Parameterized DFT

The $L = 1$ and $L = N$ setups of V-OFDM are well known cases mentioned in the literature. The $L = 1$ case turns V-OFDM into a single carrier waveform (requiring an extra N-point IFFT at the receiver) while the $L = N$ case turns V-OFDM into OFDM. We identify that V-OFDM under $L = 2$ can mitigate the mismatch between the unit of operation of the sampler and the frequency-time transform computation. As explained in Subsection 5.2.3, OFDM and variants suffer from what we refer to as the sampling-complexity trade-off. This happens because the sampler operates in a sample-by-sample basis whereas the unit of operation of the frequency-time transform computation is an N-sample symbol. Since the entire symbol must be sampled within the symbol period, the Nyquist (inter-sample) time interval decreases as N gets large but the time complexity to compute all N samples increases on N.

We identify V-OFDM can be set to mitigate the sampling-complexity trade-off. If one parameterizes L to 2, the N-subcarrier V-OFDM symbol is vectorized into only two VBs, leading to $N/2$ 2-point DFTs. Since these 2-point DFTs are completely independent from each other, they can be computed in parallel. Each 2-point transform takes $O(1)$ time complexity regardless of the value of N, therefore the entire solution requires $O(N)$ floating point operations. Although the final complexity is not $O(1)$ (as required by the sampling-complexity trade-off), the solution is multiplierless, requiring only $N/2$ complex sums. Indeed, both the indexes l and q that iterate across the frequency and time VBs (lines 10 and 8 in Algorithm 5.1, respectively), vary from 0 to 1, causing the complex

exponential to simplify to either 1 or -1. The two time domain VBs are

$$\mathbf{y}_0 = \begin{bmatrix} X_{0\cdot N/2+0} \\ X_{0\cdot N/2+1} \\ \vdots \\ X_{0\cdot N/2+N/2-1} \end{bmatrix} e^0 + \begin{bmatrix} X_{1\cdot N/2+0} \\ X_{1\cdot N/2+1} \\ \vdots \\ X_{1\cdot N/2+N/2-1} \end{bmatrix} e^0, \tag{5.30}$$

and

$$\mathbf{y}_1 = \begin{bmatrix} X_{0\cdot N/2+0} \\ X_{0\cdot N/2+1} \\ \vdots \\ X_{0\cdot N/2+N/2-1} \end{bmatrix} e^0 + \begin{bmatrix} X_{1\cdot N/2+0} \\ X_{1\cdot N/2+1} \\ \vdots \\ X_{1\cdot N/2+N/2-1} \end{bmatrix} e^{j\pi} \tag{5.31}$$

Note that the case $L = 1$ of V-OFDM dispenses the DFT computation at the transmitter but requires an extra N-point IDFT at the receiver. In turn, the case $L = 2$ is multiplierless at both the transmitter and the receiver.

5.4 Evaluation

In this section, we present simulation results to compare the FFT and PDFT algorithms and to validate our theoretical analysis. In Subsection 5.4.1, we describe the methodology of the simulations. In Subsection 5.4.2, we discuss the performance of both algorithms under a power of two number of points, as required by the FFT algorithm. In Subsection 5.4.3, we discuss the performance of the PDFT algorithm under a non power of two number of points.

5.4.1 Tools and Methodology

We compare our proposed PDFT algorithm for V-OFDM against the FFT algorithm employed by both OFDM and V-OFDM state of the art. We implement the PDFT algorithm in C++ and refer to the FFT implementation of [Press et al., 2007] to assess the FFT algorithm. It is important to remark that the runtime performance of our chosen FFT implementation can be outperformed by highly optimized FFT libraries available in the literature e.g., [Frigo and Johnson, 2005]. However, these libraries impose several preliminary runs of distinct DFT algorithms to pick the one that perform best for the considered platform and value of N. Hence, the chosen algorithm may vary across distinct values of N and the assessed runtime is highly dependent on several hardware optimizations that vary across the chosen platform. By contrast, our focus in this work is on the asymptotic complexity improvement rather than on hardware optimizations that can be handled in future work.

We vary the number of points which is equivalent to the number of subcarriers N for both algorithms. In this simulation, we vary N as powers of two considering a relatively small number of subcarriers, as in today's FFT-based waveforms. In the other simulation, we consider non power of two points and a minimum of 10^5 subcarriers. In this simulation, we also vary the number of VBs of PDFT, as well as the number of points per VB. For each algorithm, we assess the runtime $T(N)$ (seconds) and the throughput $SC(N)$ (Megabits per second). Unless differently stated, the throughput of each algorithm was measured considering each subcarrier is BPSK-modulated.

We sampled the wall-clock runtime $T(N)$ of each algorithm with the standard C++ `timespace` library [team, 2018] under the profile `CLOCK_MONOTONIC` on a 1.8 GHz i7-4500U Intel processor with 8 GB of memory. We repeated each experiment as many times as needed in order to achieve a mean with relative error below 5% with a confidence interval of 95%. Each sample of $T(N)$ was forwarded to the Akaroa-2 tool [McNickle et al., 2010] for statistical treatment. Akaroa-2 determined the minimum number of samples required to reach the transient-free steady-state mean estimation for $T(N)$. In each execution, we assigned our CPU process with the largest real-time priority and employed the `isolcpus` Linux kernel directive to allocate one physical CPU core exclusively for each process. We generate the input points for the algorithms with the standard C++ 64-bit version of the Mersenne Twistter (MT) 19937 pseudo-random number generator [Matsumoto and Nishimura, 1998] set to the seed 1973272912 [Hechenleitner and Entacher, 2002]. In Tables 5.2 and 5.3, we report the statistics of each simulation. Both tables report the number of points, the algorithm, the runtime in μs, the throughput, the runtime's half-width of the confidence interval and the runtime's variance, respectively. No experiment demanded more than 70000 repetitions and an average of about 500 samples were discarded due to the transient stage.

5.4.2 Power of Two DFTs

In this subsection, we evaluate the performance of FFT and PDFT algorithms under power of two number of points, as required by the FFT algorithm. In Fig. 5.3, we plot the runtime of the FFT algorithm (employed by OFDM and V-OFDM) and the multiplierless PDFT algorithm we propose for V-OFDM set to two $N/2$-subcarrier vector blocks. In Fig. 5.4, we plot the total number of arithmetic instructions predicted by the theoretical complexity analysis. The overall number of arithmetic instructions performed by the FFT algorithm and the PDFT algorithm are at least $5N \log_2 N$ [Frigo and Johnson, 2005] and N (Subsection 5.3.4), respectively. The statistics of the runtime are reported in Table 5.2. We report the throughput considering the BPSK modulation in which one bit modulates one subcarrier. Thus, one can reproduce Fig. 5.5 and Fig. 5.6 just by multiplying the BPSK-based throughput with the number of bits achieved by other modulation, e.g., 6 in the case of 64-QAM.

As one can observe in Fig. 5.3 and Fig. 5.4, the exponential nature of the FFT

Table 5.2: Runtime and throughput of PDFT (V-OFDM, $L = 2$) and FFT (V-OFDM) algorithms under BPSK modulation and power of two number of points. δ is the half-width of the confidence interval with 95% of confidence and relative error below 0.05.

N	**Algorithm**	**Runtime** μs	**Throughput (Mbps)**	$\pm\delta$ μs	**Variance**
2^1	PDFT	**0.05**	**38.02**	0.001	< 0.001
	FFT	**0.42**	**4.71**	0.01	< 0.001
2^2	PDFT	**0.07**	**58.31**	0.001	< 0.001
	FFT	**0.54**	**7.35**	0.03	< 0.001
2^3	PDFT	**0.09**	**84.84**	0.001	< 0.001
	FFT	**0.72**	**11.06**	0.03	< 0.001
2^4	PDFT	**0.15**	**109.07**	0.001	< 0.001
	FFT	**1.06**	**15.13**	0.02	< 0.001
2^5	PDFT	**0.26**	**125.05**	0.01	< 0.001
	FFT	**1.89**	**16.96**	0.09	< 0.001
2^6	PDFT	**0.45**	**143.59**	0.01	< 0.001
	FFT	**3.58**	**17.86**	0.08	< 0.001
2^7	PDFT	**0.80**	**159.96**	0.01	< 0.001
	FFT	**7.54**	**16.97**	0.37	0.02
2^8	PDFT	**1.58**	**161.66**	0.08	$<$0.001
	FFT	**15.65**	**16.36**	0.51	0.05
2^9	PDFT	**2.96**	**172.94**	0.01	$<$0.001
	FFT	**33.97**	**15.07**	1.26	0.29
2^{10}	PDFT	**6.43**	**159.24**	0.30	0.02
	FFT	**73.58**	**13.92**	2.79	1.39
2^{11}	PDFT	**12.99**	**157.71**	0.35	0.02
	FFT	**158.28**	**12.94**	0.55	0.05
2^{12}	PDFT	**24.35**	**168.22**	0.16	$<$0.001
	FFT	**362.43**	**11.30**	2.82	1.42
2^{13}	PDFT	**48.93**	**167.43**	0.46	0.04
	FFT	**790.96**	**10.36**	6.01	6.45
2^{14}	PDFT	**97.60**	**167.87**	0.18	0.01
	FFT	**1786.68**	**9.17**	3.13	1.76
2^{15}	PDFT	**220.81**	**148.40**	0.13	$<$0.001
	FFT	**4193.85**	**7.81**	3.55	2.25
2^{16}	PDFT	**442.09**	**148.24**	0.38	0.03
	FFT	**9154.79**	**7.16**	60.18	647.40
2^{17}	PDFT	**899.34**	**145.74**	6.74	8.13
	FFT	**19805.5**	**6.62**	54.58	532.5
2^{18}	PDFT	**1845.65**	**142.03**	11.34	23.0
	FFT	**54415.6**	**4.82**	245.92	1482

Table 5.3: Runtime and throughput of PDFT algorithm under BPSK modulation and non power of two number of points. δ is the half-width of the confidence interval with 95% of confidence and relative error below 0.05.

N	**Algorithm**	**Runtime** μs	**Throughput (Mbps)**	$\pm\delta$ μs	**Variance**
100000	PDFT L=2	**616.27**	**162.27**	2.55	1.16
	PDFT L=3	**13194.70**	**7.58**	18.36	60.25
	PDFT L=4	**19661.60**	**5.09**	28.12	141.31
	PDFT L=5	**26566.00**	**3.76**	130.42	3040.57
200000	PDFT L=2	**1260.86**	**158.62**	1.06	0.20
	PDFT L=3	**26664.20**	**7.50**	23.73	100.66
	PDFT L=4	**39414.40**	**5.07**	37.15	246.64
	PDFT L=5	**53084.40**	**3.77**	39.02	272.09
300000	PDFT L=2	**1933.58**	**155.15**	7.33	9.60
	PDFT L=3	**40969.50**	**7.32**	33.04	195.16
	PDFT L=4	**59452.20**	**5.05**	595.27	63339.50
	PDFT L=5	**80230.30**	**3.74**	57.35	587.81
400000	PDFT L=2	**2556.17**	**156.48**	5.00	4.46
	PDFT L=3	**52958.40**	**7.55**	26.59	126.36
	PDFT L=4	**79045.20**	**5.06**	43.66	340.75
	PDFT L=5	**106685.00**	**3.75**	136.26	3318.80
500000	PDFT L=2	**3250.60**	**153.82**	2.05	0.75
	PDFT L=3	**67125.20**	**7.45**	409.26	29939.60
	PDFT L=4	**100663.00**	**4.97**	807.14	116450.00
	PDFT L=5	**134902.00**	**3.71**	969.38	167969.00
600000	PDFT L=2	**3832.85**	**156.54**	3.06	1.68
	PDFT L=3	**79383.40**	**7.56**	29.29	153.30
	PDFT L=4	**118633.00**	**5.06**	57.44	589.81
	PDFT L=5	**159963.00**	**3.75**	294.60	15513.50

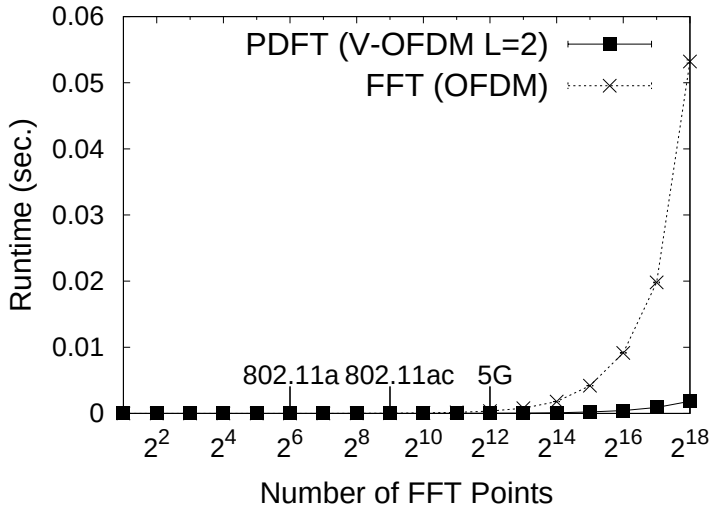

Figure 5.3: FFT vs. PDFT (proposed): Simulation runtime.

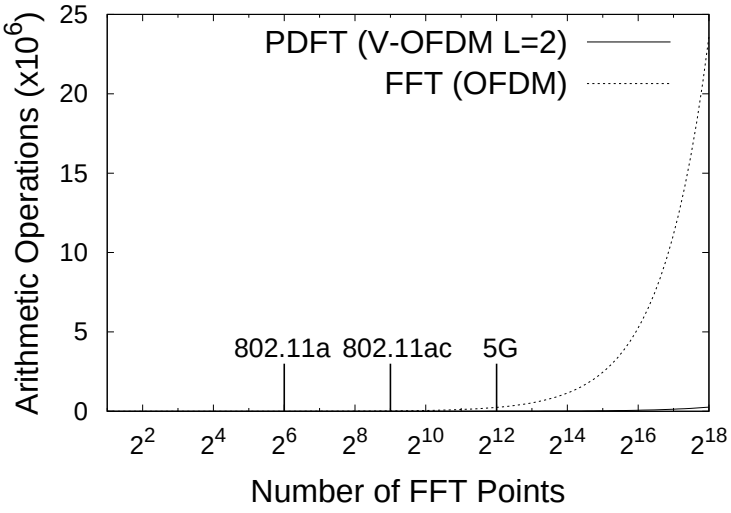

Figure 5.4: FFT vs. PDFT (proposed): Complexity.

complexity becomes clear after $N = 2^{12} = 4096$ points. Because the FFT algorithm demands N to grow as a power of two 2^i (for some $i > 0$), the number of DFT points must at least double in novel standards that adopt more subcarriers to improve throughput. Consequently, the complexity of the FFT algorithm grows accordingly. We highlight the performance of FFT for the largest number of points of different wireless communication standards. In the case of the IEEE 802.11a [IEEE 802.11, 2012], IEEE 802.11ac [802.11, 2013] and 5G [3GPP, 2018] standards the maximum number of FFT points are 64, 512 and 4096, respectively. Considering the $5N \log_2 N$ arithmetic instructions of the Cooley-Tukey algorithm [Frigo and Johnson, 2005], no less than 1920, 23040 and 245760 arithmetic instructions must be performed by FFT in those standards, respectively. In our simulation, these complexities caused the FFT runtime to grow at least one order of magnitude, which corresponded to 3.58 μs, 33.97 μs and 363.8 μs, respectively, as reported in Fig. 5.3.

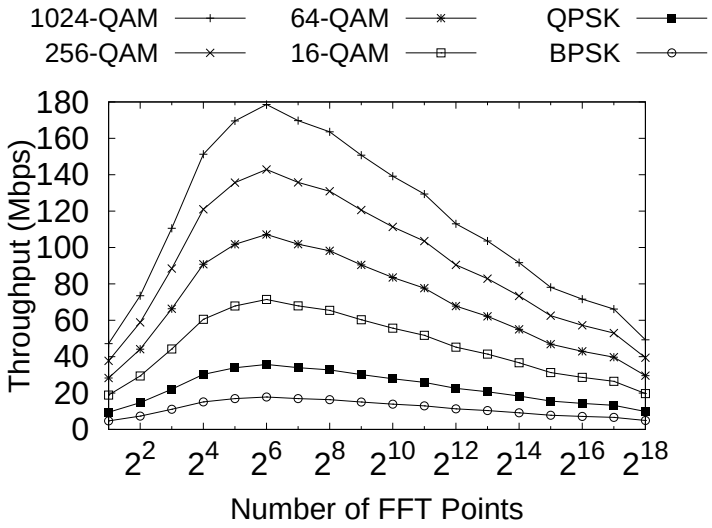

Figure 5.5: Throughput of FFT algorithm under different signal constellation mappers.

The wall-clock runtime of FFT can be improved if FFT is implemented on dedicate hardware such as ASICs. However, as shown in Fig. 5.4, the overall number of arithmetic instructions remains exponential irrespective of the implementation technology. Thus, the FFT complexity represents a serious concern for other relevant performance indicators of future networks like manufacturing cost, area (device portability) and power consumption.

By contrast, the proposed PDFT algorithm performed about two orders of magnitude better than FFT for all scenarios, even under the power of two constraint of FFT. Also, the FFT algorithm nullifies on N. In the simulation, this behavior can be observed by noting that the FFT throughput reaches the maximum value for $N = 2^6$ but achieves nearly the same value for $N = 2^2$ and $N = 2^{18}$ (Fig. 5.5). In turn, the PDFT algorithm keeps nearly the same throughput after $N = 2^7$ (Fig. 5.6). According to our theoretical analyses, this stems from the fact that both the PDFT complexity and the number of processed bits grows linearly on N. Therefore, the PDFT throughput tends to a non-null constant as N gets arbitrarily large.

5.4.3 Non Power of Two DFTs

In this subsection, we evaluate the performance of the PDFT algorithm under a non power of two number of points N. We vary N through $1 \cdot 10^5, 2 \cdot 10^5, \cdots, 6 \cdot 10^5$. In Figs. 5.7 and 5.8, we plot the runtime and throughput performance of the proposed PDFT algorithm, respectively. We vary the number of vector blocks $L = 2, 3, 4, 5$ and plot the performance of the FFT algorithm by setting N to the existing powers of two in the interval $[1 \cdot 10^5, 6 \cdot 10^5]$, namely $2^{17} = 131072$, $2^{18} = 262144$ and $2^{19} = 524288$. PDFT requires the length N/L of each vector block to be an integer. This requisite is met by all chosen values of N and L except $L = 3$. In this case, we decrease N by $N \mod 3$ to ensure N/L is an

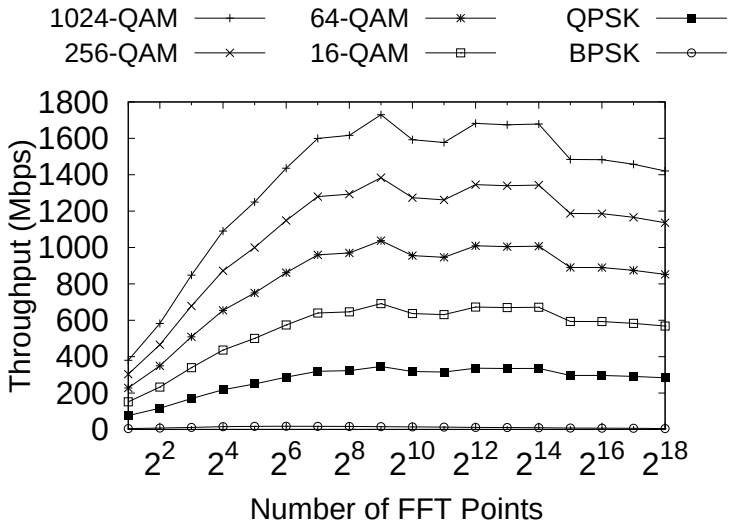

Figure 5.6: Throughput of PDFT algorithm under different signal constellation mappers.

integer ($x \mod y$ returns the remainder of division of x by y). Thus, for $L = 3$ the values of N 10^5, $2 \cdot 10^5$, $4 \cdot 10^5$ and $5 \cdot 10^5$ are subtracted by -1, -2, -1 and -2, respectively. The runtime and throughput of the FFT and PDFT algorithms are taken from Table 5.2 and Table 5.3, respectively. Both tables have the same structure of columns, as we explained in Subsection 5.4.2.

As one can see in Fig. 5.7, the runtime performance of PDFT improves for lower values of L. The best performance is achieved for $L = 2$ in which PDFT becomes multiplierless and performs $N/2$ 2-point transforms. Although the PDFT performance worsens for larger L, its complexity remains linear on N for all evaluated setups. This happens because PDFT exploits the parameterization technique to perform $\mathsf{M} = N/L$ independent L-point DFTs. By setting L to $\Theta(1)$, each independent DFT takes $L^2 = \Theta(1)$ time complexity, yielding a total of $(N/L) \cdot \Theta(1) = O(N)$ complexity.

The lowest complexity of PDFT (achieved with $L = 2$) translates into the fastest throughput among all algorithms, which is about two orders of magnitude above all other algorithms, as one can see in Fig. 5.8 where throughput is plotted considering one bit per point (i.e., BPSK modulation). Despite that, PDFT sustains a non-null throughput for all values of L whereas FFT nullifies as N grows.

The throughput nullification happens because the complexity grows asymptotically faster than the number of modulated bits as N grows. In the case of PDFT, the throughput remains constant as N grows even considering the fact that complexity grows too. Besides, because PDFT relies on the classic DFT algorithm rather than FFT, the number of points can grow in an unitary manner rather than doubling. Considering the range of the experiment $[1 \cdot 10^5, \cdots, 6 \cdot 10^5]$ for example, there exist 250001, 166667, 125001 and 100001 possible setup choices of N for PDFT under $L = 2$, $L = 3$, $L = 4$ and $L = 5$, respectively. By contrast, there are only three choices of N for the FFT algorithm in the same

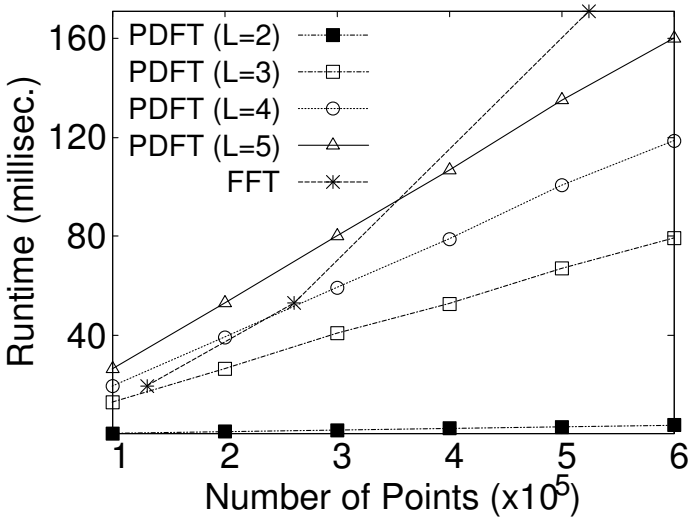

Figure 5.7: Runtime of FFT and the proposed PDFT algorithms for a number of points $N = 1 \cdot 10^5, 2 \cdot 10^5, \cdots, 6 \cdot 10^5$. For FFT, only the powers of two $2^{17} = 131072$, $2^{18} = 262144$ and $2^{19} = 524288$ are considered.

range, they are $2^{17} = 131072$, $2^{18} = 262144$ and $2^{19} = 524288$. *This can provide standardization bodies with more setup choices for future multicarrier wireless communication standards.*

5.5 Summary

In this chapter, we demonstrated that the Fast Fourier Transform (FFT) algorithm can be too complex for the post-5G generation of multicarrier waveforms. The constraint that the number of points N must grow as a power of two 2^i (for some $i > 0$) along with the unprecedented growth in the number of subcarriers, cause FFT to run in the exponential complexity $O(2^i \cdot i)$. Also, because this complexity grows faster than the number of modulated bits, the FFT throughput nullifies as N grows. We generalized this result to show that the throughput of any DFT algorithm nullifies on N unless the lower bound complexity of the DFT problem verifies as $\Omega(N)$, which is an open conjecture in computer science.

To overcome the scalability limitations of FFT, we consider the alternative formulation of frequency-time transform of Vector OFDM (V-OFDM) [Xiang-Gen Xia, 2001], a waveform that replaces an N-point FFT by N/n ($n > 0$) smaller FFTs to mitigate the cyclic prefix overhead of OFDM. In this sense, we replace FFT by DFT to relax the power of two constraint on N and to provide V-OFDM with flexible numerology (e.g. $n = 3$, $N = 156$). Besides, by parameterizing n to $\Theta(1)$, we identify that the resulting DFT-based solution (we refer to as Parameterized DFT, PDFT) runs linearly on N rather than exponentially on i.

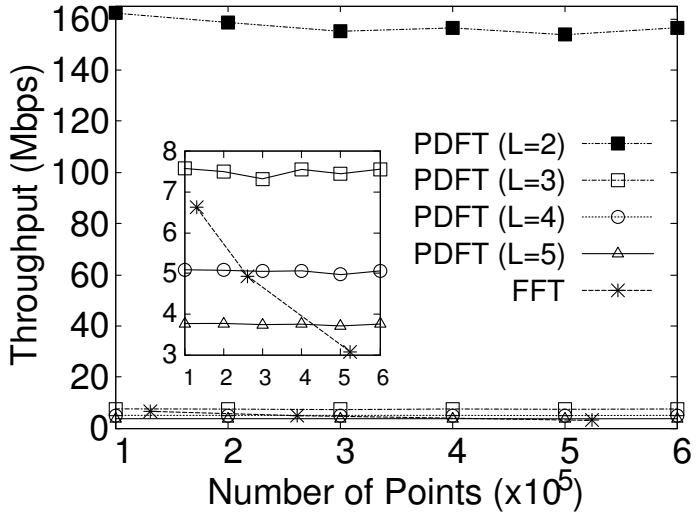

Figure 5.8: Throughput of FFT and the proposed PDFT algorithms for a number of points $N = 1 \cdot 10^5, 2 \cdot 10^5, \cdots, 6 \cdot 10^5$. For FFT, only the powers of two $2^{17} = 131072$, $2^{18} = 262144$ and $2^{19} = 524288$ are considered.

We also formulate what we refer to as the sampling-complexity (Nyquist-Fourier) trade-off, which stems from the fact that the N-point DFT algorithm operates on a batch of N samples but its associated sampler operates on a sample by sample basis. As N grows, the Nyquist inter-sample time interval demanded by the sampler decreases but the DFT complexity to compute all samples increases. We demonstrate that the asymptotic solution of the trade-off would require $\Theta(1)$ DFT algorithms. Since DFT algorithms grows linearly on N at best, i.e., $\Omega(N)$, no DFT algorithm can meet the Nyquist deadline as N grows. However, we identify that the trade-off can be countered in practice if V-OFDM is set to two $N/2$-subcarrier vector blocks (i.e., $n = 2$). In that case, the transform simplifies to $N/2$ complex sums that can be performed in parallel both at the transmitter and receiver. Thus, the N-point DFT becomes multiplierless and each sample that feeds the DAC/ADC comes only from two – rather than N – other samples. We believe these results turn V-OFDM into a competitive candidate waveform for future broadband wireless networks.

Therefore, our results constitute a relevant step towards the practical deployment of extremely wide multicarrier signals that are expected for the post-5G generation of waveforms. In future work, the PDFT algorithm can be coupled to an analog Terahertz radio. Also, the optimal parameterization for the PDFT complexity can be identified for different channel propagation conditions.

Chapter 6

Conclusions and Future Work

"Everything that has a beginning has an end, Neo."

(The Oracle)

Contents

This chapter overviews the Spectro-Computational (SC) complexity model in terms of issues addressed, relevance for the fields of computational complexity and information theory, and future possibilities. The remainder of this chapter is organized as follows. The Section 6.1 summarizes this thesis. The Section 6.2 and Section 6.3 present the main contributions and the possible future directions of this thesis, respectively.

6.1 Synthesis of the Thesis

This thesis presents a mathematical model for the unified analysis of computational complexity and throughput of a communication signal. The model exploits the fact that throughput and complexity are both functions of the signal spectrum bandwidth. Furthermore, the ratio between the number of modulated bits and the complexity to modulate them is a reasonable measure of throughput for a single or a sequence of communication signal algorithms. Based on that, novel conclusions have been achieved throughout this thesis, as we now summarizes.

After introducing the basic concepts of the computational complexity and information theory and reviewing the related literature in performance evaluation of signal waveforms, Chapter 2 concludes that a model enabling a joint analysis of indicators of computational complexity and data rate (such as throughput, spectral efficiency and capacity) still lacks in that related work.

In Chapter 3, the underlying conclusion is that computational complexity as well as the indicators of data rate can be, both, expressed as function of the signal's spectrum bandwidth. Based on that, the SC throughput of a signal processing algorithm (or a sequence, as in the case of waveforms) can be given by the ratio between number of modulated bits per symbol and computational complexity to process the symbol. Also, classic concepts and definitions from both computational complexity and information theory can be specialized by having the SC throughput as performance indicator, e.g. optimal complexity algorithm, spectral efficiency, and throughput upper-bound (i.e., capacity). Based on the proposed specialized definitions, a novel signal regime is defined, namely, the *comp-limited signal* in which the computational complexity overhead causes the signal capacity to nullify as the bandwidth gets arbitrarily large. By means of a step-by-step SC analysis, the chapter finishes by concluding that the N-point Fourier transform problem causes the basic OFDM waveform to be comp-limited unless its lower bound complexity verifies as $\Omega(N)$ (i.e., grows at least linearly on N), which remains a "fascinating" open question in computer science [Lokam, 2009].

The main conclusion of Chapter 4 is that the ideal mapping setup of OFDM with Index Modulation (OFDM-IM) is not computationally intractable. Under the 'ideal' mapping setup OFDM-IM reaches the maximal spectral efficiency gain over OFDM but the resulting computational complexity was conjectured as intractable by the literature [Lu et al., 2018], [Basar et al., 2017]. Guided by an analysis based on the SC model, the chapter calculates the exact mapping complexity required for the ideal setup and presents an OFDM-IM mapper that is able to reach the required complexity in practice.

Chapter 5 concludes that the SC throughput of the basic OFDM waveform nullifies as the spectrum bandwidth grows, unless the lower bound complexity of the N-point Fourier transform problem verifies as $\Omega(N)$. This means that the Fast Fourier Transform (FFT) algorithm is not fast enough to sustain non null throughput as the bandwidth gets arbitrarily large. Also, because FFT demands N to be a power of two 2^i $(i > 0)$, the spectrum widening leads to an exponential complexity on i, i.e. $O(2^i i)$. Based on the SC analysis, we verify that the scalability limitation can be solved with Vector OFDM (V-OFDM)[Xiang-Gen Xia, 2001], a waveform that replaces an N-point FFT by N/n $(n = 2^j > 0)$ smaller FFTs to mitigate the cyclic prefix overhead of OFDM. We propose to apply the parameterized complexity technique on the classic $O(N^2)$ DFT algorithm, getting what we refer to as the Parameterized DFT (PDFT) algorithm. By setting n to $\Theta(1)$ (i.e., a constant), we show that PDFT runs linearly on N rather than exponentially on i while relaxing the power of two constraint of FFT in V-OFDM.

6.2 Contributions

The central contribution of this thesis consists of an unified SC analytical model that encompasses two classes of performance indicators of wireless communic-

ation signal waveforms, namely, indicators of data rate – such as throughput, spectral efficiency and capacity – and indicators of computational complexity, such as runtime processing and (mainly) number of computational instructions. From the perspective of computer science, the SC analysis specializes the asymptotic analysis of signal processing algorithms guided by two performance targets, namely, input length (i.e., throughput) maximization and complexity minimization. From the perspective of the information theory and the communication signal fields, the SC analysis can guide the design and comparison of waveforms operating in extremely wide spectral bandwidths, as expected for the future generation of wireless communications.

Other contributions derived from the application of the proposed model to optimize two variants of OFDM in terms complexity and throughput. In summary, the following contributions were achieved:

- **Contribution 1, The Spectro-Computational (SC) Complexity Analysis**
  The SC complexity analysis unifies signal throughput and complexity analysis through two steps. Firstly, it exploits the fact that both performance indicators can be written as functions of variables of spectrum such as bandwidth or number of subcarriers. Secondly, the SC analysis counts complexity in the total transmission time considered by the symbol throughput formula, yielding the SC throughput of a communication signal algorithm (subsection 3.2.1). With the unprecedented growth of spectrum expected for the post-5G generation of waveforms, the asymptotic analysis of the SC throughput having the spectral bandwidth as variable (subsection 3.2.4) can reveal whether the complexity of a given waveform solution does nullify throughput. The entire SC complexity analysis is presented in chapter 3;

- **Contribution 2, Novel Definitions Towards a Unified Theory of Waveform Throughput and Computational Complexity**
  This contribution comprises a family of novel formal definitions that enhances classical concepts of information theory. The SC capacity (presented in subsection 3.2.1) builds on the concepts of channel capacity (from information theory) and and lower bound complexity of a problem (from theoretical computer science). The definition of the computation-limited signal regime is homologous to the classic power- and band-limited signal regimes defined from the Shannon capacity. This definition enables one to calculate the asymptotic lower bound for the throughput of a given waveform proposal. Based on that, the feasibility of the waveform design for arbitrarily large number of subcarriers N can be verified;

- **Contribution 3, The Optimal Mapper for OFDM with Index Modulation**
  This contribution ensures that the optimal mapping setup of OFDM with Index Modulation (OFDM-IM) is not computationally intractable, as it has been conjectured by the literature [Lu et al., 2018], [Basar et al., 2017]. The optimal mapping setup is such that the spectral efficiency gain

of OFDM-IM over OFDM maximizes. Based on the SC analysis, it is shown that the the index selector algorithm required by the N-subcarrier OFDM-IM mapper must run in $\Theta(N)$ time complexity. OFDM-IM mappers running faster than such complexity cannot reach the maximal spectral efficiency, whereas one running slower nullifies the mapping throughput for arbitrarily large N. This theoretical assertion is demonstrated in practice by means of an open source library that supports all DSP steps to map/demap an N-subcarrier complex frequency-domain OFDM-IM symbol; The entire discussion is shown in chapter 4.

- **Contribution 4, Asymptotic Formalization of the Sampling-Complexity Trade-Off**
  This contribution identifies the asymptotic complexity lower bound of batch-oriented communication signal algorithms whose output must feed Nyquist-constrained samplers. This is the case of the Fast Fourier Transform (FFT) algorithm in OFDM. The problem is formalized as a trade-off between the Nyquist inter-sample time interval and the FFT complexity: as the Nyquist interval decreases (thereby enabling more samples in the symbol period and increasing symbol throughput) the FFT complexity increases. Subsection 5.2.3 shows that the Nyquist sampling constraint demands a lower bound complexity of $\Omega(1)$ for the N-point DFT problem, much harder than the $\Omega(N)$ lower bound which has been considered as an open possibility by theoretical computer science. Subsection 5.3.4 demonstrates how to achieve multiplierless DFT for OFDM in its vectorized form. Although the multiplierless setup does not solve the sampling-complexity trade-off in theory, the asymptotically dominant computational instruction of DFT becomes constant and only $\Theta(N)$ sums are necessary.

- **Contribution 5, Spectro-Computational Analysis of OFDM and Novel Asymptotic Limits for Fourier Transform Algorithms**
  This contribution shows that the Fast Fourier Transform (FFT) algorithm can be too complex for the post-5G generation of multicarrier waveforms. The constraint that the number of points N must grow as a power of two 2^i (for some $i > 0$) along with the unprecedented growth in the number of subcarriers, cause FFT to run in the exponential complexity $O(2^i \cdot i)$. Also, because this complexity grows faster than the number of modulated bits, the FFT throughput nullifies as N grows. This result is generalized to demonstrate that the throughput of any DFT algorithm nullifies on N unless the lower bound complexity of the DFT problem verifies as $\Omega(N)$, which is an open question in computer science. We also apply the SC model to analyze the V-OFDM waveform and identify that the strategy of replacing a single N-point FFT by several smaller n-point FFTs can prevent the SC throughput nullification. However, to relax the power of two constraint of FFT, we propose to apply the parameterized complexity technique on the classic $O(N^2)$ DFT algorithm, getting what we refer to as the Parameterized DFT (PDFT) algorithm. PDFT runs linearly on N rather than exponentially on i while relaxing the power of two constraint of FFT in V-OFDM.

6.3 Future Directions

The SC complexity analysis proposed in this thesis considers the intrinsic relationship between signal throughput and complexity. The effectiveness of the proposal to calculate the minimum required complexity for the scalability of signal throughput was verified through practical case studies, for example, in the design of an asymptotically optimal mapper for the OFDM-IM waveform [Basar et al., 2013] and the design of an asymptotically optimal frequency-time transform algorithm for the V-OFDM waveform [Xiang-Gen Xia, 2001]. Thus, future work can build on the proposed theoretical analysis as well as each particular case study.

The throughput-complexity waveform optimizations achieved by the case studies of the proposed analytic model can guide the design improvements for other waveforms, specially variants of the proposals considered in this thesis. For example, the optimal mapper achieved for OFDM with index modulation can be applied to other IM systems that rely on the same index selector of the original OFDM-IM mapper, such as spatial modulation systems [Wen et al., 2019] and dual mode OFDM-IM [Mao et al., 2017b]. In face of the huge complexity expected for Terahertz waveforms, the proposed parameterized solution achieved for vectorized OFDM can be coupled to an analog Terahertz radio and the optimal parameterization complexity for different channel propagation conditions can be investigated and implemented through automatic schemes.

Open theoretical questions of this thesis can be handled in future work. For instance, whether OFDM and OFDM-IM are comp-limited signals depend on whether the lower bound complexity of the Fourier transform problem is linear on the number of points. However, this remains an important open question on theoretical computer science. The capacity-complexity scalability solution achieved in this thesis was for the parameterized Fourier transform problem, which is slightly different from the classic Fourier transform problem and matches OFDM in its vectorized form. Approaches other than that can be exploited in future works. Instead of decreasing the asymptotic computational complexity of the frequency-time transformation, one may concern on devising clever mappers that increase the asymptotic number of bits modulated in the multicarrier symbol.

This is the case, for instance, of Multiple Mode (MM) OFDM-IM [Wen et al., 2017] that refers to permutation techniques to modulate $B(N) = O(N \log_2 N)$ bits in an N-subcarrier OFDM-like symbol. This would prevent the FFT complexity $T(N) = O(N \log_2 N)$ to nullify the waveform throughput $B(N)/T(N)$ as N gets larger. However, differently from the waveforms considered in this work, reasonable bit error rates have been achieved only under exponential time heuristics [Mao et al., 2018]. In this case, one may rely on algorithm design techniques (like parameterization) to pursue the maximum complexity predicted by the SC analysis for that novel waveform.

Finally, future works can exploit more general questions such as the enhance-

ment of the mathematical model we propose. In this sense, one possible investigation can consider the Bit Error Rate (BER) performance indicator along with complexity and throughput. This would enable one, for example, to equate the intrinsic trade-off between complexity and the transmission error rate faced by signal detection heuristics. Based on that, the minimum complexity for a given BER performance target can be calculated and compared among distinct waveforms.

References

3GPP (2018). Technical Specification Group Radio Access Network; Study on Scenarios and Requirements for Next Generation Access Technologies (Release 15). Technical Report 38.913, version 15.0.0, 3GPP Global Initiative.

802.11, I. (2013). IEEE Standard for IT– Specific requirements–Part 11: Wireless LAN Medium Access Control (MAC) and Physical Layer (PHY) Specifications–Amendment 4: Enhancements for Very High Throughput for Operation in Bands below 6 GHz. *IEEE Std 802.11ac-2013*, pages 1–425.

Afshani, P., Freksen, C. B., Kamma, L., and Larsen, K. G. (2019). Lower Bounds for Multiplication via Network Coding. In Baier, C., Chatzigiannakis, I., Flocchini, P., and Leonardi, S., editors, *46th International Colloquium on Automata, Languages, and Programming (ICALP 2019)*, volume 132 of *Leibniz International Proceedings in Informatics (LIPIcs)*, pages 10:1–10:12, Dagstuhl, Germany. Schloss Dagstuhl–Leibniz-Zentrum fuer Informatik.

Ailon, N. (2015). Tighter fourier transform lower bounds. In Halldórsson, M. M., Iwama, K., Kobayashi, N., and Speckmann, B., editors, *Automata, Languages, and Programming*, pages 14–25, Berlin, Heidelberg. Springer Berlin Heidelberg.

Akyildiz, I. F., Lee, W.-Y., Vuran, M. C., and Mohanty, S. (2006). Next generation/dynamic spectrum access/cognitive radio wireless networks: A survey. *Computer Networks*, 50(13):2127 – 2159.

Albreem, M. A., Juntti, M., and Shahabuddin, S. (2019). Massive mimo detection techniques: A survey. *IEEE Communications Surveys Tutorials*, 21(4):3109–3132.

Aldirmaz, S., Acar, Y., and Basar, E. (2018). Adaptive dual-mode OFDM with index modulation. *Physical Communication*, 30:15–25.

Alouini, M. . and Goldsmith, A. J. (1999). Area spectral efficiency of cellular mobile radio systems. *IEEE Transactions on Vehicular Technology*, 48(4):1047–1066.

Alouini, M.-S. and Goldsmith, A. (1997). Area spectral efficiency of cellular mobile radio systems. In *1997 IEEE 47th Vehicular Technology Conf.. Technology in Motion*, volume 2, pages 652–656 vol.2.

Bachmann, P. (1894). *Die Analytische Zahlentheorie [Analytic Number Theory]*. B. G. Teubner, zahlentheorie, band 2 edition.

Basar, E., Aygolu, U., Panayirci, E., and Poor, H. V. (2012). Orthogonal frequency division multiplexing with index modulation. In *2012 IEEE Global Comm. Conf. (GLOBECOM)*, pages 4741–4746.

Basar, E., Aygolu, U., Panayirci, E., and Poor, H. V. (2013). Orthogonal frequency division multiplexing with index modulation. *IEEE Trans. Signal Process.*, 61(22):5536–5549.

Basar, E., Wen, M., Mesleh, R., Renzo, M. D., Xiao, Y., and Haas, H. (2017). Index modulation techniques for next-generation wireless networks. *IEEE Access*, 5:16693–16746.

Bianchi, G. (2000). Performance analysis of the IEEE 802.11 distributed coordination function. *IEEE Journal on Selected Areas in Communications*, 18(3):535–547.

Blume, H., Hubert, H., Feldkamper, H. T., and Noll, T. G. (2002). Model-based exploration of the design space for heterogeneous systems on chip. In *Proc. IEEE International Conf. on Application- Specific Systems, Architectures, and Processors*, pages 29–40.

Botsinis, P., Ng, S. X., and Hanzo, L. (2013). Quantum search algorithms, quantum wireless, and a low-complexity maximum likelihood iterative quantum multi-user detector design. *IEEE Access*, 1:94–122.

Buckles, B. P. and Lybanon, M. (1977). Algorithm 515: Generation of a vector from the lexicographical index [g6]. *ACM Trans. Math. Softw.*, 3(2):180–182.

Chaitin, G. J. (1987). *Algorithmic Information Theory*. Cambridge Tracts in Theoretical Computer Science. Cambridge University Press.

Chen, A., Datta, S., Hu, X. S., Niemier, M. T., Rosing, T. ., and Yang, J. J. (2019). A survey on architecture advances enabled by emerging beyond-cmos technologies. *IEEE Design Test*, 36(3):46–68.

Chen, J., Kanj, I. A., and Xia, G. (2006). Improved parameterized upper bounds for vertex cover. In Kralovic, R. and Urzyczyn, P., editors, *Mathematical Foundations of Computer Science 2006, 31st International Symposium, MFCS 2006, Stará Lesná, Slovakia, August 28-September 1, 2006, Proceedings*, volume 4162 of *Lecture Notes in Computer Science*, pages 238–249. Springer.

Chen, Y., Eldar, Y. C., and Goldsmith, A. J. (2013). Shannon meets nyquist: Capacity of sampled gaussian channels. *IEEE Transactions on Information Theory*, 59(8):4889–4914.

Chen, Y., Goldsmith, A. J., and Eldar, Y. C. (2014). Channel capacity under sub-nyquist nonuniform sampling. *IEEE Transactions on Information Theory*, 60(8):4739–4756.

Chen, Y., Goldsmith, A. J., and Eldar, Y. C. (2017). On the minimax capacity loss under sub-nyquist universal sampling. *IEEE Transactions on Information Theory*, 63(6):3348–3367.

Chen, Y., Zhang, S., Xu, S., and Li, G. Y. (2011). Fundamental trade-offs on green wireless networks. *IEEE Communications Magazine*, 49(6):30–37.

Cheng, P., Tao, M., Xiao, Y., and Zhang, W. (2011). V-ofdm: On performance limits over multi-path rayleigh fading channels. *IEEE Transactions on Communications*, 59(7):1878–1892.

Chiang, M., Hande, P., Lan, T., and Tan, C. W. (2008). Power control in wireless cellular networks. *Found. Trends Netw.*, 2(4):381–533.

Conceição, F., Gomes, M., Silva, V., Dinis, R., ao Silva, A., and Castanheira, D. (2020). A survey of candidate waveforms for beyond 5g systems. *Electronics*, 10:21.

Cook, S. A. and Reckhow, R. A. (1972). Time-bounded random access machines. In *Proceedings of the Fourth Annual ACM Symposium on Theory of Computing*, STOC '72, pages 73–80, New York, NY, USA. ACM.

Cooley, J. and Tukey, J. (1965). An algorithm for the machine calculation of complex fourier series. *Mathematics of Computation*, 19(90):297–301.

Cormen, T. H., Leiserson, C. E., Rivest, R. L., and Stein, C. (2009). *Introduction to Algorithms, Third Edition*. The MIT Press, 3rd edition.

Crouse, D. F. (2007). Remark on algorithm 515: Generation of a vector from the lexicographical index combinations. *ACM Trans. Math. Softw.*, 33(2).

Daneshgaran, F., Laddomada, M., Mesiti, F., Mondin, M., and Zanolo, M. (2008). Saturation throughput analysis of IEEE 802.11 in the presence of non ideal transmission channel and capture effects. *Communications, IEEE Transactions on*, 56(7):1178–1188.

Davila, H. L., Liu, C., Liu, W., Huang, S., Jou, S., and Chen, S. (2015). A 802.15.3c/802.11ad compliant 24 gb/s fft processor for 60 ghz communication systems. In *2015 28th IEEE International System-on-Chip Conference (SOCC)*, pages 44–48.

Deutsch, D. (1985). Quantum theory, the church-turing principle and the universal quantum computer. 400:97–117.

Doré, J.-B., Gerzaguet, R., Cassiau, N., and Ktenas, D. (2017). Waveform contenders for 5g: Description, analysis and comparison. *Physical Communication*, 24.

Downey, R. G. and Fellows, M. R. (2012). *Parameterized Complexity*. Springer Publishing Company, Incorporated.

Drozdenko, B., Zimmermann, M., Dao, T., Chowdhury, K., and Leeser, M. (2018). Hardware-software codesign of wireless transceivers on zynq heterogeneous systems. *IEEE Transactions on Emerging Topics in Computing*, 6(4):566–578.

Er, M. (1985). Lexicographic ordering, ranking and unranking of combinations. *International J. of Computer Mathematics - IJCM*, 17:277–283.

Fan, R., Yu, Y. J., and Guan, Y. L. (2014). Orthogonal frequency division multiplexing with generalized index modulation. In *2014 IEEE Global Commun. Conf.*, pages 3880–3885.

Fan, R., Yu, Y. J., and Guan, Y. L. (2015). Generalization of orthogonal frequency division multiplexing with index modulation. *IEEE Trans. on Wireless Commun.*, 14(10):5350–5359.

Fan, R., Yu, Y. J., and Guan, Y. L. (2016). Improved orthogonal frequency division multiplexing with generalised index modulation. *IET Commun.*, 10(8):969–974.

Fortnow, L. and Homer, S. (2003). A short history of computational complexity. *Bulletin of the EATCS*, 80:95–133.

Frenger, P. K. and Svensson, N. A. B. (1999). Parallel combinatory OFDM signaling. *IEEE Trans. Commun.*, 47(4):558–567.

Frigo, M. and Johnson, S. G. (2005). The design and implementation of fftw3. *Proceedings of the IEEE*, 93(2):216–231.

Gerzaguet, R., Bartzoudis, N., Baltar, L. G., Berg, V., Doré, J.-B., Kténas, D., Font-Bach, O., Mestre, X., Payaró, M., Färber, M., and Roth, K. (2017). The 5g candidate waveform race: a comparison of complexity and performance. *EURASIP J. on Wireless Commun. and Networking*, 2017(1):13.

Gokceli, S., Basar, E., Wen, M., and Kurt, G. K. (2017). Practical implementation of index modulation-based waveforms. *IEEE Access*, 5:25463–25473.

Guerreiro, J., Dinis, R., and Montezuma, P. (2013). Optimum and sub-optimum receivers for ofdm signals with strong nonlinear distortion effects. *IEEE Transactions on Communications*, 61(9):3830–3840.

H. Chen, G. and Chern, M.-S. (1986). Parallel generation of permutations and combinations. *BIT*, 26:277–283.

Harel, D. (1987). *Algorithmics: The Spirit of Computing*. Addison-Wesley Longman Publishing Co., Inc., Boston, MA, USA.

Haron, N. Z. and Hamdioui, S. (2008). Why is cmos scaling coming to an end? In *2008 3rd International Design and Test Workshop*, pages 98–103.

Hartmanis, J. and Stearns, R. (1965). On the computational complexity of algorithms. *Transactions of The American Mathematical Society - TRANS AMER MATH SOC*, 117:285–285.

Harvey, D. and Hoeven, J. V. D. (2020). Integer multiplication in time o(n log n). *Annals of Mathematics*.

Hechenleitner, B. and Entacher, K. (2002). On shortcomings of the ns-2 random number generator. In *Proceedings of Communication Networks and Distributed Systems Modeling and Simulation (CNDS), Texas, USA*, pages 71–77.

Hei, Y., Zhang, C., and Song, W. (2019). Energy and spectral efficiency tradeoff in massive mimo systems with multi-objective adaptive genetic algorithm. *Springer Soft. Comput.*, 23:7163–7179.

Heideman, M., Johnson, D., and Burrus, C. (1985). Gauss and the history of the fast fourier transform. *Archive for History of Exact Sciences*, 34:265–277.

Heliot, F., Imran, M. A., and Tafazolli, R. (2012). On the energy efficiency-spectral efficiency trade-off over the mimo rayleigh fading channel. *IEEE Transactions on Communications*, 60(5):1345–1356.

Hellstrom, H., Luvisotto, M., Jansson, R., and Pang, Z. (2019). Software-defined wireless communication for industrial control: A realistic approach. *IEEE Industrial Electronics Magazine*, 13(4):31–37.

Hessar, M., Najafi, A., Iyer, V., and Gollakota, S. (2020). Tinysdr: Low-power SDR platform for over-the-air programmable iot testbeds. In *17th USENIX Symposium on Networked Systems Design and Implementation (NSDI 20)*, pages 1031–1046, Santa Clara, CA. USENIX Association.

Hu, Z., Chen, F., Wen, M., Ji, F., and Yu, H. (2018). Low-complexity llr calculation for ofdm with index modulation. *IEEE Wireless Communications Letters*, 7(4):618–621.

Huang, T., Yang, W., Wu, J., Ma, J., Zhang, X., and Zhang, D. (2019). A survey on green 6g network: Architecture and technologies. *IEEE Access*, 7:175758–175768.

IEEE (2019). IEEE Draft Standard for Information Technology – Telecommunications and Information Exchange Between Systems Local and Metropolitan Area Networks – Specific Requirements Part 11: Wireless LAN Medium Access Control (MAC) and Physical Layer (PHY) Specifications Amendment Enhancements for High Efficiency WLAN. *IEEE P802.11ax/D6.0, November 2019*, pages 1–780.

IEEE 802.11 (2012). IEEE Standard for Information technology– Part 11: Wireless LAN MAC and PHY Specifications Amendment 5: Enhancements for Higher Throughput. *IEEE Std 802.11-2012*.

IEEE 802.11 (2016). IEEE Standard for Information technology–TeleCommun. and information exchange between systems Local and metropolitan area networks–Specific requirements - Part 11: Wireless LAN Medium Access Control (MAC) and Physical Layer (PHY) Specifications. *IEEE Std 802.11-2016 (Revision of IEEE Std 802.11-2012)*, pages 1–3534.

Ishikawa, N., Sugiura, S., and Hanzo, L. (2016). Subcarrier-index modulation aided OFDM - will it work? *IEEE Access*, 4:2580–2593.

Jain, R., Molnar, D., and Ramzan, Z. (2005). Towards a model of energy complexity for algorithms [mobile wireless applications]. In *IEEE Wireless Communications and Networking Conference, 2005*, volume 3, pages 1884–1890 Vol. 3.

Jaradat, A. M., Hamamreh, J. M., and Arslan, H. (2018). Ofdm with subcarrier number modulation. *IEEE Wireless Communications Letters*, 7(6):914–917.

Karp, R. (1972). Reducibility among combinatorial problems. In Miller, R. and Thatcher, J., editors, *Complexity of Computer Computations*, pages 85–103. Plenum Press.

Kim, K. and Park, H. (2019). New design of constellation and bit mapping for dual mode ofdm-im. *IEEE Access*, 7:52573–52580.

Knuth, D. E. (1997). *The Art of Computer Programming, Volume 1 (3rd Ed.): Fundamental Algorithms*. Addison Wesley Longman Publishing Co., Inc., USA.

Knuth, D. E. (2011). *The Art of Computer Programming: Combinatorial Algorithms, Part 1*. Addison-Wesley Professional, 1st edition.

Kokosiński, Z. (1995). Algorithms for unranking combinations and their applications. In *7th IASTED/ISMM International Conference on Parallel and Distributed Computing and Systems*, pages 216–224, Washington D.C., USA.

Kolmogorov, A. (1998). On tables of random numbers. *Theoretical Computer Science*, 207(2):387 – 395.

Kreher, D. L. and Stinson, D. R. (1999). Combinatorial algorithms: Generation, enumeration, and search. *SIGACT News*, 30(1):33–35.

Kumar, G. G., Sahoo, S. K., and Meher, P. K. (2019). 50 years of fft algorithms and applications. *Circuits Syst. Signal Process*, 38(12):5665 – 5698.

Landau, E. (1909). *Handbuch der Lehre von der Verteilung der Primzahlen*. Teubner, Leipzig. 2 volumes. Reprinted by Chelsea, New York, 1953.

Lanhua, X., Chen, H., and Zhao, F. (2017). Area spectral efficiency and energy efficiency tradeoff in ultradense heterogeneous networks. *Wireless Communications and Mobile Computing*, 2017:1–8.

Letaief, K. B., Chen, W., Shi, Y., Zhang, J., and Zhang, Y. A. (2019). The roadmap to 6g: Ai empowered wireless networks. *IEEE Communications Magazine*, 57(8):84–90.

Li, J., Dang, S., Wen, M., Jiang, X., Peng, Y., and Hai, H. (2019a). Layered orthogonal frequency division multiplexing with index modulation. *IEEE Systems Journal*, pages 1–10.

Li, Q., Wen, M., Dang, S., Basar, E., Poor, H. V., and Chen, F. (2019b). Opportunistic spectrum sharing based on ofdm with index modulation. *IEEE Transactions on Wireless Communications*, 19(1):192–204.

Li, Y., Ngebani, I., Xia, X., and Host-Madsen, A. (2012). On performance of vector ofdm with linear receivers. *IEEE Transactions on Signal Processing*, 60(10):5268–5280.

Liao, R., Bellalta, B., Oliver, M., and Niu, Z. (2016). Mu-mimo mac protocols for wireless local area networks: A survey. *IEEE Communications Surveys Tutorials*, 18(1):162–183.

Liu, Y., Ji, F., Wen, M., Wan, D., and Zheng, B. (2017). Vector ofdm with index modulation. *IEEE Access*, 5:20135–20144.

Liu, Y., Li, C., Xia, X., Quan, X., Liu, D., Xu, Q., Pan, W., Tang, Y., and Kang, K. (2019). Multiband user equipment prototype hardware design for 5g communications in sub-6-ghz band. *IEEE Transactions on Microwave Theory and Techniques*, 67(7):2916–2927.

Lokam, S. V. (2009). *Complexity Lower Bounds Using Linear Algebra*. Now Publishers Inc., Hanover, MA, USA.

Lu, S., Hemadeh, I. A., El-Hajjar, M., and Hanzo, L. (2018). Compressed-sensing-aided space-time frequency index modulation. *IEEE Trans. Veh. Technol.*, 67(7):6259–6271.

Luke, H. D. (1999). The origins of the sampling theorem. *IEEE Communications Magazine*, 37(4):106–108.

Luzzatto, A. and Shirazi, G. (2016). *Wireless transceiver design : mastering the design of modern wireless equipment and systems*. 2nd edition.

MacWilliams, F. and Sloane, N. (1978). *The Theory of Error-Correcting Codes*. North-holland Publishing Company, 2nd edition.

Madanayake, A., Cintra, R. J., Akram, N., Ariyarathna, V., Mandal, S., Coutinho, V. A., Bayer, F. M., Coelho, D., and Rappaport, T. S. (2020a). Fast radix-32 approximate dfts for 1024-beam digital rf beamforming. *IEEE Access*, pages 1–1.

Madanayake, A., Cintra, R. J., Akram, N., Ariyarathna, V., Mandal, S., Coutinho, V. A., Bayer, F. M., Coelho, D., and Rappaport, T. S. (2020b). Fast radix-32 approximate dfts for 1024-beam digital rf beamforming. *IEEE Access*, 8:96613–96627.

Madey, G., Xiang, X., Cabaniss, S. E., and Huang, Y. (2005). Agent-based scientific simulation. *Computing in Science & Engineering*, 2(01):22–29.

Makki, B., Fang, C., Svensson, T., Nasiri-Kenari, M., and Zorzi, M. (2017). Delay-sensitive area spectral efficiency: A performance metric for delay-constrained green networks. *IEEE Trans. on Commun.*, 65(6):2467–2480.

Mao, T., Wang, Q., and Wang, Z. (2017a). Generalized dual-mode index modulation aided ofdm. *IEEE Commun. Letters*, 21(4):761–764.

Mao, T., Wang, Q., Wang, Z., and Chen, S. (2018). Novel index modulation techniques: A survey. *IEEE Commun. Surveys Tuts*, 21(1):315–348.

Mao, T., Wang, Z., Wang, Q., Chen, S., and Hanzo, L. (2017b). Dual-mode index modulation aided OFDM. *IEEE Access*, 5:50–60.

Martínez, C. and Molinero, X. (2001). A generic approach for the unranking of labeled combinatorial classes. *Random Struct. Algorithms*, 19:472–497.

Maruta, K. and Falcone, F. (2020). Massive mimo systems: Present and future. *Electronics*, 9(3).

Matsumoto, M. and Nishimura, T. (1998). Mersenne twister: A 623-dimensionally equidistributed uniform pseudo-random number generator. *ACM Trans. Model. Comput. Simul.*, 8(1):3–30.

McCaffrey, J. D. (2004). Generating the mth lexicographical element of a mathematical combination. *MSDN Library*.

McNickle, D., Pawlikowski, K., and Ewing, G. (2010). AKAROA2: A controller of discrete-event simulation which exploits the distributed computing resources of networks. In *European Conf. on Modelling and Simulation, ECMS 2010, Kuala Lumpur, Malaysia, June 1-4, 2010*, pages 104–109.

Moore, G. E. (2003). No exponential is forever: but "forever" can be delayed! [semiconductor industry]. In *2003 IEEE International Solid-State Circuits Conference, 2003. Digest of Technical Papers. ISSCC.*, pages 20–23 vol.1.

Mousavi, S., Taghiabadi, M. M. R., and Ayanzadeh, R. (2019). A survey on compressive sensing: Classical results and recent advancements. *ArXiv*, abs/1908.01014.

Mukherjee, S. and Mohammed, S. K. (2015). Energy-spectral efficiency trade-off for a massive su-mimo system with transceiver power consumption. In *2015 IEEE International Conference on Communications (ICC)*, pages 1938–1944.

Myung, H. G., Lim, J., and Goodman, D. J. (2006). Single carrier fdma for uplink wireless transmission. *IEEE Vehicular Technology Magazine*, 1(3):30–38.

Nawaz, S. J., Sharma, S. K., Wyne, S., Patwary, M. N., and Asaduzzaman, M. (2019). Quantum machine learning for 6g communication networks: State-of-the-art and vision for the future. *IEEE Access*, 7:46317–46350.

Nyquist, H. (1928). Certain topics in telegraph transmission theory. *Transactions of the American Institute of Electrical Engineers*, 47(2):617–644.

Ochiai, H. (2003). Performance of optimal and suboptimal detection for uncoded ofdm system with deliberate clipping and filtering. In *GLOBECOM '03. IEEE Global Telecommunications Conference (IEEE Cat. No.03CH37489)*, volume 3, pages 1618–1622 vol.3.

OEIS Foundation Inc. (2018). Sequence Number A001405. *The On-Line Encyclopedia of Integer Sequences*. (entry by Charles R Greathouse IV).

Ozturk, E., Basar, E., and Cirpan, H. A. (2017). Generalized frequency division multiplexing with flexible index modulation. *IEEE Access*, 5:24727–24746.

Pancaldi, F., Vitetta, G. M., Kalbasi, R., Al-Dhahir, N., Uysal, M., and Mheidat, H. (2008). Single-carrier frequency domain equalization. *IEEE Signal Processing Magazine*, 25(5):37–56.

Parque, V. and Miyasita, T. (2018). Towards the succinct representation of m out of n. In *11th International Conf., IDCS 2018*, pages 16–26, Tokyo, Japan.

Press, W. H., Teukolsky, S. A., Vetterling, W. T., and Flannery, B. P. (2007). *Numerical Recipes 3rd Edition: The Art of Scientific Computing*. Cambridge University Press, USA, 3 edition.

Proakis, J. and Salehi, M. (2008). *Digital Communications*. McGraw-Hill, 5th edition.

Qaisar, S., Bilal, R. M., Iqbal, W., Naureen, M., and Lee, S. (2013). Compressive sensing: From theory to applications, a survey. *Journal of Communications and Networks*, 15(5):443–456.

Queiroz, S. (2013). All-at-once or piece-by-piece: How to access wide channels in WLANs with channel width diversity? *Communications Letters, IEEE*, 17(11):2188–2191.

Queiroz, S. (2020). lib-ofdmim: The OFDM with index modulation library mapper. `https://github.com/sauloqueiroz/lib-ofdmim`.

Queiroz, S., Silva, W., Vilela, J. P., and Monteiro, E. (2020). Maximal spectral efficiency of OFDM with index modulation under polynomial space complexity. *IEEE Wireless Communications Letters*, 9(5):1–4.

Queiroz, S., Vilela, J., and Monteiro, E. (2019). What is the cost of the index selector task for OFDM with index modulation? In *IFIP/IEEE Wireless Days (WD) 2019*, Manchester, UK.

Queiroz, S., Vilela, J. P., and Monteiro, E. (2020). Is FFT fast enough for beyond-5G communications? Technical Report ArXiv 2012.07497, CISUC (University of Coimbra) and Federal University of Technology – Paraná.

Queiroz, S., Vilela, J. P., and Monteiro, E. (2020). Optimal mapper for OFDM with index modulation: A spectro-computational analysis. *IEEE Access*, 8:68365–68378.

Rao, A. and Yehudayoff, A. (2020). *Communication Complexity: and Applications*. Cambridge University Press.

Rappaport, T. S., Xing, Y., Kanhere, O., Ju, S., Madanayake, A., Mandal, S., Alkhateeb, A., and Trichopoulos, G. C. (2019). Wireless Communications and Applications Above 100 GHz: Opportunities and Challenges for 6G and Beyond. *IEEE Access*, 7:78729–78757.

Richter, F., Fehske, A. J., and Fettweis, G. P. (2009). Energy efficiency aspects of base station deployment strategies for cellular networks. In *2009 IEEE 70th Vehicular Technology Conference Fall*, pages 1–5.

Salah, M., Omer, O. A., and Mohammed, U. S. (2019). Spectral efficiency enhancement based on sparsely indexed modulation for green radio communication. *IEEE Access*, 7:31913–31925.

Salh, A., Audah, L., and Shah, N. (2019). Trade-off energy and spectral efficiency in a downlink massive mimo system. *Springer Wireless Pers. Commun.*, 106:897–910.

Sandell, M., Tosato, F., and Ismail, A. (2016). Low complexity max-log LLR computation for nonuniform pam constellations. *IEEE Commun. Letters*, 20(5):838–841.

Schaich, F. and Wild, T. (2014). Waveform contenders for 5g – ofdm vs. fbmc vs. ufmc. In *2014 6th International Symposium on Communications, Control and Signal Processing (ISCCSP)*, pages 457–460.

Schonhage, A. and Strassen, V. (1971). Schnelle multiplikation grosser zahlen. *Computing*, 7(3-4):281–292.

Shannon, C. E. (1948). A mathematical theory of communication. *Bell Syst. Tech. J.*, 27(3):379–423.

Shannon, C. E. (1949). Communication in the presence of noise. *Proceedings of the IRE*, 37(1):10–21.

Shi, Y., Lu, X., Gao, K., Zhu, J., and Wang, S. (2019). Subblocks set design aided orthogonal frequency division multiplexing with all index modulation. *IEEE Access*, 7:52659–52668.

Shimizu, T., Fukunaga, T., and Nagamochi, H. (2014). Unranking of small combinations from large sets. *Journal of Discrete Algorithms*, 29(C):8–20.

Siddiq, A. I. (2016). Low complexity ofdm-im detector by encoding all possible subcarrier activation patterns. *IEEE Commun. Letters*, 20(3):446–449.

Solomonoff, R. J. (1960). A preliminary report on a general theory of inductive inference. In *Tech. Report ZTB-138, Zator Company, Cambridge*.

Sugiura, S., Ishihara, T., and Nakao, M. (2017). State-of-the-art design of index modulation in the space, time, and frequency domains: Benefits and fundamental limitations. *IEEE Access*, 5:21774–21790.

Tan, K., Liu, H., Zhang, J., Zhang, Y., Fang, J., and Voelker, G. M. (2011). Sora: High-performance software radio using general-purpose multi-core processors. *Commun. ACM*, 54(1):99–107.

Tariq, F., Khandaker, M. R. A., Wong, K. K., Imran, M. A., Bennis, M., and Debbah, M. (2020). A speculative study on 6g. *IEEE Wireless Communications*, 27(4):118–125.

team, C. (2018). The c++ timespec library.

Thompson, C. D. (1979). Area-time complexity for vlsi. In *Proceedings of the Eleventh Annual ACM Symposium on Theory of Computing*, STOC '79, pages 81–88, New York, NY, USA. Association for Computing Machinery.

Thompson, C. D. (1980). *A Complexity Theory for VLSI*. PhD thesis, USA. AAI8100621.

Thomson, J., Baas, B., Cooper, E. M., Gilbert, J. M., Hsieh, G., Husted, P., Lokanathan, A., Kuskin, J. S., McCracken, D., McFarland, B., Meng, T. H., Nakahira, D., Ng, S., Rattehalli, M., Smith, J. L., Subramanian, R., Thon, L., Yi-Hsiu Wang, Yu, R., and Xiaoru Zhang (2002). An integrated 802.11a baseband and mac processor. In *2002 IEEE International Solid-State Circuits Conference. Digest of Technical Papers (Cat. No.02CH37315)*, volume 1, pages 126–451 vol.1.

Traversa, F., Ramella, C., Bonani, F., and Ventra, M. D. (2015). Memcomputing np-complete problems in polynomial time using polynomial resources and collective states. *Science Advances*, 1.

Viswanathan, M. and Mathuranathan, V. (2018). *Wireless Communication Systems in Matlab: (Black & White Edition)*. Independently Published.

Wen, M., Basar, E., Li, Q., Zheng, B., and Zhang, M. (2017). Multiple-mode orthogonal frequency division multiplexing with index modulation. *IEEE Trans. Commun.*, 65(9):3892–3906.

Wen, M., Li, Q., Basar, E., and Zhang, W. (2018). A generalization of multiple-mode OFDM with index modulation. In *2018 IEEE 23rd International Conf. on Digital Signal Process. (DSP)*, pages 1–5.

Wen, M., Li, Q., Basar, E., and Zhang, W. (2018). Generalized multiple-mode OFDM with index modulation. *IEEE Trans. Wireless Commun.*, 17(10):6531–6543.

Wen, M., Zhang, Y., Li, J., Basar, E., and Chen, F. (2016). Equiprobable subcarrier activation method for OFDM with index modulation. *IEEE Commun. Lett.*, 20(12):2386–2389.

Wen, M., Zheng, B., Kim, K. J., Di Renzo, M., Tsiftsis, T. A., Chen, K., and Al-Dhahir, N. (2019). A survey on spatial modulation in emerging wireless systems: research progresses and applications. *IEEE J. Sel. Areas Commun.*, 37(9):1949–1972.

Wikipedia (2020). Nyquist–shannon sampling theorem.

Xiang-Gen Xia (2001). Precoded and vector ofdm robust to channel spectral nulls and with reduced cyclic prefix length in single transmit antenna systems. *IEEE Transactions on Communications*, 49(8):1363–1374.

Xiao, M., Mumtaz, S., Huang, Y., Dai, L., Li, Y., Matthaiou, M., Karagiannidis, G. K., Bjornson, E., Yang, K., I, C., and Ghosh, A. (2017). Millimeter wave communications for future mobile networks. *IEEE Journal on Selected Areas in Communications*, 35(9):1909–1935.

Yoon, E., Kim, S., Kwon, S., and Yun, U. (2019). An efficient index mapping algorithm for OFDM-index modulation. *IEEE Access*, 7:184194–184206.

Yu, H., Lee, H., and Jeon, H. (2017). What is 5g? emerging 5g mobile services and network requirements. *Sustainability*, 9(10).

Zacheo, G., Djukic, D., Dorni, A., Babich, F., and Ricciato, F. (2012). A software-defined radio implementation of an 802.11 ofdm physical layer transceiver. In *Proceedings of 2012 IEEE 17th International Conference on Emerging Technologies Factory Automation (ETFA 2012)*, pages 1–4.

Zaidi, A. A., Baldemair, R., Tullberg, H., Bjorkegren, H., Sundstrom, L., Medbo, J., Kilinc, C., and Da Silva, I. (2016). Waveform and numerology to support 5G services and requirements. *IEEE Communications Magazine*, 54(11):90–98.

Zhang, W., Gao, X., Li, Z., and Shi, Y. (2020). Pilot-assisted mimo-v-ofdm systems: Compressed sensing and deep learning approaches. *IEEE Access*, 8:7142–7159.

Zhang, X., Bie, H., Ye, Q., Lei, C., and Tang, X. (2017). Dual-mode index modulation aided OFDM with constellation power allocation and low-complexity detector design. *IEEE Access*, 5:23871–23880.

Zhao, Y., Yu, G., and Xu, H. (2019). 6g mobile communication network: Vision, challenges and key technologies. *SCIENTIA SINICA Informationis*, 49(8):963–987.

Zheng, B., Chen, F., Wen, M., Ji, F., Yu, H., and Liu, Y. (2015). Low-complexity ml detector and performance analysis for OFDM with in-phase/quadrature index modulation. *IEEE Commun. Letters*, 19(11):1893–1896.